PROGRESS TOWARD THE TOTAL SYNTHESIS OF MARINEOSIN A AND THE SYNTHESIS AND OPTIMIZATION OF A SELECTIVE DOPAMINE RECEPTOR 4 ANTAGONIST FOR USE AS A PET TRACER AND AN *IN VIVO* TOOL TO STUDY COCAINE ADDICTION

By

Cynthia Bollinger Berry

Thesis

Submitted to the Faculty of the

Graduate School of Vanderbilt University

in partial fulfillment of the requirements

for the degree of

MASTER OF SCIENCE

in

CHEMISTRY

December, 2014

Nashville, Tennessee

Approved:

Craig W. Lindsley, Ph.D.

Gary A. Sulikowski, Ph.D.

"For surely I know the plans I have for you,"
says the Lord, "plans for your welfare and
not for harm, to give you a future with hope."

Jeremiah 29:11

"Hold tight and pretend it's a plan!"

The Doctor

ACKNOWLEDGMENTS

There are so many people to thank for getting me where I am today. First, I thank God for giving me a passion and the talents needed to pursue that passion. Through Him, nothing is impossible.

A big acknowledgment to my advisor, Craig Lindsley. Craig provided me the best opportunity possible to follow my career goals. He has also been my guide as I grew as a chemist, showing me how to think about and fix problems.

I thank all the members of the Lindsley lab, past and present, for making my graduate experience fun and educational. It really is great to be friends with your co-workers. A special acknowledgment to Leslie Aldrich, who was my first mentor in lab and taught me almost everything I needed to know. To Brittney Bates, my best friend in lab: without you, graduate school would not have been the wonderful experience it was. You provided advice, support, and lots of laughter.

My family has always supported me in following my dreams. While they won't understand much of what is written in this document, they will likely be the only ones to try.

Finally, to my husband, Jordan: you have been amazing throughout our time together. You never questioned my need to spend late hours and weekends in lab. You have supported my career aspirations by following me to Nashville and now following me to San Diego. You have been a shoulder to cry on, a launching pad, an escape. You complete me and I am so excited to start our next adventure together.

TABLE OF CONTENTS

LIST OF SCHEMES

LIST OF FIGURES

LIST OF TABLES

ABBREVIATIONS

5-HT	serotonin receptor
α	adrenaline receptors
[α]	specific rotation
Å	angstrom
AC	adenylyl cyclase
ADHD	Attention Deficit Hyperactivity Disorder
Ag_2O	silver(I) oxide
ancill. pharm.	ancillary pharmacology
aq.	aqueous
ArI	aryl iodide
BBB	blood-brain barrier
$BF_3{\cdot}OEt_2$	boron trifluoride diethyl etherate
Bn	benzyl
BnBr	benzyl bromide
Boc	*tert*-butyloxycarbonyl
Boc_2O	di-*tert*-butyl dicarbonate
$B(OMe)_3$	trimethyl borate
B:P	brain to plasma ratio
brsm	based on recovered starting material
bs	broad singlet
°C	degrees Celsius
c	concentration
cAMP	cyclic adenosine monophosphate
CAN	ceric ammonium nitrate
CB_1	cannabinoid receptor 1
$CDCl_3$	deuterated chloroform
$CHCl_3$	chloroform
CH_2Cl_2	dichloromethane
$(CH_2Cl)_2$	1,2-dichloroethane

CH_3CN	acetonitrile
cmp	compound
CNS	central nervous system
COSY	correlation spectroscopy
Cs_2CO_3	cesium carbonate
CuBr	copper(I) bromide
CuI	copper(I) iodide
Cy	cyclohexyl
CYP	cytochrome P450 enzyme
δ	chemical shift in ppm
d	doublet
D_{2L}	dopamine receptor 2 long form
D_{2S}	dopamine receptor 2 short form
D_4	dopamine receptor 4
DA	dopamine
DAST	diethylaminosulfur trifluoride
DAT	dopamine transporter
dd	doublet of doublets
ddd	doublet of doublet of doublets
dddd	doublet of doublet of doublet of doublets
DDQ	2,3-dichloro-5,6-dicyano-1,4-benzoquinone
ddt	doublet of doublet of triplets
DEPT	distortionless enhancement by polarization transfer
DIBAL-H	diisobutylaluminum hydride
DIPEA	*N*,*N*-diisopropylethylamine
dm	doublet of multiplets
DMAP	4-dimethylaminopyridine
DMF	*N*,*N*-dimethylformamide
DMP	Dess–Martin periodinane
DMPK	drug metabolism and pharmacokinetics
DMSO	dimethylsulfoxide

dq	doublet of quartets
dr	diastereomeric ratio
DRD4	D_4 receptor gene
dt	doublet of triplets
E	*entgegen* (opposite)
EDC	1-ethyl-3-(3-dimethylaminopropyl)carbodiimide
ee	enantiomeric excess
eq	equivalent
ESI	electrospray ionization
Et	ethyl
Et_2O	diethyl ether
Et_3N	triethylamine
Et_4NOH	tetraethylammonium hydroxide
EtOAc	ethyl acetate
FDA	Food and Drug Administration
f_u	fraction unbound
g	gram(s)
GIRK	G-protein coupled inwardly-rectifying potassium channel
GPCR	G-protein coupled receptor
h	hour(s)
H	histamine receptor
H_2	hydrogen gas
H_2O	water
HBr	hydrogen bromide
HCl	hydrogen chloride
HCT-116	human colorectal carcinoma
HF	hydrogen fluoride
HMBC	heteronuclear multiple-bond correlation spectroscopy
HOBt	hydroxybenzotriazole
HPLC	high-performance liquid chromatography
HRMS	high-resolution mass spectrometry

HSQC	heteronuclear single-quantum correlation spectroscopy
HWE	Horner-Wadsworth-Emmons
Hz	hertz
IC_{50}	half maximal inhibitory concentration
IL3	third intracellular loop
ImH	imidazole
in situ	in the reaction mixture
in vacuo	in a partial or full vacuum
Inh.	inhibition
IP	intraperitoneal dosing
IPA	isopropylalcohol
i-Pr	isopropyl
J	coupling constant
K_2CO_3	potassium carbonate
K_3PO_4	tripotassium phosphate
K_d	dissociation constant
kg	kilogram(s)
K_i	binding affinity
KO^tBu	potassium *tert*-butoxide
L	liter(s)
LCMS	liquid chromatography-mass spectrometry
$LiBH_4$	lithium borohydride
LiCl	lithium chloride
LiOH	lithium hydroxide
log P	partition coefficient
LTMP	lithium 2,2,6,6-tetramethylpiperidide
μM	micromolar
μW	microwave
m	multiplet
M	molar concentration
M	muscarinic receptor

MBC	4-methoxy-2,2’-bipyrrole-5-carbaldehyde
Me	methyl
Me_3OBF_4	trimethyloxonium tetrafluoroborate
MeI	iodomethane
MeOH	methanol
Mes	2,4,6-trimethylphenyl (mesityl)
mg	milligram(s)
MHz	megahertz
min	minute(s)
mL	milliliter(s)
MLPCN	Molecular Libraries Probe Production Centers Network
mmol	millimole(s)
MnO_2	manganese dioxide
mol%	mole percent
MS	molecular sieves
m/z	mass to charge ratio
n	number of independently performed experiments
Na_2CO_3	sodium carbonate
Na_2SO_4	sodium sulfate
$NaBH_4$	sodium borohydride
NaH	sodium hydride
$NaHCO_3$	sodium bicarbonate
NaH_2PO_4	monosodium phosphate
NaO_2Cl	sodium chlorite
NaOCl	sodium hypochlorite
NaOH	sodium hydroxide
n-BuLi	*n*-butyllithium
NCI	National Cancer Institute
NCS	*N*-chlorosuccinimide
NET	norepinephrine transporter
NHP	non-human primate

NH_4Cl	ammonium chloride
NH_4OH	ammonium hydroxide
NH_4OAc	ammonium acetate
nM	nanomolar
nm	nanometer(s)
NMO	*N*-methylmorpholine *N*-oxide
NMP	*N*-methyl-2-pyrrolidone
NMR	nuclear magnetic resonance
nOe	nuclear Overhauser effect
NOESY	nuclear Overhauser effect spectroscopy
O_3	ozone
OCD	Obsessive-Compulsive Disorder
o/n	overnight
PD	Parkinson's Disease
$Pd/BaSO_4$	palladium on barium sulfate
Pd/C	palladium on carbon
$Pd(OAc)_2$	palladium(II) acetate
$Pd(PPh_3)_4$	tetrakis(triphenylphosphine)palladium(0)
$Pd_2(dba)_3$	tris(dibenzylideneacetone)dipalladium(0)
PET	positron emission tomography
PG	protecting group
pH	measure of hydrogen ion concentration
Ph	phenyl
Ph_3P	triphenylphosphine
PhH	benzene
PhMe	toluene
$PhNTf_2$	*N*-phenyl-bis(trifluoromethanesulfonimide)
Piv	trimethylacetyl (pivaloyl)
PK	pharmacokinetic
PMB	*para*-methoxybenzyl
$POCl_3$	phosphorus oxychloride

$P(OEt)_3$	triethyl phosphite
ppm	parts per million
p-TsOH	*para*-toluenesulfonic acid
pyr	pyridine
q	quartet
Q-TOF	quadrupole-time of flight
quant.	quantitative
quin	quintet
R	*Rectus* (right)
rCL_{HEP}	hepatic clearance in rat
RCM	ring-closing metathesis
Red-Al	sodium bis(2-methoxyethoxy)aluminum hydride
R_T	retention time
rt	room temperature
σ	sigma receptor
s	singlet
S	*Sinister* (left)
SAR	structure-activity relationship
SEM	2-(trimethylsilyl)ethoxymethyl
sext	sextet
SFC	supercritical fluid chromatography
SM	starting material
SMe_2	dimethyl sulfide
S_N2	bimolecular nucleophilic substitution
S_NAR	nucleophilic aromatic substitution
SO_3	sulfur trioxide
SPhos	2-dicyclohexylphosphino-2',6'-dimethoxybiphenyl
t	triplet
TBAF	tetra-*n*-butylammonium fluoride
TBAI	tetrabutylammonium iodide
TBDPS	*tert*-butyldiphenylsilyl

TBHP	*tert*-butyl hydroperoxide
temp	temperature
TES	triethylsilyl
Tf_2O	trifluoromethanesulfonic anhydride
THF	tetrahydrofuran
THP	tetrahydropyran
$TiCl_4$	titanium tetrachloride
TIPS	triisopropylsilyl
TLC	thin layer chromatography
TMSOTf	trimethylsilyl trifluoromethanesulfonate
TOCSY	total correlation spectroscopy
TPAP	tetrapropylammonium perruthenate
Ts	*para*-toluenesulfonyl (tosyl)
UV	ultraviolet
VNTR	variable number of tandem repeats
$VO(acac)_2$	vanadyl acetylacetonate
v/v	volume to volume
wt%	weight percent
XantPhos	4,5-Bis(diphenylphosphino)-9,9-dimethylxanthene
Z	*zusammen* (together)
$ZnBr_2$	zinc bromide

Chapter I

Progress toward the Total Synthesis of Marineosin A

1.1. Introduction

Natural products have been important in traditional medicine, the development of chemical methodology, and the pharmaceutical industry for hundreds of years. The synthesis of natural products has played a significant role in the growth of organic chemistry, and natural products are the inspiration for approximately half of the approved drugs in the United States.[1] The Lindsley lab was attracted to the total synthesis of marineosin A for these reasons. Herein describes the synthetic efforts put forth to synthesize this interesting natural product.

1.2. Marineosins A and B

The marineosins (**Figure 1.1**) were discovered in 2008 by Fenical and co-workers from a marine-derived *Streptomyces*-related actinomycete.[2] These natural products have a novel structure containing two pyrrole functionalities, a 12-membered macrocycle, and a spiroiminal center. Marineosins A and B differ only at two stereocenters, the spirocenter (C8) and the methoxy substituent (C7). In the HCT-116 human colon tumor cell line, marineosin A displayed an IC_{50} = 0.5 μM while marineosin B was much weaker at 46 μM. When further tested in the National Cancer Institute (NCI) 60 cell line panel, marineosin A showed considerable cytotoxic selectivity against melanoma and leukemia without affecting other cell lines.[2]

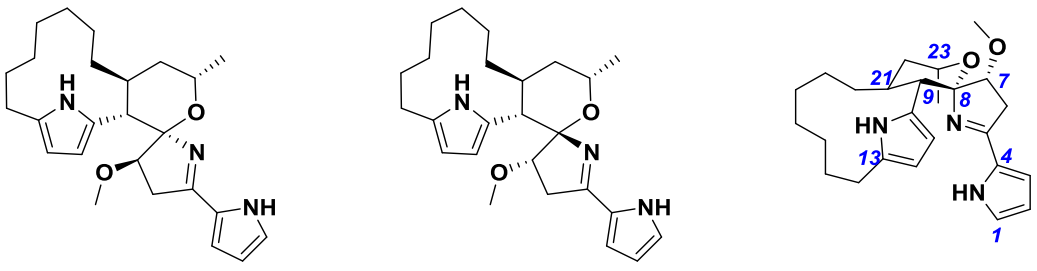

Marineosin A, 1.1 **Marineosin B, 1.2** **1.1**

Figure 1.1. Chemical structures of the marineosins.

The marineosins belong to the same family of natural products as the prodigiosin alkaloids (**Figure 1.2**). The prodigiosins are a large family of molecules consisting of a pyrrolylpyrromethene core with varying alkyl substituents at C13.[3] Prodigiosin family members exhibit a wide range of biological activities including antibacterial, antimalarial, anticancer and, most significant in the clinic, immunosuppressive activity.[3] There has been much interest in the prodigiosins, and many total syntheses of these compounds have been reported.

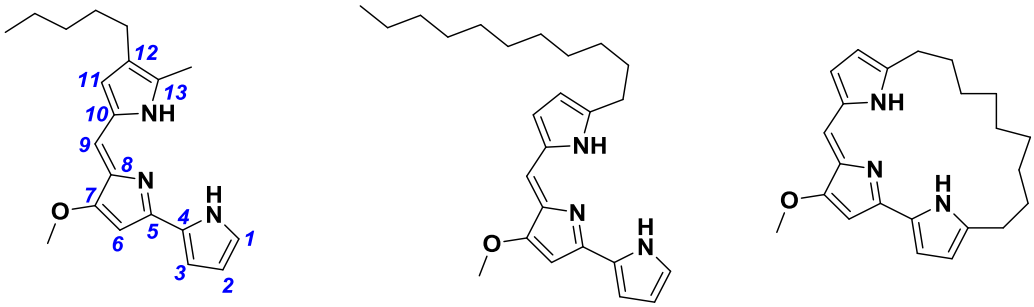

Figure 1.2. Representative members of the prodigiosin family.

1.3. Literature Review

1.3.1. Proposed Biosyntheses

In his initial report, Fenical proposed a biosynthesis of the marineosins from a known prodigiosin intermediate (**Scheme 1.1**).[2] This route encompasses the condensation of 4-methoxy-2,2'-bipyrrole-5-carbaldehyde (MBC, **1.6**), precursor of the prodigiosins, with pyrrole **1.7**. The product of this reaction could undergo an inverse-electron-demand hetero-Diels–Alder cyclization to form spiroiminal **1.9**. This Diels–Alder would ultimately give rise to the diastereomers that are marineosins A and B, as cyclization can occur from above or below the enone plane of **1.8**. Further reduction would provide the natural products.

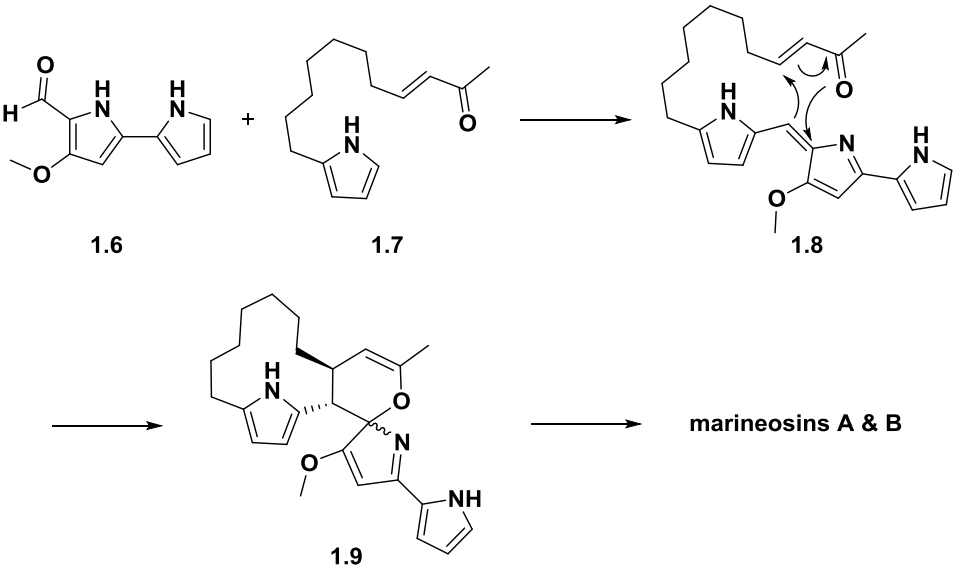

Scheme 1.1. Fenical's proposed biosynthesis of the marineosins.[2]

An attempt at a biomimetic total synthesis of marineosin A based on Fenical's proposed biosynthesis was reported from our lab in 2010.[4] Chemistry was developed to synthesize both precursors **1.11** and **1.7** in four steps each (**Scheme 1.2**). The aldehyde and enone smoothly underwent condensation to form the inverse-electron-demand hetero-Diels–Alder substrate (**1.8**). Unfortunately, all conditions attempted failed to affect the desired cyclization to spiroiminal **1.9**. Molecular modeling revealed that **1.8** is unlikely to reach a favorable conformation (key atoms being within three Angstroms of each other) for the Diels–Alder reaction to occur. This study concluded that laboratory conditions would not be able to prove this biosynthetic proposal.[4] Several intermolecular Diels–Alder conditions were attempted but also proved unsuccessful, suggesting that the dienophile is insufficient as a coupling partner. This is likely due to the removal of electron density through the highly conjugated system.

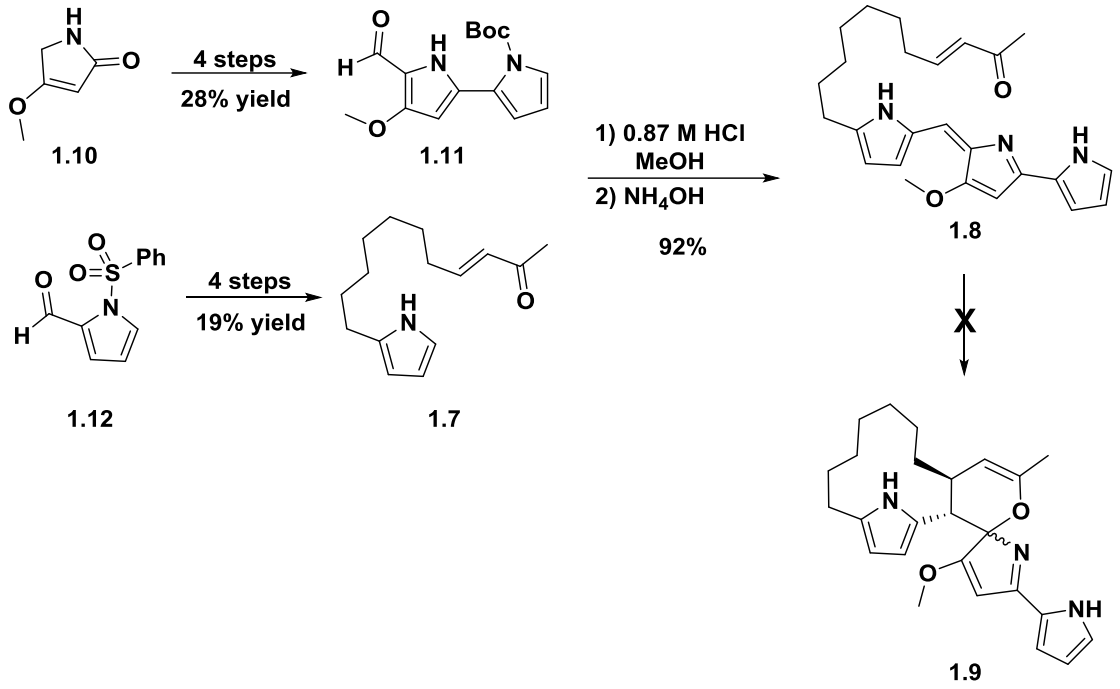

Scheme 1.2. Attempted biomimetic synthesis of marineosin A.[4]

Snider envisioned a different biosynthetic pathway to the marineosins. He did not favor the six-electron oxidation followed by four-electron reduction that Fenical's route required.[5] Snider proposed a biosynthesis starting from undecylprodigiosin (**1.4**, **Figure 1.2**) that only required one enzyme to perform a single two-electron oxidation. Using his proposal as a guide, Snider began work on a model system to test this strategy for the synthesis of the spiroiminal core of the marineosins (**Scheme 1.3**).

Vinylmagnesium bromide addition into lactone **1.13** followed by triethyl silyl (TES) protection afforded enone **1.14**. Addition of 2-(trimethylsilyl)ethoxymethyl (SEM) protected pyrrolyl oxime **1.15** proceeded in 73% yield to form isoxazoline **1.16**. Incorporation of an unprotected pyrrole lead to degradation and byproducts in subsequent reactions, so the group resorted to the SEM-protected pyrrole. Isoxazoline **1.16** underwent hydrogenolysis with Raney nickel followed by bis-methylation of the alcohols. Hydrochloric acid (HCl) was utilized to hydrolyze the silyl ether, affect the loss of methanol, and close the spiroiminal. This step gave a mixture of three diastereomers after two weeks of equilibration time. Deprotection with tetra-butylammonium fluoride (TBAF) yielded the three diastereomers shown.

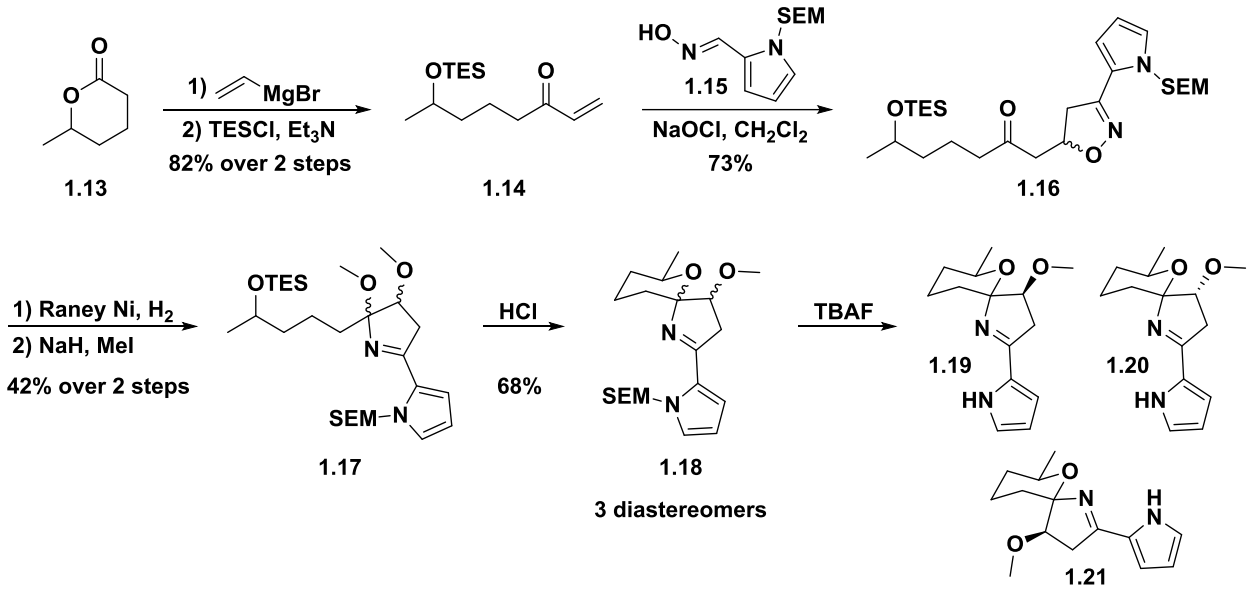

Scheme 1.3. Snider's route to the spiroiminal core of the marineosins.[5]

The fused macrocyclic ring of the marineosins forces the methyl group into an axial position, but in these smaller systems, the methyl group resides in an equatorial position. Of the three diastereomers, **1.20** has the same spirocenter and methoxy configuration as marineosin B; however, none have the absolute stereochemistry exhibited by marineosin A.

In his dissertation in 2012, S. Salem of the Reynolds lab sequenced the gene cluster responsible for the biosynthesis of the marineosins.[6] He reported that the enzyme MarG oxidizes hydroxyundecylprodigiosin (**1.22**) and that the following macrocyclization and spiroiminal formation give dehydromarineosin A (**1.23**, **Scheme 1.4**). MarG is a RedG homologue, an enzyme known to catalyze the production of the prodigiosins. Salem also reports that the enzyme MarA catalyzes the final reduction to yield marineosin A.[6]

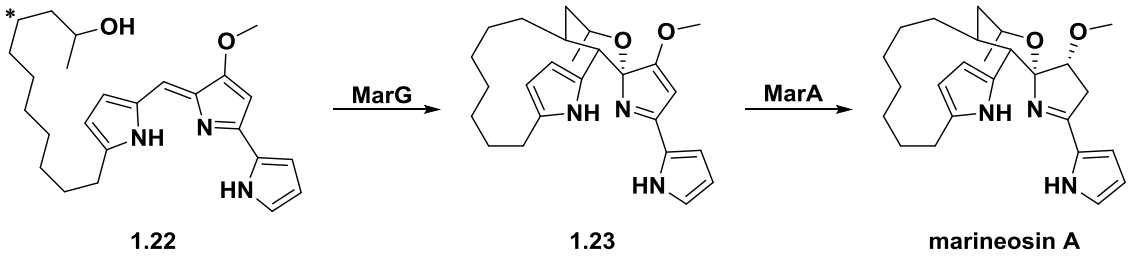

Scheme 1.4. Reynolds/Salem's biosynthesis of marineosin A.[6]

Snider wanted to test Salem's final reduction of the enol ether to marineosin A chemically.[7] Treatment of **1.24**, an intermediate in his previous model system, with hydrofluoric acid (HF) in tetrahydrofuran (THF) gave 3-methoxypyrrole **1.25** (**Scheme 1.5**). Reaction of **1.25** with manganese dioxide (MnO_2) in acetone gave two separable spiroiminals, **1.26** and **1.27**. Hydrogenation of these two compounds with palladium on barium sulfate ($Pd/BaSO_4$) provided four diastereomers, thus mimicking the reduction claimed by Salem to be the last step in the biosynthesis of marineosin.

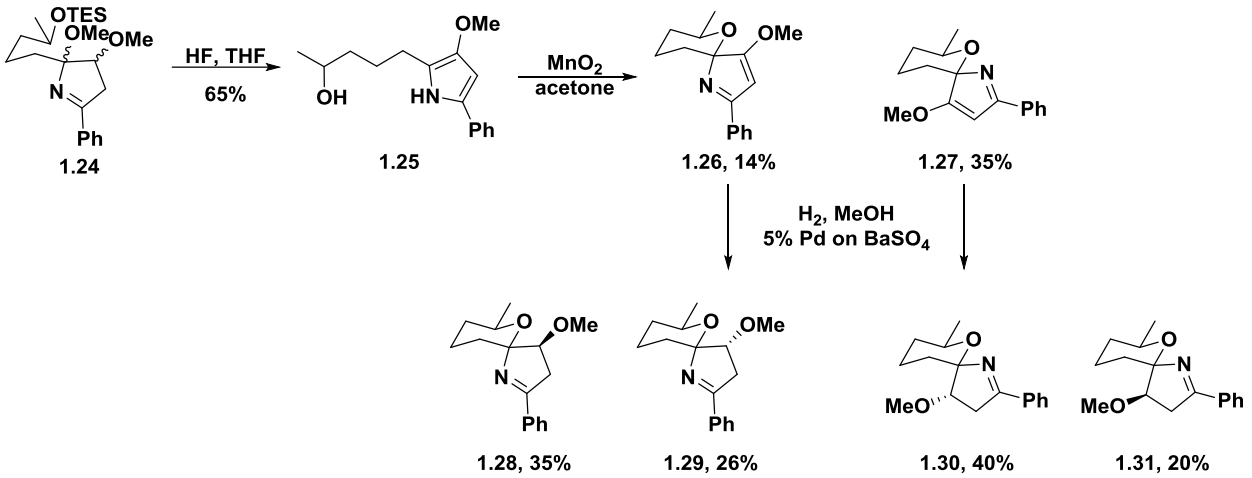

Scheme 1.5. Snider's chemical proof of Salem's biosynthetic reduction.[7]

Spiroiminal **1.30** was formed in 40% yield, and although it has the same relative stereochemistry as marineosin A, it exhibits a very different conformation.[7] Whereas marineosin A's macrocyclic ring locks the tetrahydropyran ring into a formation with the nitrogen and methyl in axial positions, **1.30** prefers the nitrogen and methyl groups to be equatorial due to steric interactions. Snider's next goal was to prepare a more substituted model system that would exhibit the same conformation as marineosin A.

1.3.2. Snider's Advanced Model System and Progress toward the Total Synthesis of Marineosin A

In order to synthesize a more substituted model system with hopes of preparing a compound with the same conformation as marineosin A, Snider added phenyl and propyl groups to his initial model system.[7] From parasorbic acid (**1.32**), the iodolactone was formed and

subsequent Buchwald–Hartwig coupling yielded phenyl lactone **1.33** (**Scheme 1.6**). Conjugate addition with allylmagnesium bromide followed by hydrogenation provided trisubstituted lactone **1.34**. Transformation to the Weinreb amide with *N,O*-dimethylhydroxylamine was followed by protection of the secondary alcohol and addition of vinyl Grignard to yield enone **1.35**. The next four steps, developed in their previous model system, gave two diastereomers, **1.37** and **1.38**. The isomer matching the stereochemistry of marineosin A (**1.38**) was the major product in a 7:1 ratio and was shown to adopt the same conformation as marineosin A.[7]

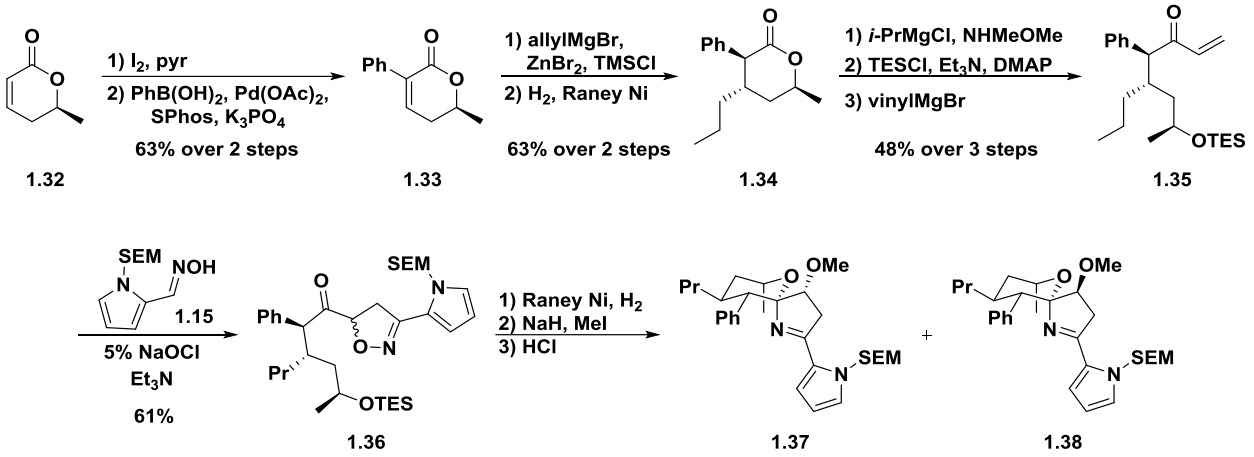

Scheme 1.6. Snider's more functionalized model system.[7]

After completing the synthesis of spiroiminal **1.38**, Snider's focus turned to the pyrrole-containing macrocycle of marineosin A (**Scheme 1.7**).[7] Aldehyde **1.39** was subjected to 1,2-addition followed by Ley oxidation[8] and subsequent reduction with sodium borohydride to give pyrrole **1.40**. This pyrrole was then *t*-butoxycarbonyl (Boc) protected and transformed to boronic acid **1.41** with lithium 2,2,6,6-tetramethylpiperidide (LTMP) and trimethyl borate. Suzuki coupling with iodolactone **1.42** afforded pyrrolyl lactone **1.43**. Conjugate addition of allyl Grignard gave a 5:4 mixture of the undesired *cis* isomer (**1.44**) and Boc-migrated compound (**1.45**) in 56% yield. Treatment of this mixture with trimethylsilyl (TMS) triflate removed the Boc groups and afforded the desired *trans* isomer (**1.46**). Ring closing metathesis (RCM) with 30 mol% Grubbs II at reflux for 16 hours yielded the macrocycle in 41% yield, and hydrogenation gave saturated ring system **1.47**.

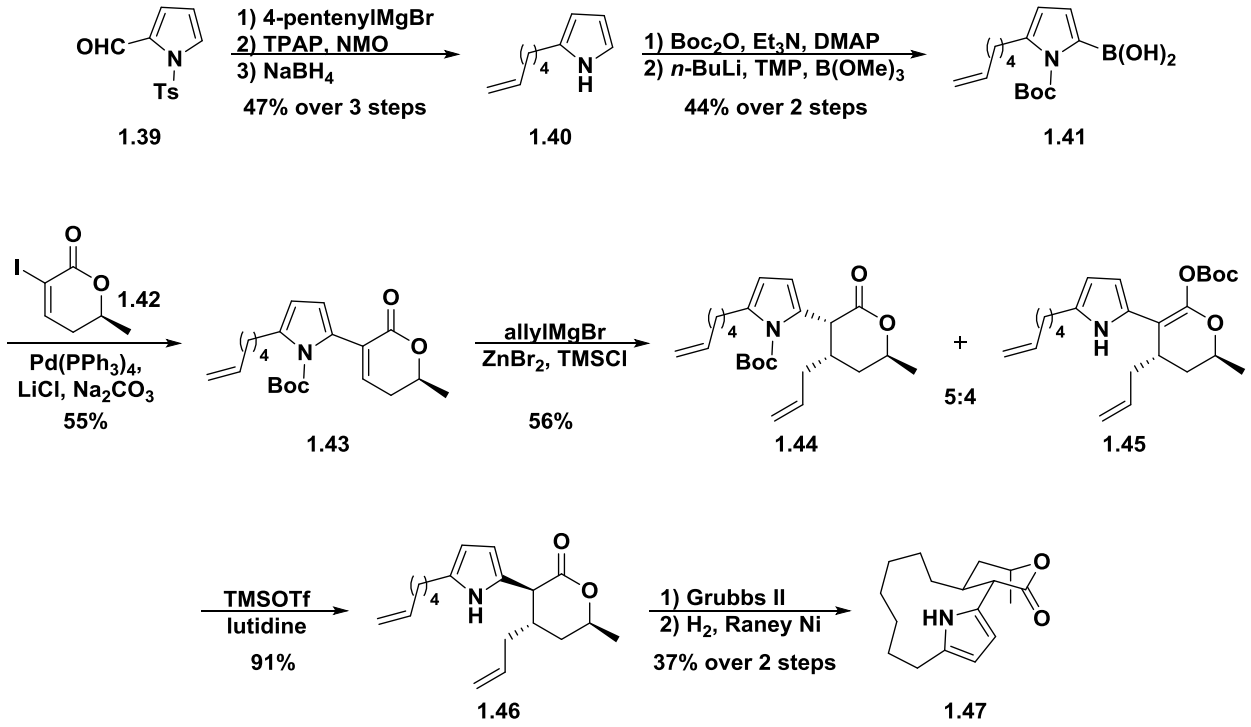

Scheme 1.7. Snider's synthesis of the macrocyclic pyrrole.[7]

An X-ray crystal structure of macrocycle **1.47** confirmed the stereocenter conformation and indicated that the lactone adopts a boat conformation with the pyrrole nitrogen perpendicular to the macrocycle (**Figure 1.3**).[7]

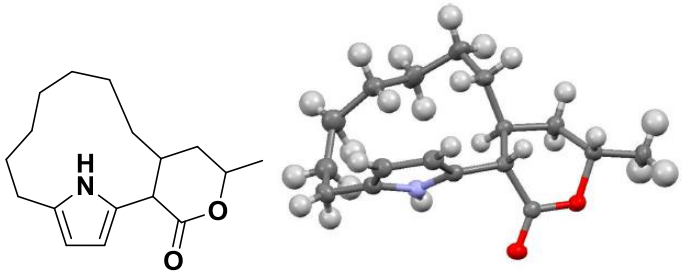

Figure 1.3. X-ray crystal structure of macrocycle **1.47**.[7]

In attempt to complete the total synthesis of marineosin A, Snider combined his model system syntheses.[7] From pyrrole macrocycle **1.47**, the lactone was opened via Weinreb amide formation, and the alcohol was TES protected (**Scheme 1.8**). Enone **1.48** was synthesized by 1,2-addition of vinyl lithium into the amide. Cycloaddition with SEM-protected pyrrole **1.15** gave

isoxazoline **1.49**, and hydrogenolysis gave imine **1.50**. Only three steps remained from intermediate **1.50** to marineosin A. Unfortunately, a variety of methylation conditions failed to methylate the diol. These hydroxyl groups appear to be more hindered than in the model systems, and hemi-iminal **1.50** decomposed under all conditions tested. In addition, Snider and co-workers tried to form the spiroiminal before methylation but only decomposition was seen. Hemi-iminal **1.50** is the furthest reported intermediate Snider achieved using this method; however, one can assume that Snider's efforts to complete the total synthesis are still underway.

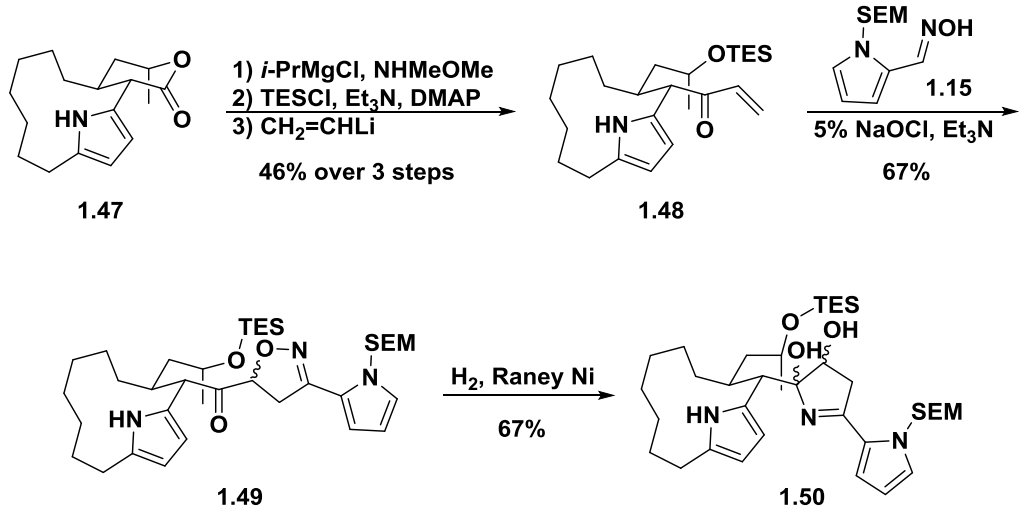

Scheme 1.8. Snider's efforts toward the total synthesis of marineosin A.[7]

1.4. Progress toward the Total Synthesis of Marineosin A

The Lindsley lab recently reported our progress toward the total synthesis of marineosin A.[9,10] This work includes the completion of the first 21 steps of a 29 step proposal *en route* to the natural product, an advanced model system to test late reactions of the synthesis, and a smaller model system to test the installation of pyrrole in the last step.

1.4.1. Synthesis toward Marineosin A

Several of the Lindsley lab's first attempts to synthesize marineosin A failed due to early installation of the pyrrole rings. In light of this, we imagined a retrosynthetic route that involved late stage installation of both pyrrole units.[10] As shown in **Scheme 1.9**, the last step will be pyrrole addition into the lactam. The spirocenter will be formed by acid-mediated cyclization. Ring

closing metathesis and Paal–Knorr pyrrole synthesis will yield the macrocyclic pyrrole. Diketone **1.53** will be formed via Stetter reaction. A regioselective epoxide opening will set the stereochemistry of the methoxy group. A conjugate addition and aldol addition will set two stereocenters via Evan's oxazolidinone, which leads us to the starting materials: chiral epoxide **1.59**, vinylmagnesium bromide, and Evan's auxiliary phosphonate **1.58**.

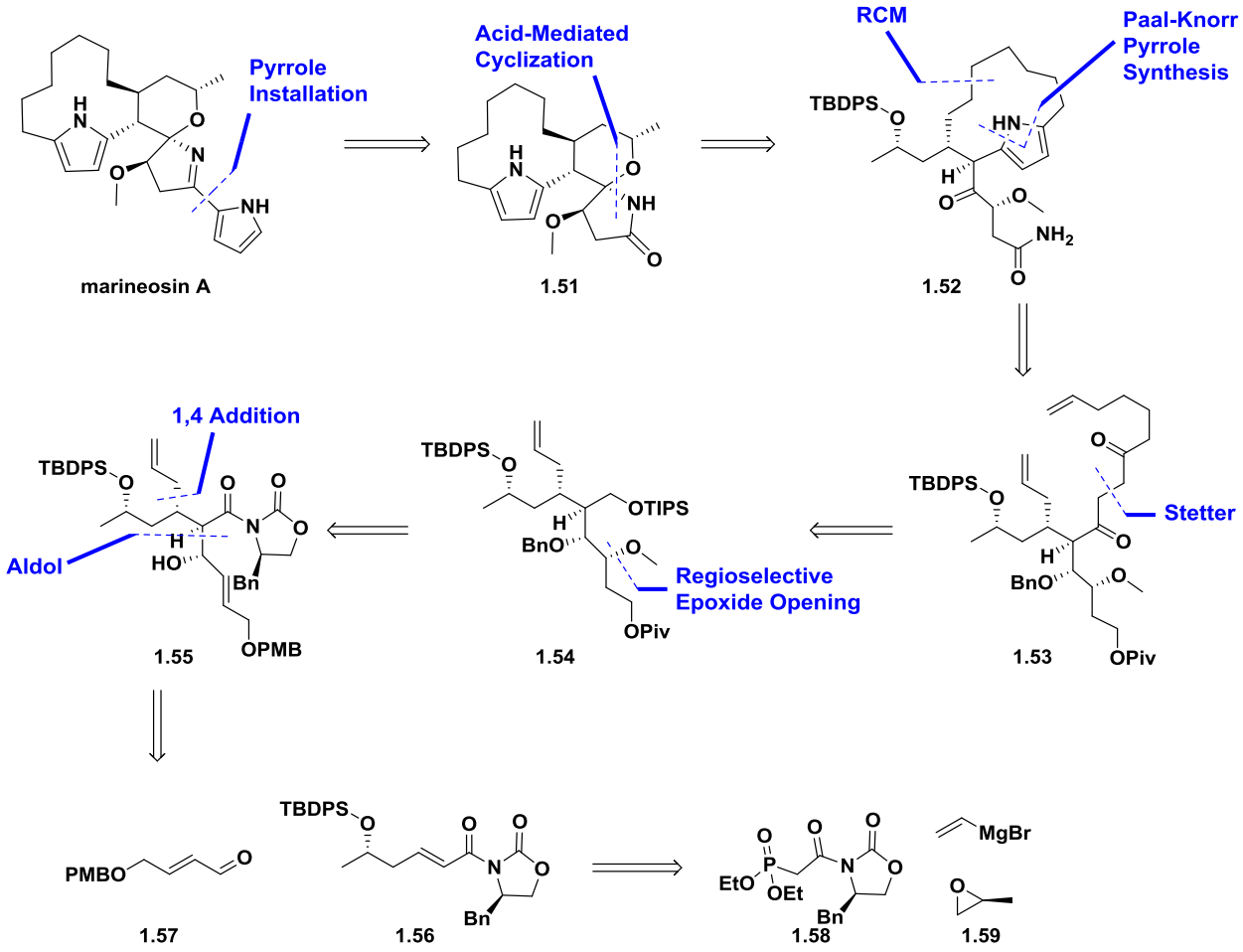

Scheme 1.9. Retrosynthetic analysis of marineosin A.

Forward synthesis began with the opening of (*S*)-propylene oxide via copper-promoted Grignard addition followed by protection of the resulting alcohol as a *tert*-butyldiphenylsilyl (TBDPS) ether (**Scheme 1.10**).[10] Ozonolysis converted terminal olefin **1.62** to aldehyde **1.63** in 84% yield. To synthesize the required Horner–Wadsworth–Emmons (HWE) phosphonate **1.58**, (*R*)-oxazolidinone **1.60** was acylated with bromoacetyl bromide to give **1.61** which then underwent

the Arbuzov reaction with triethyl phosphite. Phosphonate **1.58** underwent HWE olefination with aldehyde **1.63** to afford the acyloxazolidinone (**1.56**) in 75% yield.

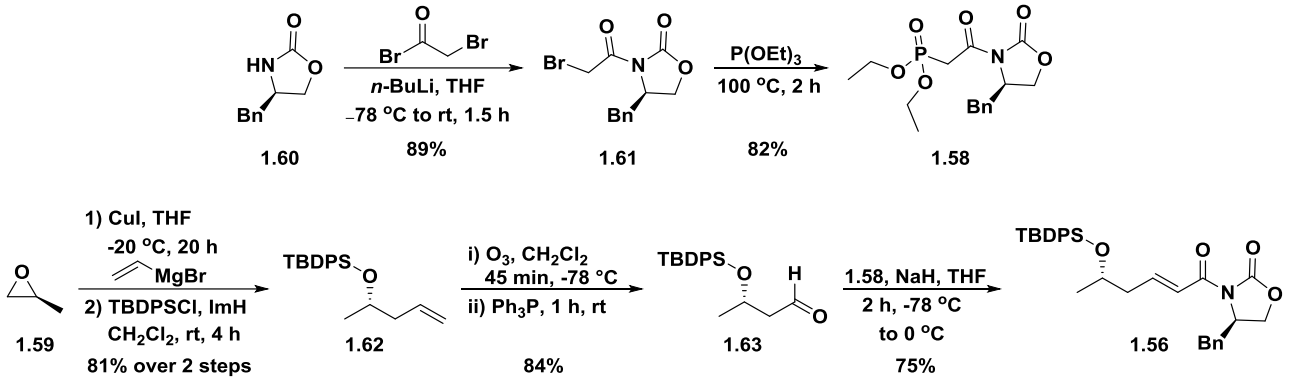

Scheme 1.10. Synthesis of acyloxazolidinone **1.56**.

The above synthesis was a substantial improvement over the original route to oxazolidinone **1.56** (**Scheme 1.11**). Initially, Grubbs II catalyzed cross metathesis between olefin **1.62** and methyl acrylate. Hydrolysis followed by addition of oxazolidinone **1.60** provided acyloxazolidinone **1.56**. In addition to removing one linear step and increasing overall yield, the new route reduced reaction time by three days and reduced cost by avoiding the use of Grubbs II in an early step of the total synthesis.

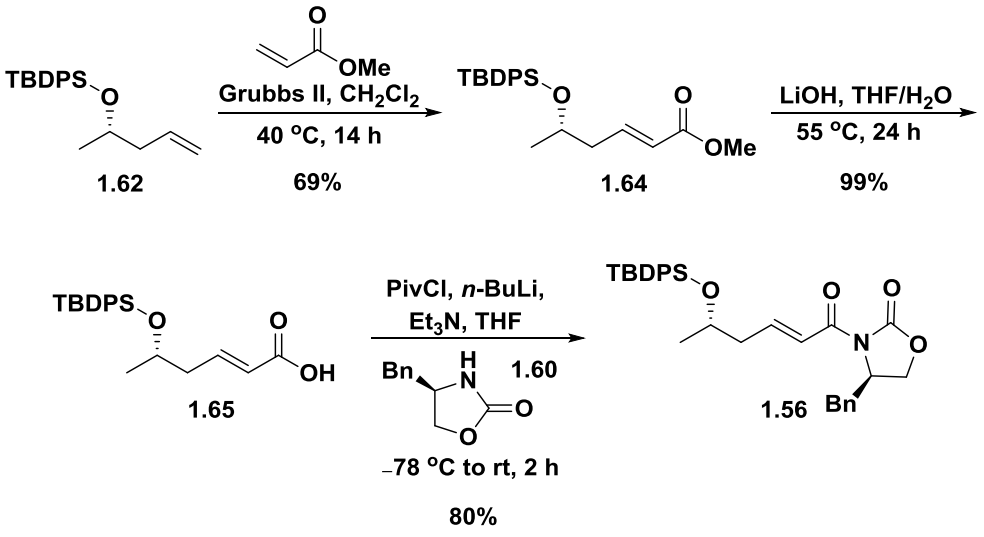

Scheme 1.11. Original route to acyloxazolidinone **1.56**.

Conjugate addition with allylmagnesium bromide and copper bromide proceeded through a chelated transition state to set one of the marineosin A stereocenters and provide oxazolidinone **1.68** (**Scheme 1.12**).[11] The necessary aldehyde for the aldol addition was synthesized from *cis*-butene-1,4-diol. Mono-*para*-methoxybenzyl (PMB) protection followed by allylic oxidation with manganese dioxide (MnO_2) afforded aldehyde **1.57**. This compound was used in the Crimmins' aldol reaction with titanium(IV) chloride to provide *syn* adduct **1.55**.[12] The Evan's auxiliary was hydrolyzed with lithium borohydride to give the free primary alcohol which was transformed to the triisopropyl silyl (TIPS) ether (**1.70**). Being important that the auxiliary removal be kept below 0 °C, the mixture was separated into smaller reaction vessels and set up in icy salt water. When the reaction was run at 0 °C, yields were only 33-36%.

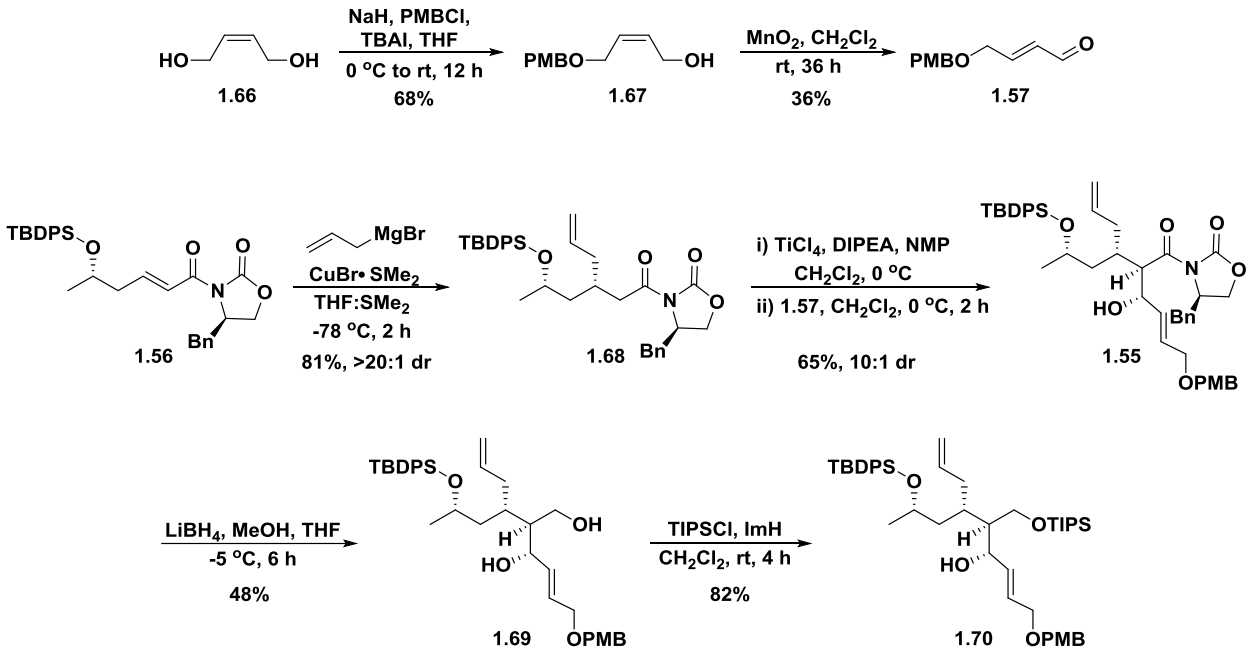

Scheme 1.12. Synthesis of intermediate **1.70**.

Oxirane **1.71** was formed via hydroxyl-directed vanadyl acetoacetate ($VO(acac)_2$) epoxidation in 95% yield (**Scheme 1.13**).[13] The secondary alcohol was benzyl protected, and the PMB group was reductively removed with 2,3-dichloro-5,6-dicyano-1,4-benzoquinone (DDQ) to provide alcohol **1.73**. Red-Al selectively opened the epoxide to 1,3-diol **1.74**.[14] The primary alcohol was protected as a pivalate ester, and the secondary alcohol was methylated to provide key intermediate **1.54**.

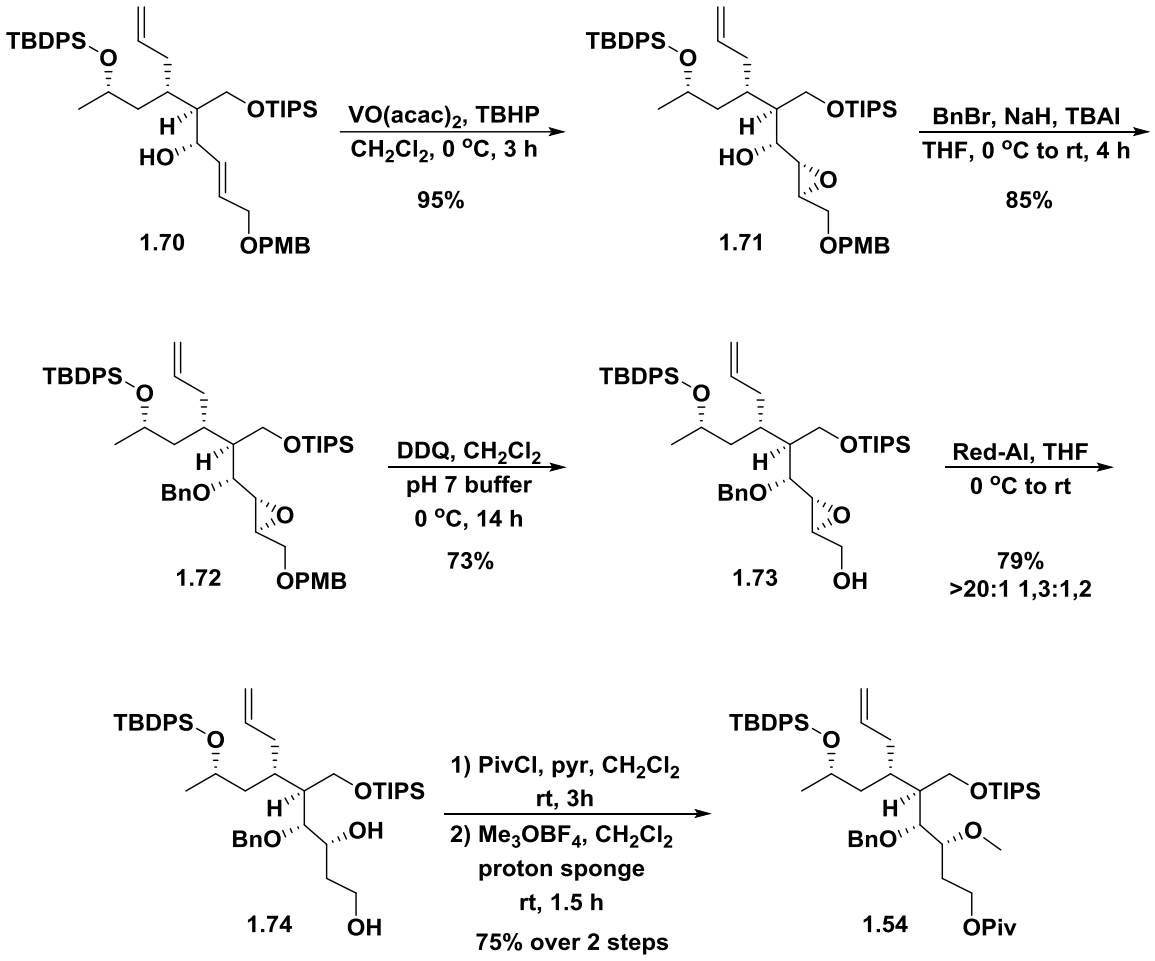

Scheme 1.13. Synthesis of intermediate **1.54**.

From intermediate **1.54**, the TIPS group was removed with boron trifluoride diethyl etherate ($BF_3{\cdot}OEt_2$), and the subsequent alcohol was oxidized to aldehyde **1.76** under Parikh–Doering conditions[15] (**Scheme 1.14**). Addition into the aldehyde with vinylmagnesium bromide followed by oxidation provided enone **1.77**. This oxidation was originally performed with MnO_2 (62% yield), but the yield was increased (91%) and reaction time decreased using Dess–Martin periodinane[16] (DMP). A Stetter reaction[17] with 6-heptenal (**1.78**) gave key 1,4-dione **1.53**. RCM with Grubbs I afforded a 1:1 mixture of the *cis* and *trans* olefins, which were carried on together. Finally, Paal–Knorr pyrrole synthesis[18,19] was completed in five hours thermally. The reaction time was improved to 20 minutes under microwave conditions to provide macrocyclic pyrrole **1.80**. This is our most advanced intermediate in the total synthesis of marineosin A, attained in 21 steps and 0.93% yield from (*S*)-propylene oxide.

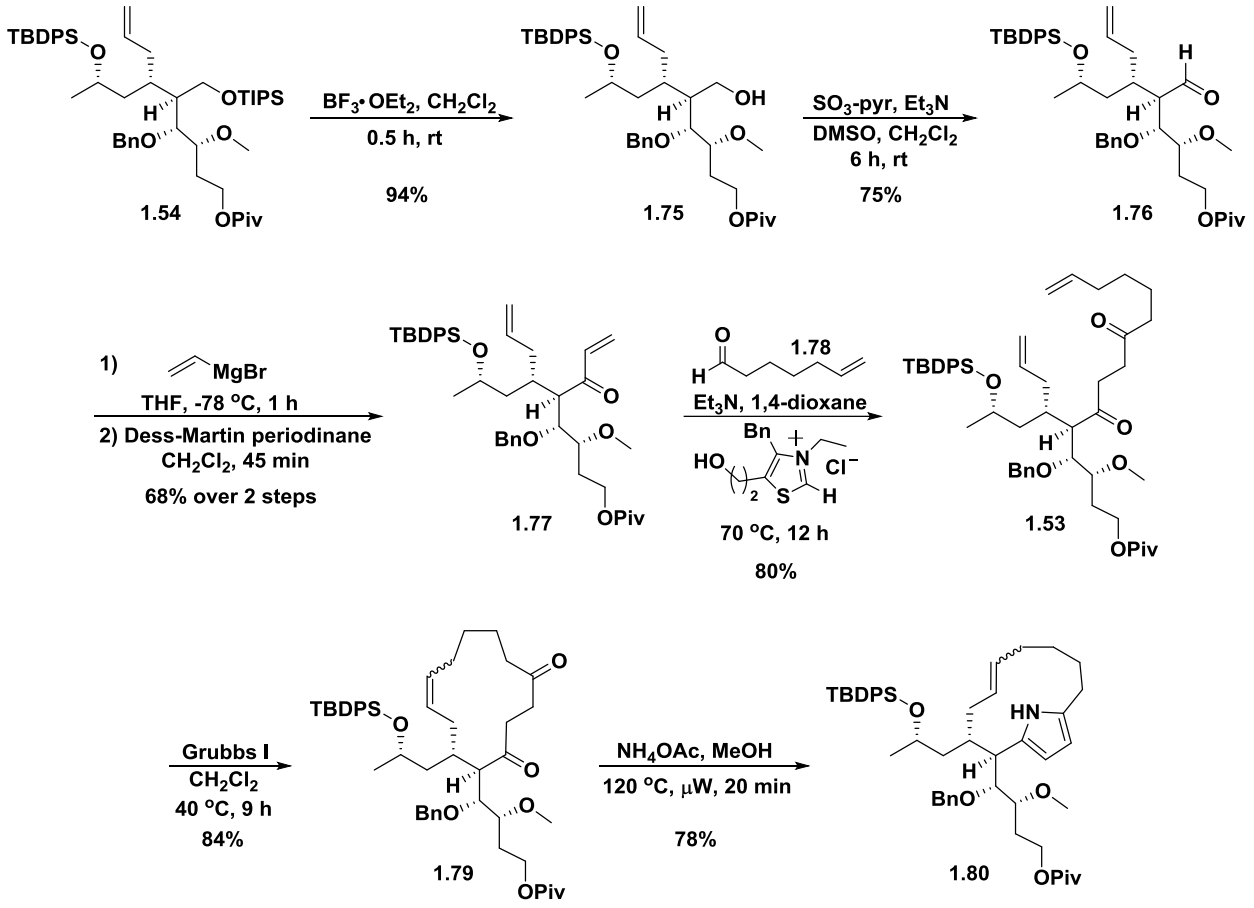

Scheme 1.14. Synthesis of our most advanced intermediate, pyrrole **1.80**.

The initial conditions and yield for the RCM to macrocycle **1.79** proved problematic, calling for an investigation of reaction conditions (**Table 1.1**). The use of Grubbs I in toluene (PhMe) and 1,2-dichloroethane ($(CH_2Cl)_2$) showed no improvement despite their ability to reach higher temperatures. Alkylidene Grubbs I (**1.82**)[20] and catalyst **1.83**[21] were both claimed to be ideal for closing 12- to 14-membered rings, but neither led to reaction completion. Grubbs II and Hoveyda–Grubbs II showed complete conversion but with the same high catalyst loadings as Grubbs I. Use of the molybdenum Schrock catalyst (**1.86**) did not progress the reaction. Finally, microwave conditions were used to lower the catalyst loading, but the necessary high dilution, and thus low throughput, was not ideal for this reaction. After this study, it was decided to continue performing this RCM with Grubbs' first generation catalyst.

Table 1.1. Results of various RCM conditions by TLC.

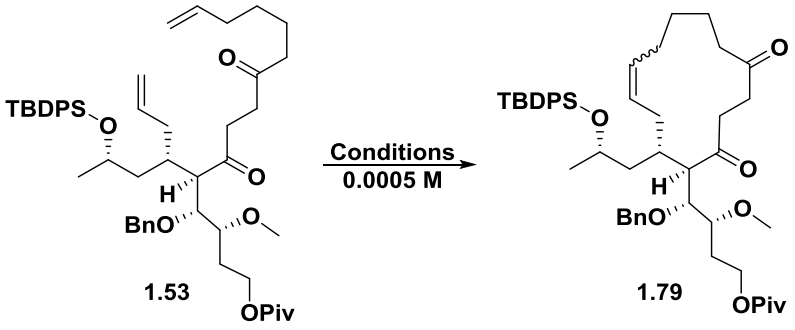

Catalyst	Solvent	Temp (°C)	Eq.	Notes on Progress
Grubbs I	CH_2Cl_2	40	1.1	Consumption of SM
Grubbs I	PhMe	110	0.25	No conversion
Grubbs I	$(CH_2Cl)_2$	55	1.1	Consumption of SM
Alkylidene Grubbs I	CH_2Cl_2	40	1.0	Not complete
Catalyst A	PhH	80	0.85	Not complete but cleaner than entry 1
Grubbs II	$(CH_2Cl)_2$	65	1.1	Consumption of SM
Hoveyda Grubbs II	CH_2Cl_2	40	1.2	Consumption of SM
Schrock	PhH	80	1.0	No conversion
Grubbs II	PhMe	μW 160	0.3	35 min, 60% conversion

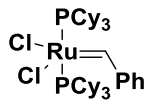

1.81
Grubbs I

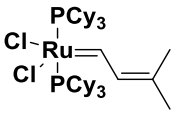

1.82
Alkylidene Grubbs I

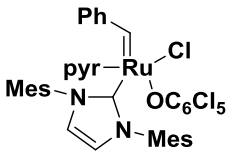

1.83
Catalyst A

Mes =

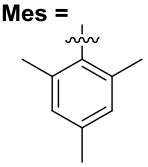

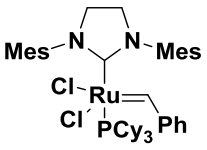

1.84
Grubbs II

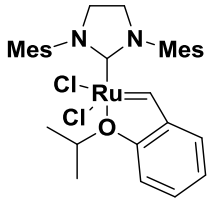

1.85
Hoveyda Grubbs II

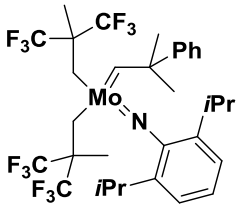

1.86
Schrock

1.4.2. Substituted Model System

In order to save advanced material and test the late synthetic steps, a model system was developed from key intermediate **1.54** (**Scheme 1.15**).[10] The pivalate ester was reductively removed with diisobutylaluminum hydride (DIBAL-H), and the resulting alcohol was oxidized with Parikh–Doering[15] then Pinnick[22] conditions to carboxylic acid **1.88**. Coupling with ammonium chloride (NH_4Cl) provided the amide[23] which then underwent hydrogenolysis of the benzyl protecting group and hydrogenation of the olefin. Ley oxidation transformed the alcohol to ketone **1.90**,[8] and cyclization was achieved with 0.01 M HCl in 86% yield.

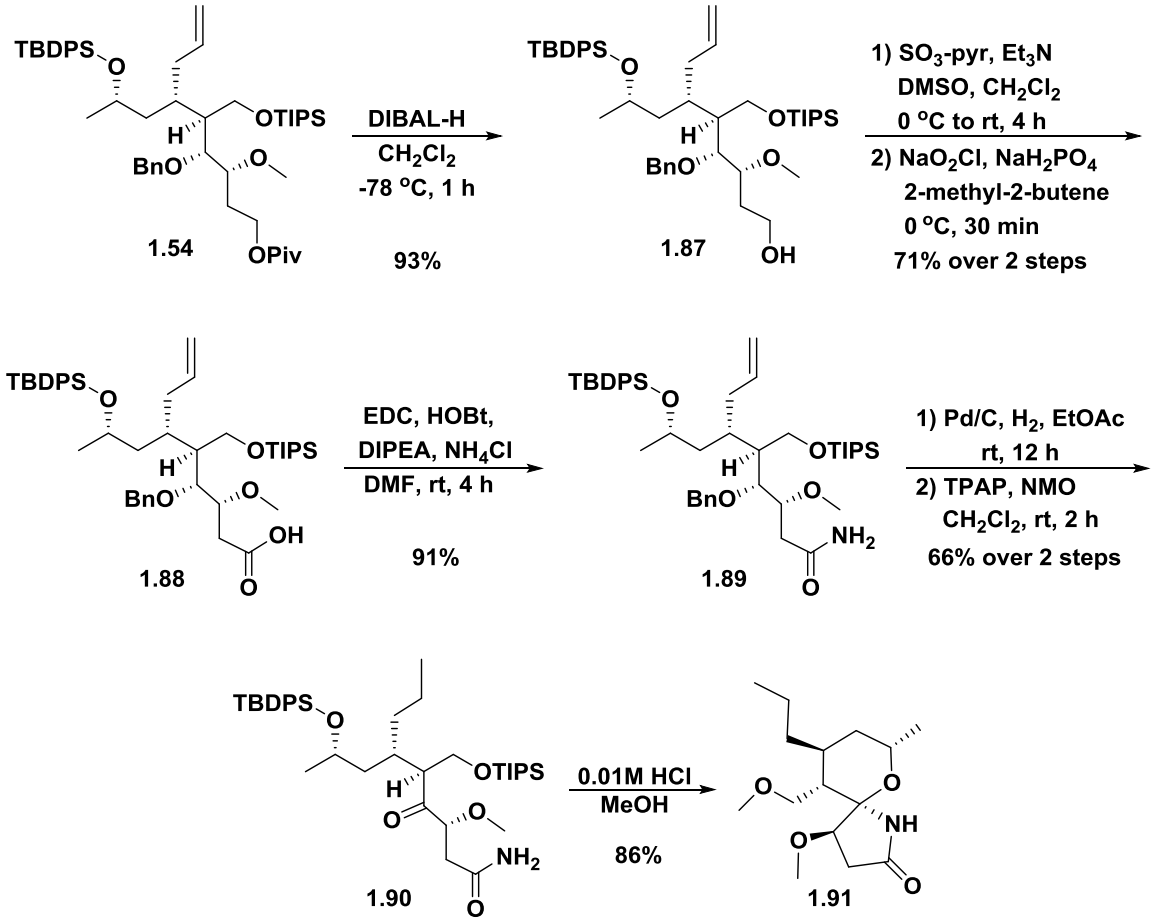

Scheme 1.15. Synthesis of model spiroaminal **1.91**.

1D and 2D NMR experiments were used to confirm the conformation of the stereocenters of spiroaminal **1.91** (**Figure 1.4**). This model system represents marineosin A with the same absolute stereochemistry at all stereocenters. The relative stereochemistry was determined by the

methyl group of the pyran ring, which was set by (*S*)-propylene oxide at the beginning of the synthesis.

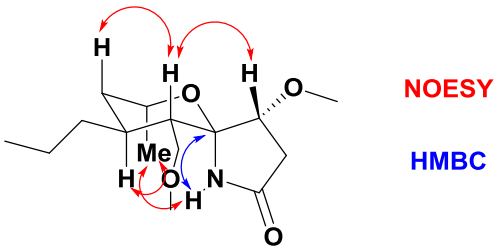

Figure 1.4. NMR correlations of **1.91**.

1.4.3. Late Stage Pyrrole Installation

In order to complete marineosin A, our synthesis calls for pyrrole installation onto a lactam as the last step. To test conditions for this reaction, another model system was synthesized (inspired by Huang *et al*.[24]) with fewer substituents on the pyran ring.[9]

First, THF was opened with aqueous hydrobromic acid (HBr) followed by hydroxyl group protection with tetrahydropyran (THP) (**Scheme 1.16**). The resulting THP ether (**1.94**) was stirred with magnesium to form Grignard reagent **1.95**. The maleimide fragment (**1.98**) was prepared from a known condensation of (*R*)-hydroxysuccinic acid and PMB amine.[25] Silver oxide mediated alkylation with iodomethane gave maleimide **1.98**.

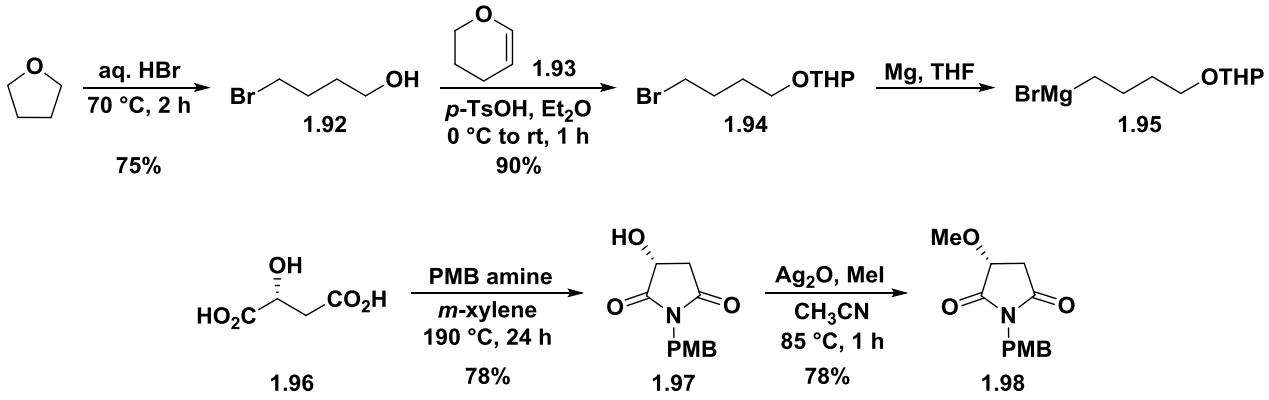

Scheme 1.16. Synthesis of coupling partners, **1.95** and **1.98**.

Grignard addition of **1.95** into maleimide **1.98** proceeded in 80% yield to give tertiary alcohol **1.99** (**Scheme 1.17**). Treatment with *para*-toluenesulfonic acid (*p*-TsOH) cleaved the THP

ether and generated an iminium salt that was regioselectively attacked by the hydroxyl group to give spiroaminal **1.101**. The PMB group was then removed with ceric ammonium nitrate (CAN), providing the desired spiroaminal (**1.102**) to test pyrrole installation conditions.

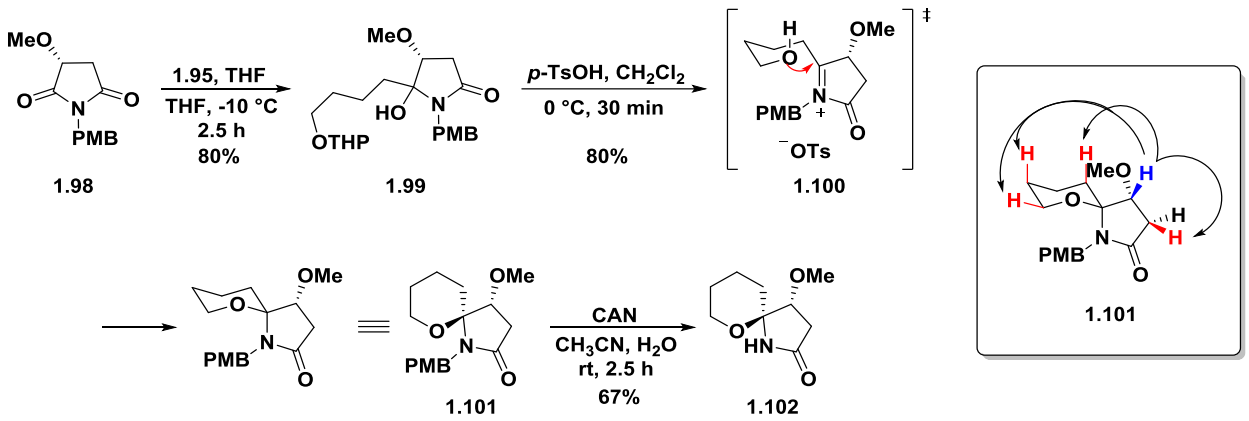

Scheme 1.17. Synthesis of spiroaminal **1.102** and nOe correlations of **1.101**.

NMR experiments showed that, in comparison to marineosin A, lactam **1.101** possesses the same stereochemistry at the methoxy substituent but has the opposite stereochemistry at the spirocenter (**Scheme 1.17**). The spirocenter likely does not take on the desired configuration due to the lack of substitution on the pyran ring, which does not favor the marineosin A conformation. Although the stereochemistry is not the same as marineosin A, this model system was still valuable as a substrate to test final reaction conditions.

Compound **1.102** was tested under many reaction conditions to install pyrrole onto the spirolactam (**Scheme 1.18**). Vilsmeier-type chemistry using phosphoryl chloride[26] as well as treatment with acid and pyrrole failed to provide **1.105**. Likewise, transformation of the carbonyl into the triflate followed by Suzuki coupling to 2-pyrrole boronic acid failed under many attempted conditions, including various metal sources, bases, solvents, and temperatures.

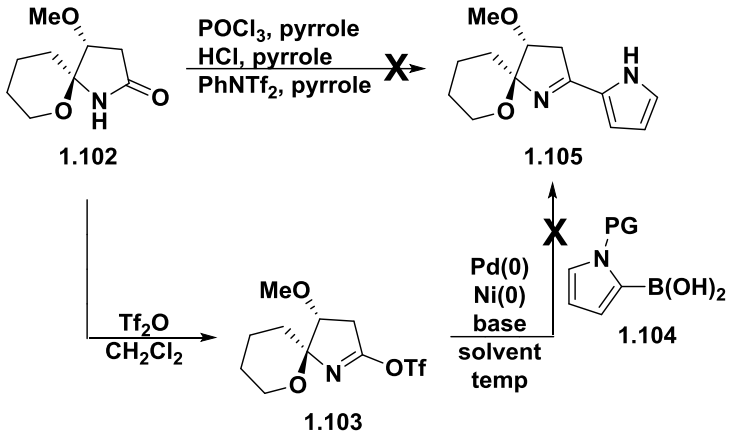

Scheme 1.18. Failed methods of installing pyrrole.

Based on the precedent set by Balenkova, the reaction shown in **Scheme 1.19** was attempted.[27] This method generates an iminium triflate salt *in situ*, and pyrrole acts as an intercepting nucleophile. Various conditions were tested with differing equivalents of reagents; the best result yielded 36% **1.105** in 15 minutes with 1.0 equivalent triflic anhydride and 5.0 equivalents pyrrole. nOe studies of adduct **1.105** (**Scheme 1.19**) revealed no equilibration of the spirocenter with installation of pyrrole, even after two weeks in $CDCl_3$.

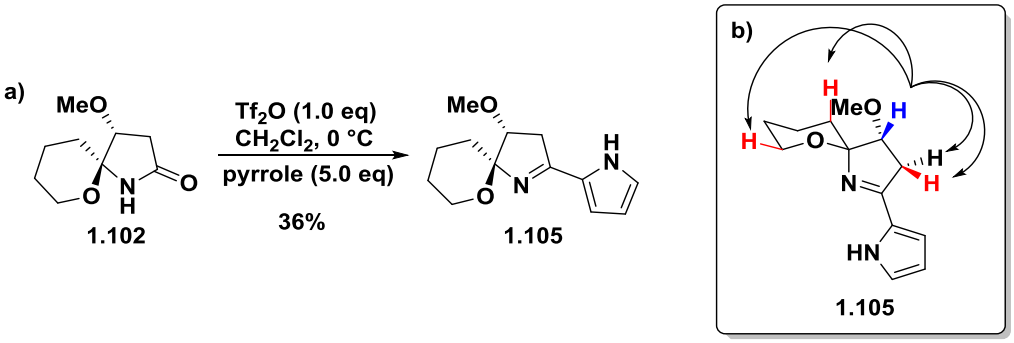

Scheme 1.19. (a) Conditions for pyrrole addition. **(b)** nOe correlations.

Repetition of this reaction sequence starting with (*S*)-hydroxysuccinic acid afforded a model system reminiscent of marineosin B in 9% overall yield (**Scheme 1.20**). Both of these model systems were then tested in a HCT-116 human colon carcinoma cytotoxicity assay to ascertain if they contained the minimal pharmacophore of the marineosins' activity. Both were

determined to be inactive, suggesting that either the larger construct and/or stereochemical conformation are important for biological activity.[9]

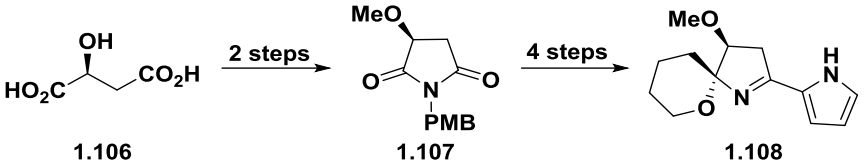

Scheme 1.20. Synthesis of the model system representing marineosin B.

Shortly after this synthesis was reported, Shi and co-workers published a very similar model system and pyrrole installation.[28] Using 2.0 equivalents triflic anhydride in neat distilled pyrrole, they were able to yield 91% of spiroiminal **1.20** (**Scheme 1.21**). Their model system contains the marineosins' methyl substituent on the pyran ring, similar to Snider's first model system. Three diastereomers were obtained from this route: **1.20**, **1.19** (representing marineosin B), and **1.110**; however, Shi was not able to synthesize the marineosin A-like diastereomer, **1.21**, using this method.

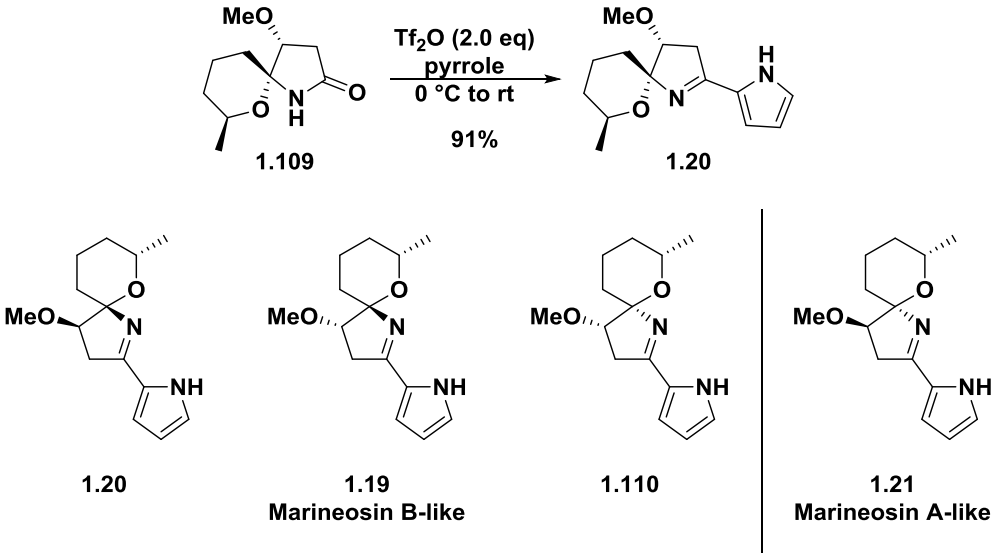

Scheme 1.21. Shi's pyrrole addition with the isomers obtained in his study (**1.20**, **1.19**, and **1.110**) and the one not obtained (**1.21**).

Upon reading this paper, we attempted our reported conditions with distilled pyrrole and increased the yield to 80% (**Table 1.2**). When Shi's exact conditions were tested on our substrate, a 71% yield was obtained. With these results, we feel confident that this procedure will provide marineosin A in the last step of our synthesis.

Table 1.2. Yield of pyrrole installation under various conditions.

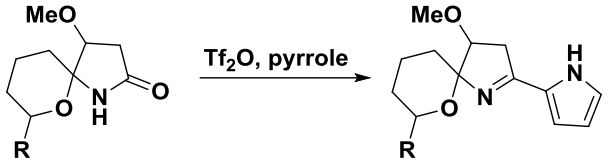

	Reported Yield	In Our Hands	Conditions
Lindsley *et al*. R = H	36%	36%	0.1 M CH_2Cl_2, 1.0 eq Tf_2O, 5.0 eq pyrrole, 0 °C, 13 min
Shi *et al*. R = Me	90%	71%	0.1 M distilled pyrrole, 2.0 eq Tf_2O, 0 °C to rt, 3 h
		80%	0.1 M CH_2Cl_2, 1.0 eq Tf_2O, 5.0 eq distilled pyrrole, 0 °C, 13 min

1.4.4. Synthesis to Complete Marineosin A

Based on the two model systems that have been completed for marineosin A, we are confident in the proposed final reactions toward the total synthesis of the natural product. All of the reactions have been tested on substrates similar to those shown in **Scheme 1.22**. From our most advanced intermediate, **1.80**, DIBAL-H will remove the pivalate ester. Parikh–Doering and Pinnick oxidations followed by EDC coupling will provide primary amide **1.112**. Hydrogenolysis and Ley oxidation will afford ketone **1.52**. Acid-mediated deprotection and cyclization will give spirolactam **1.51**. Finally, pyrrole installation via triflate displacement will yield marineosin A.

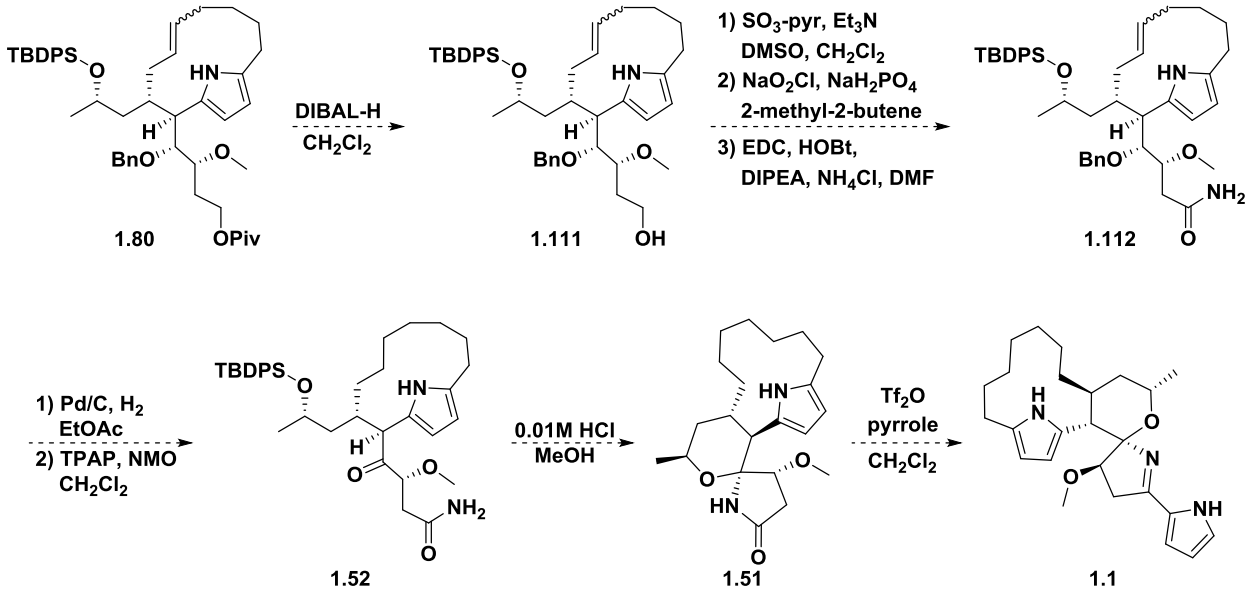

Scheme 1.22. Synthesis of marineosin A from pyrrole **1.80** based on model system syntheses.

1.5. Conclusions

While there have been many successful efforts to synthesize prodiginine alkaloids, marineosin A has yet to succumb to total synthesis. Our lab has completed a 21-step synthesis to an advanced macrocyclic pyrrole intermediate *en route* to marineosin A. This intermediate contains most of the carbon backbone, lacking only the final pyrrole, and four of the five stereocenters of marineosin A. In addition, we have completed two model systems that have allowed us to explore chemistry to form the spirocenter and install the final pyrrole ring. Through the study of these two model systems, we have laid the groundwork for the completion of the total synthesis of marineosin A.

1.6. Experimental Methods

All reagents and solvents were commercial grade and purified prior to use when necessary. Analytical thin layer chromatography (TLC) was performed on Sorbent Technologies HL 0.25 mm silica gel plates with UV indicator. Visualization was accomplished by irradiation under a 254 nm UV lamp and/or the use of an iodine chamber or potassium permanganate stain. Chromatography on silica gel was performed using Silica Gel 60 (230-400 mesh) from Sorbent Technologies. ^{1}H and ^{13}C NMR spectra were recorded on a Bruker DRX-400 (400 and 100 MHz, respectively) NMR instrument. Chemical shifts are reported in ppm from the solvent resonance as an internal standard. Data are reported as follows: chemical shift, multiplicity (s = singlet, d = doublet, t = triplet, m = multiplet, bs = broad singlet), coupling constant (Hz), and number of protons. Optical rotations were measured on a JASCO P-2000 digital polarimeter at room temperature. Concentration (c) in g/100 mL and solvent are given in parentheses. A Micromass Q-Tof API-US mass spectrometer was used to acquire high resolution mass spectrometry (HRMS) data. The value Δ is the error in the measurement (in ppm) given by the equation Δ = [(*M*E – *M*T)/ *M*T] × 106, where *M*E is the experimental mass and *M*T is the theoretical mass. The HRMS results were obtained with ES as the ion source and leucine enkephalin as the reference.

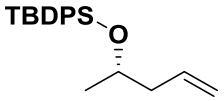

1.62

(*S*)-*tert*-butyl(pent-4-en-2-yloxy)diphenylsilane (1.62). Cuprous iodide (1.64 g, 8.61 mmol) was suspended in anhydrous tetrahydrofuran (17.5 mL) the resulting solution was cooled to -20 °C with vigorous stirring. Vinylmagnesium bromide (1.0 M in THF, 100 mL) was cannulated under a positive stream of argon into the stirring cuprous iodide over 20 min. The resulting black solution was stirred for 30 min before a solution of (*S*)-propylene oxide **1.59** (3.02 g, 43.04 mmol) in anhydrous tetrahydrofuran (5.5 mL) was added dropwise. The reaction mixture was stirred for 20 h at -20 °C. At this time, the reaction was quenched by slow addition of saturated aqueous ammonium chloride and warmed to room temperature. The mixture was extracted with diethyl ether, dried over sodium sulfate, and filtered through celite. The organic layer was carefully concentrated under reduced pressure to avoid evaporation of the volatile homoallylic alcohol. The remaining solvent was removed by gently blowing air across the surface of the crude reaction

mixture. After 20 min, the remaining yellow oil was carried on to the next step without further purification. The crude homoallylic alcohol was suspended in dichloromethane (108 mL) and to this imidazole (5.86 g, 86.1 mmol) was added followed by *tert*-butyldiphenylchlorosilane (16.5 mL, 64.6 mmol) at room temperature. The reaction was stirred for 2 h at room temperature and quenched by the addition of water when complete. The mixture was extracted with dichloromethane, dried over sodium sulfate, and concentrated *in vacuo* to give a thick, yellow oil. The crude oil was purified by chromatography (0-10% ethyl acetate in hexanes) and condensed under reduced pressure to give silyl ether **1.62** as a clear yellow oil (11.3 g, 81% over 2 steps).

^{1}H NMR ($CDCl_3$, 400 MHz) δ (ppm): 1.14 (s, 9H), 1.145 (d, *J* = 3.0 Hz, 3H), 2.22-2.33 (m, 2H), 3.98 (sext, *J* = 6.0 Hz, 1H), 5.01-5.06 (m, 2H), 5.84 (dddd, *J* = 17.0, 11.2, 10.4, 7.6 Hz, 1H), 7.41-7.49 (m, 6H), 7.75-7.78 (m, 4H). **^{13}C NMR** ($CDCl_3$, 100 MHz) δ (ppm): 19.4, 23.0, 27.2, 44.1, 69.3, 116.9, 127.6, 127.6, 129.6, 129.6, 134.6, 134.9, 135.2, 136.0, 136.0. **HRMS**: $C_{21}H_{28}ONaSi$, Calculated $[M+Na]^+$: 347.1807, Found $[M+Na]^+$: 347.1804. $[\alpha]_D^{20}$ = -15.7 (c = 1.0, $CHCl_3$).

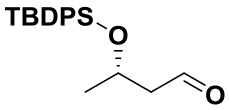

1.63

(*S*)-3-((*tert*-butyldiphenylsilyl)oxy)butanal (1.63). Olefin **1.62** (8.15 g, 25.1 mmol) was suspended in dichloromethane (251 mL) and cooled to -78 °C. Ozone was bubbled in until the solution turned blue (about 45 min). Triphenylphosphine (7.90 g, 30.1 mmol) was then added and the flask was purged with argon. This was stirred at room temperature under an atmosphere of argon for 1 h. The solution was then concentrated under vacuum and purified by column chromatography (0-5% ethyl acetate in hexanes) to give colorless oil **1.63** (6.90 g, 84%).

^{1}H NMR ($CDCl_3$, 400 MHz) δ (ppm): 1.12 (s, 9H), 1.24 (d, *J* = 6.4 Hz, 3H), 2.53-2.65 (m, 2H), 4.43 (sext, *J* = 6.0 Hz, 2H), 7.42-7.48 (m, 6H), 7.75 (dd, *J* = 8.0, 1.6 Hz, 4H), 9.79 (t, *J* = 6.4, 1H). **^{13}C NMR** ($CDCl_3$, 100 MHz) δ (ppm): 19.1, 23.8, 26.9, 52.7, 65.6, 127.6, 127.7, 129.7, 129.8, 133.5, 134.0, 135.8, 201.7. **HRMS**: $C_{20}H_{26}O_2NaSi$, Calculated $[M+Na]^+$: 349.1600, Found $[M+Na]^+$: 349.1601. Spectral data matches that recorded by S. Barluenga, *et al*.[29]

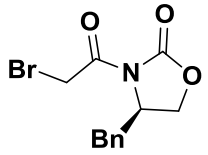

1.61

(*R*)-4-benzyl-3-(2-bromoacetyl)oxazolidin-2-one (1.61). (*R*)-4-benzyl-2-oxazolidinone **1.60** (12.5 g, 70.5 mmol) was dissolved in anhydrous tetrahydrofuran (282 mL) and cooled to -78 °C before adding *n*-butyl lithium (2.5 M in hexanes, 71.9 mmol) dropwise. This solution was stirred for 10 min at -78 °C. Bromoacetyl bromide (6.27 mL, 71.9 mmol) was added neat and this solution was stirred for 10 min at -78 °C then 1.5 h at room temperature. When the reaction was complete by TLC, it was quenched with saturated aqueous ammonium chloride, extracted with ethyl acetate, dried over sodium sulfate, and condensed *in vacuo*. The resulting oil was purified by column chromatography (0-50% ethyl acetate in hexanes) to give the product as a yellow oil (18.6 g, 88%). **^{1}H NMR** ($CDCl_3$, 400 MHz) δ (ppm): 2.81 (dd, *J* = 13.2, 9.6 Hz, 1H), 3.33 (dd, *J* = 13.6, 3.2 Hz, 1H), 4.21-4.30 (m, 2H), 4.54 (d, *J* = 3.2 Hz, 2H), 4.67-4.73 (m, 1H), 7.20-7.37 (m, 5H). **^{13}C NMR** ($CDCl_3$, 100 MHz) δ (ppm): 28.2, 37.4, 55.4, 66.6, 127.5, 129.0, 129.4, 134.7, 152.9, 165.9. **HRMS**: $C_{12}H_{13}NO_3Br$, Calculated $[M+H]^+$: 298.0079, Found $[M+H]^+$: 298.0081. $[\alpha]_D^{20}$ = -34.5 (c = 0.5, $CHCl_3$). Spectral data matches that recorded by D.A. Evans and A. Weber.[30]

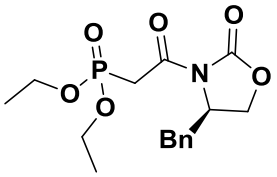

1.58

(*R*)-diethyl (2-(4-benzyl-2-oxooxazolidin-3-yl)-2-oxoethyl)phosphonate (1.58). Acyloxazolidinone **1.61** (1.49 g, 5.00 mmol) was suspended neat in triethylphosphite (1.74 mL, 10.0 mmol). A reflux condenser was attached to the flask and the solution was heated at 100 °C for 2 h. This solution was loaded directly onto a column for chromatography (0-75% ethyl acetate in hexanes). This yielded the pure product as a yellow oil (1.45 g, 82%).

^{1}H NMR ($CDCl_3$, 400 MHz) δ (ppm): 1.35 (t, *J* = 7.2, 6H), 2.75 (dd, *J* = 13.2, 10 Hz, 1H), 3.35 (dd, *J* = 13.2, 3.2 Hz, 1H), 3.80 (dq, *J* = 30.8, 19.7 Hz, 2H), 4.10-4.24 (m, 6H), 4.68-4.74 (m, 1H), 7.21-7.35 (m, 5H). **^{13}C NMR** ($CDCl_3$, 100 MHz) δ (ppm): 16.2, 16.3, 33.6, 34.9, 37.6, 55.4, 62.7,

65.9, 127.3, 128.9, 129.4, 135.0, 153.3, 165.0. **HRMS**: $C_{16}H_{23}NO_6P$, Calculated $[M+H]^+$: 356.1263, Found $[M+H]^+$: 356.1264. $[\alpha]_D^{20}$ = -35.3 (c = 1.0, $CHCl_3$).

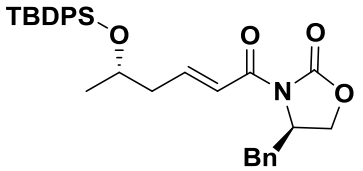

1.56

(*R*)-4-benzyl-3-((*S*,*E*)-5-((tert-butyldiphenylsilyl)oxy)hex-2-enoyl)oxazolidin-2-one (1.56). Phosphonate **1.58** (10.8 g, 30.4 mmol) was suspended in anhydrous tetrahydrofuran (204 mL) and cooled to 0 °C. Sodium hydride (60% dispersion in mineral oil, 29.2 mmol) was added and the resulting solution was stirred for 15 min at 0 °C then 45 min at room temperature. This solution was cooled to -78 °C before adding aldehyde **1.63** (7.95 g, 24.3 mmol) in anhydrous tetrahydrofuran (98.0 mL). This was stirred at -78 °C for 10 min then allowed to warm to 0 °C. At 2 h, the reaction was complete by TLC and the solution was quenched with pH 7 phosphate buffer, extracted with ethyl acetate, dried over sodium sulfate, and concentrated *in vacuo*. The resulting oil was purified by column chromatography (0-25% ethyl acetate in hexanes; 100% ethyl acetate to recover excess phosphonate **1.58**) to give the pale yellow oil of acyloxazolidinone **1.56** (9.60 g, 75%).

^{1}H NMR ($CDCl_3$, 400 MHz) δ (ppm): 1.07 (s, 9H), 1.13 (d, *J* = 6.2 Hz, 3H), 2.43 (q, *J* = 5.6 Hz, 2H), 2.78 (dd, *J* = 13.0, 9.6 Hz, 1H), 3.33 (dd, *J* = 13.5, 3.2 Hz, 1H), 4.03 (sext, *J* = 5.9 Hz, 1H), 4.19-4.23 (m, 2H), 4.73 (ddd, *J* = 13.2, 7.2, 3.4 Hz, 1H), 7.19-7.43 (m, 14 H), 7.68-7.70 (m, 4H). **^{13}C NMR** ($CDCl_3$, 100 MHz) δ (ppm): 19.4, 23.4, 26.5, 27.1, 38.0, 42.7, 55.4, 66.2, 68.7, 122.5, 127.4, 127.7, 127.8, 129.1, 129.6, 129.7, 129.8, 134.1, 134.5, 135.5, 136.0, 136.0, 148.2, 153.5, 164.8. **HRMS**: $C_{32}H_{37}NO_4NaSi$, Calculated $[M+Na]^+$: 550.2390, Found $[M+Na]^+$: 550.2393. $[\alpha]_D^{20}$ = -52.8 (c = 1.0, $CHCl_3$).

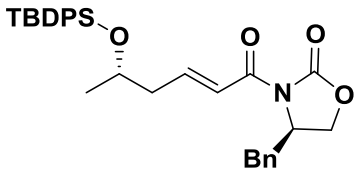

1.68

(*R*)-4-benzyl-3-((*S*)-3-((*S*)-2-((*tert*-butyldiphenylsilyl)oxy)propyl)hex-5-enoyl) oxazolidin-2-one (1.68). Recrystallized CuBr-S(CH_3)$_2$ complex (23.3 g, 113 mmol) (Procedure for recrystallization: 50 g CuBr-S(CH_3)$_2$ was dissolved in 250 mL dimethyl sulfide at 50 °C before dripping in 1 L hexanes and filtering off solvent) was suspended in dimethyl sulfide and tetrahydrofuran (1:2 v/v, 226 mL) and cooled to -78 °C. This solution was cannulated into a -78 °C solution of allylmagnesium bromide (1.0 M in diethyl ether, 90.6 mmol). The resulting thick, black solution was vigorously stirred for 1 h at -78 °C and then acyloxazolidinone **1.56** (11.9 g, 22.6 mmol) in anhydrous tetrahydrofuran (75 mL) was slowly added over 20 min. The reaction mixture was stirred for an additional 1.5 h at -78 °C and then quenched with saturated aqueous ammonium chloride and warmed to room temperature. The black mixture was extracted with diethyl ether, dried over sodium sulfate, the solvent volume reduced to approximately 200 mL by rotary evaporation, and the resulting solid/oil mixture filtered through a celite plug with liberal diethyl ether washes. The solution was condensed *in vacuo* to give a turquoise oil that was purified by column chromatography (0-20% ethyl acetate in hexanes) to provide the desired conjugate addition adduct **1.68** as a clear, colorless oil (10.4 g, 81%) and a single diastereomer by ^{1}H NMR (>20:1).

^{1}H NMR ($CDCl_3$, 400 MHz) δ (ppm): 1.05 (s, 9H), 1.12 (d, *J* = 6.1 Hz, 3H), 1.41 (quin, *J* = 7.0 Hz, 1H), 1.60 (quin, *J* = 7.0 Hz, 1H), 1.91-2.03 (m, 2H), 2.22 (quin, *J* = 6.1 Hz, 1H), 2.63 (dd, *J* = 17.9, 5.8 Hz, 1H), 2.68 (dd, *J* = 13.0, 10.0 Hz, 1H), 2.87 (dd, *J* = 17.9, 7.2 Hz, 1H), 3.28 (dd, *J* = 13.4, 3.3 Hz, 1H), 3.92 (sext, *J* = 6.2 Hz, 1H), 4.10-4.20 (m, 3H), 4.65 (ddd, *J* = 13.4, 6.9, 3.2 Hz, 1H), 4.92-4.91 (m, 2H), 5.62 (dddd, *J* = 16.7, 10.2, 9.0, 7.2 Hz, 1H), 7.20-7.43 (m, 11H), 7.66-7.70 (m, 4H). **^{13}C NMR** ($CDCl_3$, 100 MHz) δ (ppm): 19.3, 23.6, 26.5, 27.2, 30.4, 38.1, 38.4, 39.5, 43.8, 55.3, 66.2, 67.7, 77.4, 116.9, 127.5, 127.6, 127.7, 129.0, 129.1, 129.6, 129.6, 134.4, 134.9, 135.5, 136.1, 136.1, 136.3, 153.5, 172.5. **HRMS**: $C_{35}H_{43}NO_4NaSi$, Calculated $[M+Na]^+$: 592.2859, Found $[M+Na]^+$: 592.2854. $[\alpha]_D^{20}$ = -41.0 (c = 0.5, $CHCl_3$).

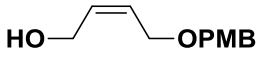

1.67

(*Z*)-4-((4-methoxybenzyl)oxy)but-2-en-1-ol (1.67). Sodium hydride (4.77 g, 119 mmol, 60% dispersion in mineral oil) was suspended in anhydrous tetrahydrofuran (227 mL). The solution was cooled to 0 °C and 1,4-*cis*-buten-1-ol **1.66** (10.0 g, 114 mmol) was added dropwise. The resulting mixture was stirred for 30 min at 0 °C at which time *p*-methoxybenzyl chloride (16.9 mL, 125 mmol) was added dropwise followed by addition of *tert*-butyl ammonium iodide (4.19 g, 11.4 mmol). The mixture was warmed to room temperature and stirred for 12 h. The reaction was quenched by dropwise addition of saturated aqueous ammonium chloride solution. The resulting mixture was extracted with ethyl acetate, dried over sodium sulfate, and concentrated under reduced pressure. The oil was purified by column chromatography (0-60% ethyl acetate in hexanes) to give PMB ether **1.67** (13.8 g, 68%).

^{1}H NMR ($CDCl_3$, 400 MHz) δ (ppm): 3.80 (s, 3H), 4.05 (d, *J* = 6.0 Hz, 2H), 4.15 (d, *J* = 6.3 Hz, 2H), 4.45 (s, 2H), 5.76 (dm, *J* = 35.0 Hz, 2H), 6.88 (d, *J* = 8.5 Hz, 2H), 7.27 (d, *J* = 8.5, 1H). **^{13}C NMR** ($CDCl_3$, 100 MHz) δ (ppm): 55.2, 58.6, 65.3, 72.0, 113.8, 128.2, 129.4, 129.9, 132.3, 159.2. **HRMS**: $C_{12}H_{16}O_3Na$, Calculated $[M+Na]^+$: 231.0997, Found $[M+Na]^+$: 231.0995. Spectral data matches that recorded by D. Könning, *et al*.[31]

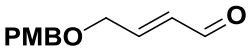

1.57

(*E*)-4-((4-methoxybenzyl)oxy)but-2-enal (1.57). PMB ether **1.67** (13.8 g, 76.7 mmol) was suspended in dichloromethane (153 mL). Manganese dioxide (80.0 g, 920 mmol) was added and the resulting heterogeneous mixture was vigorously stirred for 48 h at room temperature. The mixture was filtered through celite and condensed *in vacuo* to give a pale yellow oil. The oil was purified by column chromatography (0-40% ethyl acetate in hexanes) to provide aldehyde **1.57** as a clear, colorless oil (5.00 g, 36%).

^{1}H NMR ($CDCl_3$, 400 MHz) δ (ppm): 3.83 (s, 3H), 4.28 (dd, *J* = 4.1, 1.9 Hz, 2H), 4.54 (s, 2H), 6.41 (ddt, *J* = 15.9, 8.0, 1.9 Hz, 1H), 6.86 (dt, *J* = 15.9, 4.1 Hz, 1H), 6.92 (d, *J* = 8.4 Hz, 2H), 7.29 (d, *J* = 8.2 Hz, 2H), 9.60 (d, *J* = 7.7 Hz, 1H). **^{13}C NMR** ($CDCl_3$, 100 MHz) δ (ppm): 55.4, 68.4, 72.8, 114.1, 129.5, 129.6, 131.9, 153.4, 159.6, 193.5. **HRMS**: $C_{12}H_{14}O_3Na$, Calculated $[M+Na]^+$:

229.0841, Found $[M+Na]^+$: 229.0841. Spectral data matches that recorded by D. Könning, *et al*.[31]

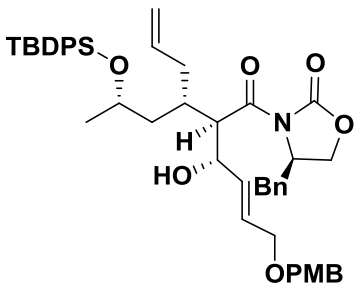

1.55

(*R*)-4-benzyl-3-((2*R*,3*S*,*E*)-2-((4*S*,6*S*)-6-((*tert*-butyldiphenylsilyl)oxy)hept-1-en-4-yl)-3-hydroxy-6-((4-methoxybenzyl)oxy)hex-4-enoyl)oxazolidin-2-one (1.55). Acyloxazolidinone **1.68** (8.81 g, 15.5 mmol) was suspended in anhydrous dichloromethane (154 mL) and cooled to 0 °C. Titanium tetrachloride (1.78 mL, 16.2 mmol) was added dropwise and the resulting yellow solution was stirred for 15 min. At 0 °C, diisopropylethylamine (2.96 mL, 17.0 mmol) was slowly added and the dark red mixture was stirred for 40 min while maintaining the temperature at 0 °C. *N*-methylpyrrolidinone (1.49 mL, 15.5 mmol) was added dropwise and the solution stirred for 10 min. Aldehyde **1.57** (3.35 g, 16.2 mmol) in anhydrous dichloromethane (65.0 mL) was added dropwise at 0 °C. After addition was complete, the solution was stirred for 1.5 h at 0 °C, quenched with saturated aqueous ammonium chloride, and warmed to room temperature. The dark orange solution was extracted with dichloromethane and filtered through a celite plug. The solvent was removed under reduced pressure at room temperature, and the resulting orange oil was purified by column chromatography (0-45% ethyl acetate in hexanes) to provide the *syn* aldol adduct **1.55** (5.24 g, 65% brsm, 10:1 dr).

^{1}H NMR ($CDCl_3$, 400 MHz) δ (ppm): 1.05 (s, 9H), 1.07 (d, *J* = 6.0 Hz, 3H), 1.49-1.56 (m, 1H), 1.61-1.67 (m, 1H), 1.80-1.86 (m, 2H), 2.01-2.09 (m, 1H), 2.11-2.18 (m, 1H), 2.48 (dd, *J* = 13.0, 10.7 Hz, 1H), 3.30 (dd, *J* = 13.2, 3.2 Hz 1H), 3.79 (s, 3H), 3.97-4.04 (m, 5H), 4.27 (t, *J* = 7.5 Hz, 1H), 4.43 (s, 3H), 4.46-4.50 (m, 1H), 4.60-4.66 (m, 1H), 4.83 (d, *J* = 17.1 Hz, 1H), 4.90 (d, *J* = 10.0 Hz, 1H), 5.55 (dddd, *J* = 16.8, 9.9, 7.2, 5.0 Hz, 1H), 5.81-5.83 (m, 2H), 6.85 (d, *J* = 8.6 Hz, 2H), 7.17-7.43 (m, 14H), 7.66-7.71 (m, 4H). **^{13}C NMR** ($CDCl_3$, 100 MHz) δ (ppm): 19.3, 23.1, 27.1, 34.7, 35.2, 38.4, 40.9, 50.6, 55.4, 55.7, 66.0, 67.6, 69.8, 72.0, 113.9, 117.1, 127.4, 127.6, 127.7, 129.1, 129.4, 129.5, 129.6, 129.7, 130.2, 130.4, 131.9, 134.5, 134.8, 135.5, 136.05, 153.8,

159.3, 173.4. **HRMS**: $C_{47}H_{58}NO_7Si$ Calculated $[M+H]^+$: 776.3983, Found $[M+H]^+$: 776.3982. $[\alpha]_D^{20}$ = -22.1 (c = 1.2, $CHCl_3$).

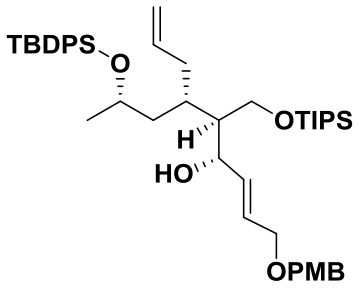

1.70

(4*S*,5*S*,6*S*,*E*)-6-((*S*)-2-((*tert*-butyldiphenylsilyl)oxy)propyl)-1-((4-methoxybenzyl)oxy-5(((triisopropylsilyl)oxy)methyl)nona-2,8-dien-4-ol (1.70). Aldol adduct **1.55** (6.11 g, 7.87 mmol) was suspended in anhydrous tetrahydrofuran (78.7 mL) and cooled to -5 °C. Anhydrous methanol (1.28 mL, 31.4 mmol) was added followed by lithium borohydride slowly (15.7 mL, 2.0 M in tetrahydrofuran), and the reaction was stirred for 6 h until complete by TLC. Water was added dropwise to quench and the solution was extracted with ethyl acetate, dried over sodium sulfate, condensed *in vacuo*, and purified by column chromatography (0-50% ethyl acetate in hexanes) to give diol **1.69** as a clear, colorless oil (2.09 g, 44%). This diol (3.34 g, 5.54 mmol) was suspended in anhydrous dichloromethane (55.0 mL) and imidazole (1.88 g, 27.7 mmol) was added followed by dropwise addition of chlorodiisopropylsilane (2.37 mL, 11.1 mmol) at room temperature. After 1 h, an additional 27.7 mmol of imidazole and 11.1 mmol of chlorodiisopropylsilane were added. After 1 h, 1.15 mL of chlorodiisopropylsilane was added and the solution was stirred for an additional 1 h and quenched by addition of water after the reaction was determined to be complete by TLC. The mixture was extracted with dichloromethane, dried over sodium sulfate, condensed *in vacuo*, and purified by column chromatography (0-30% ethyl acetate in hexanes) to give triisopropylsilyl ether **1.70** as clear, colorless oil (3.47 g, 82%).

^{1}H NMR ($CDCl_3$, 400 MHz) δ (ppm): 1.04 (s, 33H), 1.44-1.49 (m, 1H), 1.55-1.63 (m, 1H), 1.71 (quin, *J* = 7.2 Hz, 1H), 1.87-1.93 (m, 1H), 2.03-2.09 (m, 1H), 3.45 (d, *J* = 7.2 Hz, 1H), 3.76 (d, *J* = 6.8 Hz, 2H), 3.80 (s, 3H), 3.90 (sext, *J* = 6.2 Hz, 1H), 4.00 (d, *J* = 3.0 Hz, 2H), 4.25-4.29 (m, 1H), 4.45 (s, 2H), 4.84-4.91 (m, 2H), 5.49 (dddd, *J* = 16.9, 9.8, 7.2, 7.0 Hz, 1H), 5.84-5.85 (m, 2H), 6.87 (d, *J* = 8.6 Hz, 2H), 7.26 (d, *J* = 8.6 Hz, 2H), 7.34-7.43 (m, 6H), 7.66-7.69 (m, 4H). **^{13}C NMR** ($CDCl_3$, 100 MHz) δ (ppm): 11.9, 18.1, 19.3, 23.4, 27.2, 33.3, 35.1, 41.9, 47.5, 55.4, 63.4,

68.2, 70.1, 71.8, 73.9, 113.9, 116.4, 127.6, 127.7, 128.5, 129.4, 129.6, 129.7, 130.6, 133.35, 134.5, 134.9, 136.0, 136.7, 159.3. **HRMS**: $C_{46}H_{71}O_5Si_2$, Calculated $[M+H]^+$: 759.4840, Found $[M+H]^+$: 759.4836. $[\alpha]_D^{20}$ = -16.2 (c = 1.0, $CHCl_3$).

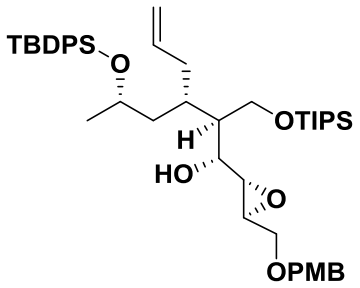

1.71

(1*R*,2*S*,3*S*)-3-((*S*)-2-((*tert*-butyldiphenylsilyl)oxy)propyl)-1-((2*S*,3*S*)-3-(((4-methoxybenzyl)oxy)methyl)oxiran-2-yl)-2-(((triisopropylsilyl)oxy)methyl)hex-5-en-1-ol (1.71). Triisopropylsilyl ether **1.70** (1.89 g, 2.45 mmol) was suspended in anhydrous dichloromethane (10.0 mL) and the solution was cooled to 0 °C. Vanadyl acetylacetonate (31.0 mg, 0.123 mmol) was added followed by dropwise addition of *tert*-butyl hydrogen peroxide (1.34 mL, ~5.5 M in decane). The resulting dark red solution was stirred at 0 °C for 4 h and an additional 5 mol% vanadyl acetylacetonate was added. Once the reaction had proceeded to completion the crude reaction mixture was transferred directly to a silica column that had been equilibrated with 1% triethylamine in hexanes and was purified using 0-25% ethyl acetate in hexanes to give oxirane **1.71** as a clear, colorless oil and a single diastereomer by ^{1}H NMR (1.79 g, 94%).

^{1}H NMR ($CDCl_3$, 400 MHz) δ (ppm): 1.03 (s, 33H), 1.46 (quin, *J* = 6.4 Hz, 1H), 1.64 (quin, 7.2 Hz, 1H), 1.72 (quin, *J* = 7.2 Hz, 1H), 1.86-1.89 (m, 2H), 2.13-2.18 (m, 1H), 2.85 (d, *J* = 4.7 Hz, 1H), 3.08 (dd, *J* = 4.4, 2.3 Hz, 1H), 3.20 (dt, *J* = 6.1, 2.2 Hz, 1H), 3.38 (dd, *J* = 11.6, 6.2 Hz, 1H), 3.76-3.86 (m, 4H), 3.80 (s, 3H), 3.92 (sext, *J* = 6.4 Hz, 1H), 4.50 (dd, *J* = 25.6, 11.6 Hz, 2H), 4.86-4.90 (m, 2H), 5.53 (dddd, *J* = 19.6, 9.8, 9.2, 7.4 Hz, 1H), 6.88 (d, *J* = 8.6 Hz, 2H), 7.27 (d, *J* = 8.6 Hz, 2H), 7.33-7.43 (m, 6H), 7.67-7.69 (m, 4H). **^{13}C NMR** ($CDCl_3$, 100 MHz) δ (ppm): 11.9, 18.1, 19.3, 23.3, 27.2, 32.9, 35.4, 42.1, 47.0, 54.5, 55.4, 56.5, 62.7, 68.3, 69.9, 70.6, 73.0, 113.9, 116.2, 127.5, 127.6, 129.5, 129.6, 130.1, 134.5, 134.9, 136.0, 137.3, 159.4. **HRMS**: $C_{46}H_{71}O_6Si_2$, Calculated $[M+H]^+$: 775.4789, Found $[M+H]^+$: 775.4785. $[\alpha]_D^{20}$ = -8.9 (c = 1.0, $CHCl_3$).

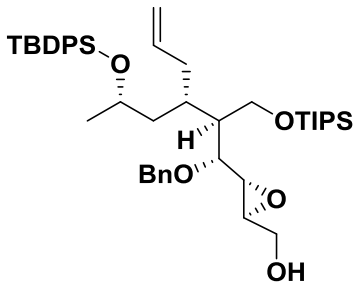

1.73

((2*S*,3*S*)-3-((1*R*,2*S*,3*S*)-1-(benzyloxy)-3-((*S*)-2-((*tert*-butyldiphenylsilyl)oxy)propyl)-2-(((triisopropylsilyl)oxy)methyl)hex-5-en-1-yl)oxiran-2-yl)methanol (1.73). Sodium hydride (60% dispersion in mineral oil, 361 mg, 9.03 mmol) was suspended in anhydrous tetrahydrofuran (45.0 mL) and the solution was cooled to 0 °C. A solution of oxirane **1.71** (3.50 g, 4.52 mmol) in tetrahydrofuran (15.0 mL) was slowly added to the sodium hydride solution, followed by immediate addition of benzyl bromide (2.14 mL, 18.1 mmol) and *tert*-butylammonium iodide (333 mg, 0.903 mmol). The solution was warmed to room temperature and stirred for 2 h. An additional 361 mg sodium hydride and 2.14 mL benzyl bromide were added at room temperature. The reaction was stirred 2 h until confirmed to be finished by LCMS. The reaction was quenched by the addition of saturated aqueous ammonium chloride, extracted with ethyl acetate, dried over sodium sulfate, and condensed *in vacuo* to give a yellow oil that was purified by column chromatography (0-15% ethyl acetate in hexanes) to provide benzyl ether (**1.72**) as a clear, colorless oil (3.10 g, 79%). This benzyl ether (1.90 g, 2.20 mmol) was suspended in a mixture of dichloromethane and pH 7 phosphate buffer (7:1 v/v, 44 mL). The solution was cooled to 0 °C and 2,3-dichloro-5,6-dicyanobenzoquinone (598 mg, 2.64 mmol) was added. The resulting biphasic solution was vigorously stirred for 12 h at 0 °C. The reaction was quenched by addition of saturated aqueous sodium bicarbonate, extracted with dichloromethane, dried over sodium sulfate, and condensed *in vacuo* to provide a yellow residue that was purified by column chromatography (0-20% ethyl acetate in hexanes) to provide alcohol **1.73** as a clear, colorless oil (1.19 g, 73%).

^{1}H NMR ($CDCl_3$, 400 MHz) δ (ppm): 1.02-1.05 (m, 33H), 1.44-1.53 (m, 2H), 1.62-1.67 (m, 1H), 1.68-1.75 (m, 1H), 1.84-1.91 (m, 1H), 1.94-2.01 (m, 1H), 2.21-2.27 (m, 1H), 3.05 (dd, *J* = 4.88, 2.2 Hz, 1H), 3.11 (quin, *J* = 2.3 Hz, 1H), 3.44 (ddd, *J* = 12.7, 7.4, 5.0 Hz, 1H), 3.63 (t, *J* = 5.1 Hz, 1H), 3.68-3.82 (m, 3H), 3.95 (sext, *J* = 6.2 Hz, 1H), 4.52 (dd, *J* = 55.6, 11.8 Hz, 2H), 4.83-4.87 (m, 2H), 5.54 (dddd, *J* = 15.3, 10.2, 7.2, 6.2 Hz, 1H), 7.25-7.42 (m, 11H), 7.68 (d, *J* = 7.2 Hz, 4H).

^{13}C NMR ($CDCl_3$, 100 MHz) δ (ppm): 12.1, 18.2, 19.3, 23.5, 27.1, 32.9, 35.9, 42.8, 47.5, 56.7,

56.8, 60.7, 61.8, 68.6, 73.8, 77.4, 115.7, 127.5, 127.6, 127.6, 128.4, 129.6, 129.6, 134.8, 135.0, 136.0, 138.3, 139.1. **HRMS**: $C_{45}H_{69}O_5Si_2$, Calculated $[M+H]^+$: 745.4684, Found $[M+H]^+$: 745.4681. $[\alpha]_D^{20}$ = -6.5 (c = 0.5, $CHCl_3$).

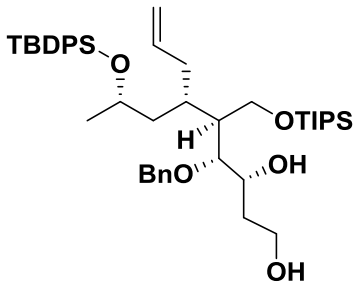

1.74

(3*R*,4*R*,5*S*,6*S*)-4-(benzyloxy)-6-((*S*)-2-((*tert*-butyldiphenylsilyl)oxy)propyl)-5-(((triisopropylsilyl)oxy)methyl)non-8-ene-1,3-diol (1.74). Alcohol **1.73** (1.74 g, 2.34 mmol) was suspended in anhydrous tetrahydrofuran (156 mL) and cooled to 0 °C. Sodium bis(2-methoxyethoxy)aluminum hydride (65 wt% in toluene, 4.35 mL, 14.0 mmol) was added dropwise and the resulting solution was warmed to room temperature and stirred for 5 h, until the reaction neared completion and the undesired free primary alcohol resulting from TIPS deprotection began to form. At this time, saturated sodium potassium tartrate solution was added dropwise and the resulting cloudy emulsion was diluted with 50 mL of ethyl acetate and stirred for 30 min until the organic layer became clear. The product was extracted with ethyl acetate, dried over sodium sulfate, and condensed *in vacuo* to give a thick, clear oil. This oil was purified by column chromatography (0-30% ethyl acetate in hexanes) to provide the desired 1,3-diol **1.74** (1.10 g, 79% based on recovered starting material) as the only product (^{1}H NMR >20:1 1,3 diol:1,2 diol).

^{1}H NMR ($CDCl_3$, 400 MHz) δ (ppm): 1.04-1.09 (m, 33H), 1.49-1.56 (m, 1H), 1.60-1.67 (m, 1H), 1.74-1.82 (m, 3H), 1.89-1.95 (m, 1H), 2.04-2.12 (m, 1H), 2.16-2.21 (m, 1H), 2.94 (bs, 1H), 3.51 (t, *J* = 6.0 Hz, 1H), 3.74-3.89 (m, 5H), 3.95-4.02 (m, 2H), 4.52 (s, 2H), 4.83-4.87 (m, 2H), 5.37-5.47 (m, 1H), 7.26-7.44 (m, 11H), 7.68-7.71 (m, 4H). **^{13}C NMR** ($CDCl_3$, 100 MHz) δ (ppm): 12.0, 18.1, 18.2, 19.3, 23.2, 27.1, 32.0, 34.8, 34.9, 42.3, 46.2, 60.9, 62.6, 68.7, 73.4, 74.6, 82.3, 116.5, 127.6, 127.6, 127.7, 127.8, 128.5, 129.6, 129.6, 134.7, 135.0, 136.0, 136.8, 138.5. **HRMS**: $C_{45}H_{71}O_5Si_2$, Calculated $[M+H]^+$: 747.4840, Found $[M+H]^+$: 747.4843. $[\alpha]_D^{20}$ = -20.0 (c = 1.0, $CHCl_3$).

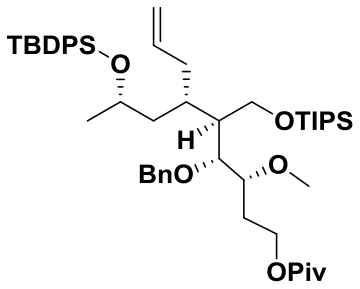

1.54

(3*R*,4*R*,5*S*,6*S*)-4-(benzyloxy)-6-((*S*)-2-((*tert*-butyldiphenylsilyl)oxy)propyl)-3-methoxy-5-(((triisopropylsilyl)oxy)methyl)non-8-en-1-yl pivalate (1.54). Diol **1.74** (978 mg, 1.31 mmol) was suspended in anhydrous dichloromethane (65.4 mL). Pyridine was added (1.05 mL, 13.1 mmol) followed by addition of pivaloyl chloride (0.970 mL, 7.85 mmol) at room temperature, and the resulting solution was stirred for 2 h. The reaction was quenched by addition of saturated aqueous sodium bicarbonate, extracted with dichloromethane, dried over sodium sulfate, and condensed *in vacuo* to give a cloudy, white residue. This residue was purified by column chromatography (0-20% ethyl acetate in hexanes) to give the pivalate ester as a clear, colorless oil (850 mg, 78%). This pivalate ester (1.10 g, 1.41 mmol) was suspended in anhydrous dichloromethane (132 mL). To this, 1,8-bis(dimethylamino) naphthalene (1.70 g, 7.94 mmol) was added followed by addition of trimethyloxonium tetrafluoroborate (0.979 g, 6.62 mmol) at room temperature. The resulting solution was stirred at room temperature for 1.5 h until TLC indicated that the reaction was complete. The reaction was quenched by addition of saturated aqueous sodium bicarbonate, extracted with dichloromethane, dried over sodium sulfate, and condensed *in vacuo* to give a pale yellow residue. This residue was purified by flash chromatography (0-15% ethyl acetate in hexanes) to provide the desired methyl ether **1.54** as a clear, colorless oil (812 mg, 73%).

^{1}H NMR ($CDCl_3$, 400 MHz) δ (ppm): 1.00-1.07 (m, 33H), 1.19 (s, 9H), 1.45 (quin, *J* = 6.8 Hz, 1H), 1.61-1.74 (m, 3H), 1.82-1.94 (m, 1H), 1.95-2.05 (m, 1H), 2.07-2.13 (m, 1H), 2.14-2.21(m, 1H), 3.36 (s, 3H), 3.55 (d, *J* = 9.2 Hz, 1H), 3.60-3.68 (m, 2H), 3.80 (dd, *J* = 8.4, 1.7 Hz, 1H), 3.92 (sext, *J* = 6.1 Hz, 1H), 4.11-4.17 (m, 1H), 4.21-4.27 (m, 1H), 4.70 (dd, *J* = 143.5, 11.4 Hz, 2H), 4.78-4.82 (m, 2H), 5.42-5.52 (m, 1H) 7.22-7.41 (m, 11H), 7.65-7.67 (m, 4H). **^{13}C NMR** ($CDCl_3$, 100 MHz) δ (ppm): 12.1, 18.3, 19.3, 23.4, 27.1, 27.4, 28.9, 33.0, 35.8, 38.8, 43.1, 46.2, 57.5, 61.9, 62.5, 68.7, 74.0, 77.4, 78.4, 81.4, 115.4, 127.3, 127.5, 127.6, 127.8, 128.3, 129.5, 129.5, 134.7,

135.2, 136.0, 138.8, 139.2, 178.7. **HRMS**: $C_{51}H_{80}O_6NaSi_2$, Calculated $[M+Na]^+$: 867.5391, Found $[M+Na]^+$: 867.5389. $[\alpha]_D^{20}$ = -7.5 (c = 1.0, $CHCl_3$).

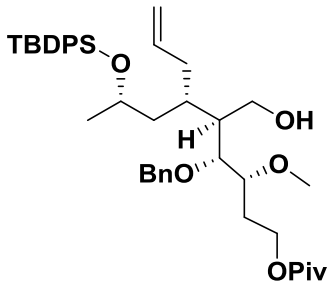

1.75

(3*R*,4*R*,5*S*,6*S*)-4-(benzyloxy)-6-((*S*)-2-((*tert*-butyldiphenylsilyl)oxy)propyl)-5-(hydroxymethyl)-3-methoxynon-8-en-1-yl pivalate (1.75). Methyl ether **1.54** (808 mg, 0.956 mmol) was suspended in anhydrous dichloromethane (95.6 mL). Boron trifluoride diethyl etherate (46.5%, 0.507 mL, 1.91 mmol) was added dropwise at room temperature and the resulting mixture was stirred for 30 min until TLC showed that the reaction had reached completion. The reaction was quenched by addition of saturated aqueous sodium bicarbonate, extracted with dichloromethane, dried over sodium sulfate, and condensed *in vacuo* to give a clear oil. This oil was purified by flash chromatography (0-30% ethyl acetate in hexanes) to give the free primary alcohol **1.75** as a clear, colorless oil (565 mg, 86%).

^{1}H NMR ($CDCl_3$, 400 MHz) δ (ppm): 1.02 (s, 9H), 1.03 (d, *J* = 6.2 Hz, 3H), 1.20 (s, 9H), 1.46 (quin, *J* = 6.6 Hz, 1H), 1.61-1.71 (m, 2H), 1.77-1.83 (m, 1H), 1.85 (t, *J* = 5.3 Hz, 1H), 1.88-1.97 (m, 1H), 1.99-2.05 (m, 1H), 2.06-2.12 (m, 1H), 3.39 (s, 3H), 3.51-3.65 (m, 3H), 3.74 (dd, *J* = 8.3, 2.2 Hz, 1H), 3.93 (sext, *J* = 6.1 Hz, 1H), 4.20 (dd, *J* = 7.7, 5.5 Hz, 1H), 4.63 (dd, *J* = 115.4, 11.6 Hz, 2H), 4.84-4.87 (m, 2H), 5.40-5.50 (m, 1H), 7.25-7.42 (m, 11H), 7.65-7.68 (m, 4H). **^{13}C NMR** ($CDCl_3$, 100 MHz) δ (ppm): 19.3, 23.2, 27.2, 27.4, 29.6, 33.1, 35.5, 38.9, 42.3, 46.0, 58.0, 60.8, 62.0, 68.8, 73.7, 77.4, 79.0, 80.6, 116.1, 127.5, 127.6, 127.6, 128.0, 128.4, 129.6, 129.6, 134.6, 134.9, 136.0, 137.9, 138.7, 178.7. **HRMS**: $C_{42}H_{60}O_6NaSi$, Calculated $[M+Na]^+$: 711.4057, Found $[M+Na]^+$: 711.4055. $[\alpha]_D^{20}$ = -9.7 (c = 0.2, $CHCl_3$).

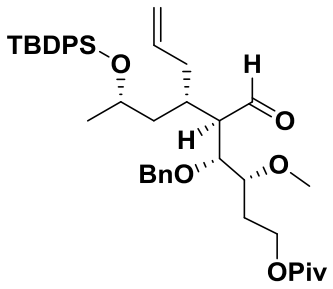

1.76

(3*R*,4*R*,5*R*,6*S*)-4-(benzyloxy)-6-((*S*)-2-((tert-butyldiphenylsilyl)oxy)propyl)-5-formyl-3-methoxynon-8-en-1-yl pivalate (1.76). Alcohol **1.75** (324 mg, 0.470 mmol) was suspended in dichloromethane/dimethylsulfoxide (4:1 v/v, 23.5 mL) and cooled to 0 °C. Triethylamine (0.660 mL, 4.70 mmol) was added followed by addition of sulfur trioxide pyridine complex (300 mg, 1.88 mmol). The resulting solution was allowed to warm to room temperature and stirred for 6 h. Additional portions of triethylamine (0.660 mL, 4.70 mmol) and sulfur trioxide pyridine complex (300 mg, 1.88 mmol) were added. The reaction was stirred for 10 h and then quenched by addition of water, extracted with dichloromethane, dried over sodium sulfate, and condensed *in vacuo* to give a pale yellow oil. This oil was purified by flash chromatography (0-15% ethyl acetate in hexanes) to provide aldehyde **1.76** as a clear, colorless oil (220 mg, 68%).

^{1}H NMR ($CDCl_3$, 400 MHz) δ (ppm): 0.99 (s, 9H), 1.01 (d, *J* = 6.4 Hz, 3H), 1.18 (s, 9H), 1.50 (ddd, *J* = 14.4, 7.6, 5.6 Hz, 1H), 1.68-1.78 (m, 2H), 1.80-1.85 (m, 1H), 2.26 (dm, *J* = 14.0 Hz, 1H), 2.34-2.41 (m, 1H), 2.71 (dt, *J* = 9.8, 2.8 Hz, 1H), 3.19-3.23 (m, 1H), 3.36 (s, 3H), 3.99 (sext, *J* = 6.0 Hz, 1H), 4.11-4.20 (m, 3H), 4.66 (dd, *J* = 123.6, 11.6 Hz, 2H), 4.90-4.97 (m, 2H), 5.53 (ddt, *J* = 23.0, 9.8, 7.2 Hz, 1H), 7.27-7.41 (m, 6H), 7.64-7.67 (m, 4H), 9.62 (d, *J* = 2.4 Hz, 1H). **^{13}C NMR** ($CDCl_3$, 100 MHz) δ (ppm): 19.3, 23.4, 27.2, 27.4, 29.4, 32.9, 35.6, 38.9, 41.4, 56.0, 58.0, 61.5, 68.1, 74.0, 75.5, 81.3, 117.1, 127.6, 127.7, 128.0, 128.5, 129.6, 129.8, 134.3, 134.9, 136.1, 136.1, 137.0, 138.4, 178.6, 202.9. **HRMS**: $C_{42}H_{58}O_6NaSi$, Calculated $[M+Na]^+$: 709.3900, Found $[M+Na]^+$: 709.3896. $[\alpha]_D^{20}$ = +3.7 (c = 0.4, $CHCl_3$).

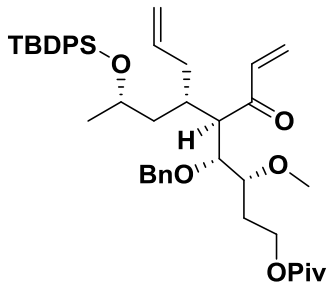

1.77

(3*R*,4*R*,5*R*,6*S*)-5-acryloyl-4-(benzyloxy)-6-((*S*)-2-((*tert*-butyldiphenylsilyl)oxy)propyl)-3-methoxynon-8-en-1-yl pivalate (1.77). Aldehyde **1.76** (200 mg, 0.291 mmol) was suspended in anhydrous tetrahydrofuran (29.0 mL). The solution was cooled to -78 °C and vinylmagnesium bromide (1.0 M in tetrahydrofuran, 0.582 mmol, 0.580 mL) was added dropwise. The resulting mixture was stirred at -78 °C for 1 h until TLC indicated the reaction had reached completion. Saturated aqueous ammonium chloride was added, and the mixture was extracted with ethyl acetate, dried over sodium sulfate, condensed *in vacuo*, and purified by flash chromatography (0-25% ethyl acetate in hexanes) to provide the allylic alcohol as a clear, colorless oil. The resultant alcohol (230 mg, 0.322 mmol) was suspended in anhydrous dichloromethane (32.0 mL). Dess–Martin Periodinane (205 mg, 0.483 mmol) was added and the cloudy white reaction was stirred for 45 minutes at room temperature. It was then quenched with saturated aqueous sodium bicarbonate, extracted with dichloromethane, dried over sodium sulfate, and concentrated *in vacuo*. The oil was purified by flash chromatography (0-20% ethyl acetate in hexanes) to provide enone **1.77** as a clear, colorless oil (208 mg, 68% over 2 steps).

^{1}H NMR ($CDCl_3$, 400 MHz) δ (ppm): 0.95 (d, *J* = 6.2 Hz, 3H), 0.98 (s, 9H), 1.15 (s, 9H), 1.17-1.21 (m, 1H), 1.43 (dt, *J* = 13.7, 6.5 Hz, 1H), 1.62 (quin, *J* = 7.0 Hz, 2H), 1.69-1.78 (m, 1H), 1.80-1.89 (m, 1H), 2.01-2.05 (m, 1H), 2.29 (quin, *J* = 6.9 Hz, 1H), 3.04 (d, *J* = 10.0 Hz, 1H), 3.09 (dd, *J* = 10.6, 2.8 Hz, 1H), 3.35 (s, 3H), 3.85 (sext, *J* = 6.2 Hz, 1H), 4.10-4.18 (m, 2H), 4.23 (d, *J* = 10.5 Hz, 1H), 4.64 (dd, *J* = 169.3, 11.4 Hz, 2H), 4.88-4.97 (m, 2H), 5.56 (dddd, *J* = 17.2, 10.2, 7.2, 7.2 Hz, 1H), 5.67 (dd, *J* = 10.3, 1.1 Hz, 1H), 6.08 (dd, *J* = 17.6, 1.0 Hz, 1H), 6.22 (dd, *J* = 17.6, 10.3 Hz, 1H), 7.24-7.41 (m, 11H), 7.61-7.67 (m, 4H). **^{13}C NMR** ($CDCl_3$, 100 MHz) δ (ppm): 19.3, 23.4, 27.2, 27.4, 29.3, 34.7, 36.1, 38.9, 41.3, 51.4, 57.9, 61.5, 68.0, 73.9, 81.0, 117.0, 127.6, 127.7, 127.9, 128.4, 128.7, 129.6, 129.7, 134.4, 134.8, 136.1, 137.4, 137.8, 138.7, 178.6, 201.4. **HRMS**: $C_{44}H_{60}O_6NaSi$, Calculated $[M+Na]^+$: 735.4057, Found $[M+Na]^+$: 735.4046. $[\alpha]_D^{20}$ = +17.5 (c = 1.0, $CHCl_3$).

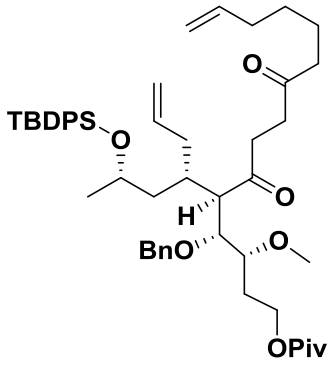

1.53

(3*R*,4*R*,5*R*)-4-(benzyloxy)-5-((4*S*,6*S*)-6-((*tert*-butyldiphenylsilyl)oxy)hept-1-en-4-yl)-3-methoxy-6,9-dioxopentadec-14-en-1-yl pivalate (1.53). Enone **1.77** (50.0 mg, 0.070 mmol) was suspended in 1,4-dioxane (1.4 mL) in a microwave vial. 3-Benzyl-5-(2-hydroxyethyl)-4-methylthiazolium chloride (18.9 mg, 0.070 mmol) was added followed by triethylamine (14.7 mg, 0.105 mmol) at room temperature. 6-hepten-1-al (**1.78**, 31.5 mg, 0.281 mmol) in 1,4 dioxane (0.2 mL) was added and the vial was capped and heated to 70 °C for 12 h. The reaction was quenched by addition of water and extracted with dichloromethane. The extract was dried over sodium sulfate, condensed *in vacuo*, and purified by flash chromatography (0-15% ethyl acetate in hexanes) to give 1,4-dione **1.53** (37.0 mg, 64 %).

^{1}H NMR ($CDCl_3$, 400 MHz) δ (ppm): 0.99 (s, 12H), 1.18 (s, 9H), 1.33-1.42 (m, 2H), 1.52-1.68 (m, 8H), 1.73-1.89 (m, 2H), 2.02-2.09 (m, 2H), 2.17-2.24 (m, 1H), 2.44 (t, *J* = 7.3 Hz, 2H), 2.49-2.57 (m, 2H), 2.59-2.70 (m, 1H), 2.89 (dd, *J* = 10.4, 3.0 Hz, 1H), 3.09 (d, *J* = 8.9 Hz, 1H), 3.32 (s, 3H), 3.92 (sext, *J* = 6.2 Hz, 1H), 4.05-4.09 (m, 1H), 4.18 (dd, *J* = 7.8, 5.5 Hz, 2H), 4.60 (dd, *J* = 158.0, 11.4 Hz, 2H), 4.87-5.03 (m, 4H), 5.52 (dddd, *J* = 17.0, 10.1, 7.0, 6.9 Hz, 1H), 5.78 (dddd, *J* = 17.4, 10.4, 7.0 6.6 Hz, 1H), 7.23-7.40 (m, 11H), 7.62-7.67 (m, 4H). **^{13}C NMR** ($CDCl_3$, 100 MHz) δ (ppm): 19.3, 23.3, 23.5, 27.2, 27.4, 28.6, 29.5, 33.7, 34.2, 35.6, 36.0, 38.9, 39.1, 41.3, 42.8, 54.2, 57.8, 62.0, 68.1, 73.7, 81.0, 114.8, 116.9, 127.6, 127.6, 127.7, 127.9, 128.4, 129.6, 129.7, 129.7, 134.6, 134.8, 136.1, 137.6, 138.7, 138.7, 178.6, 208.8, 210.3. **HRMS**: $C_{51}H_{72}O_7NaSi$, Calculated $[M+Na]^+$: 847.4945, Found $[M+Na]^+$: 847.4926. $[\alpha]_D^{20}$ = +3.2 (c = 1.0, $CHCl_3$).

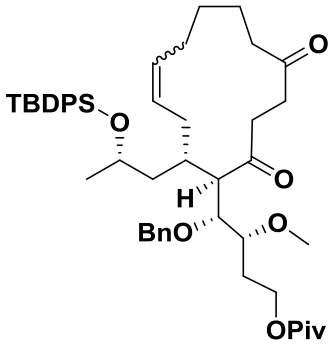

1.79

(3*R*,4*R*)-4-(benzyloxy)-4-((1*R*,2*S*)-2-((*S*)-2-((*tert*-butyldiphenylsilyl)oxy)propyl)-10,13-dioxocyclotridec-4-en-1-yl)-3-methoxybutyl pivalate (1.79). 1,4-dione **1.53** (85.0 mg, 0.103 mmol) was suspended in anhydrous dichloromethane (206 mL) with a reflux condenser attached. Grubb's first generation catalyst (25.4 mg, 0.031 mmol) was added and the resulting solution was stirred at 40 °C for 9 h. The reaction was cooled to room temperature and the dichloromethane was removed *in vacuo*. The dark brown residue was purified by flash chromatography (0-15% ethyl acetate in hexanes) to give a 1:1 mixture of the *cis*:*trans* macrocyclic alkene that were combined for the next reaction (69 mg, 84%).

^{1}H NMR ($CDCl_3$, 400 MHz) δ (ppm): 1.02 (s, 4.5 H), 1.03 (s, 4.5H), 1.04 (d, *J* = 6.2 Hz, 1.5 H), 1.06 (d, *J* = 6.2 Hz, 1.5H), 1.18 (s, 4.5H), 1.19 (s, 4.5H), 1.42-1.53 (m, 4H), 1.62- 1.83 (m, 6H), 1.84-1.93 (m, 2H), 1.97-2.04 (m, 2H), 2.10-2.14 (m, 1H), 2.15-2.23 (m, 1H), 2.27-2.32 (m, 0.5H), 2.40-2.56 (m, 2H), 2.60-2.70 (m, 1H), 2.71-2.79 (m, 1H), 2.81-2.86 (m, 1H), 2.99 (ddd, *J* = 15.4, 10.0, 3.1 Hz, 0.5H), 3.13 (d, *J* = 10.0 Hz, 0.5H), 3.16-3.19 (m, 0.5H), 3.31 (s, 1.5H), 3.39 (s, 1.5H), 3.78-3.83 (m, 1H), 3.89-3.92 (m, 1H), 4.10-4.13 (m, 1.5H), 4.16-4.22 (m, 1H), 4.57 (dd, *J* = 276.2, 11.3 Hz, 1H), 4.59 (dd, *J* = 50.6, 11.9 Hz, 1H), 4.92-4.96 (m, 0.5H), 5.14-5.19 (m, 0.5H), 5.23-5.31 (m, 1H), 7.26-7.42 (m, 11H), 7.61-7.69 (m, 4H). **^{13}C NMR** ($CDCl_3$, 100 MHz) δ (ppm): 19.3, 19.3, 22.5, 22.6, 22.8, 22.9, 25.1, 26.9, 27.1, 27.2, 27.3, 27.4, 27.9, 29.7, 29.9, 30.0, 30.3, 33.0, 34.6, 35.6, 35.8, 36.3, 38.7, 38.9, 40.3, 40.6, 41.2, 41.4, 51.8, 55.8, 58.0, 58.1, 61.5, 61.9, 68.2, 68.4, 73.4, 78.1, 78.3, 79.8, 80.7, 126.4, 127.6, 127.7, 127.7, 127.7, 127.7, 128.0, 128.0, 128.2, 128.4, 128.6, 128.7, 129.6, 129.7, 129.7, 131.9, 133.1, 134.6, 134.7, 136.0, 136.0, 136.0, 138.0, 138.6, 178.6, 210.1, 210.1, 211.5, 211.8. **HRMS**: $C_{49}H_{68}O_7NaSi$, Calculated $[M+Na]^+$: 819.4632, Found $[M+Na]^+$: 819.4630.

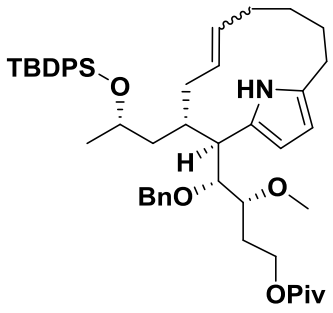

1.80

(3*R*,4*R*)-4-(benzyloxy)-4-((2*S*,3*S*)-3-((*S*)-2-((*tert*-butyldiphenylsilyl)oxy)propyl)-14-azabicyclo[9.2.1]tetradeca-1(13),5,11-trien-2-yl)-3-methoxybutyl pivalate (1.80). Macrocyclic 1,4-dione **1.79** (45.0 mg, 0.057 mmol) was suspended in anhydrous methanol (5.60 mL) in a microwave vial. Ammonium acetate (131 mg, 1.69 mmol) was added and the vial was capped and heated in the microwave at 120 °C for 20 min. The solution was cooled to room temperature, quenched with water, diluted with dichloromethane, and then extracted with dichloromethane. The extract was dried over sodium sulfate, condensed *in vacuo*, and purified by flash chromatography (0-15% ethyl acetate in hexanes) to give the pyrrolophane **1.80** (40.0 mg, 91 %).

^{1}H NMR ($CDCl_3$, 400 MHz) δ (ppm): 0.88-0.90 (m, 1H), 0.97 (d, *J* = 6.6 Hz, 1H), 1.03 (s, 9H), 1.04-1.07 (m, 4H), 1.09 (s, 9H), 1.20-1.33 (m, 4H), 1.50-1.65 (m, 5H), 1.71-1.89 (m, 2H), 2.47-2.58 (m, 2H), 2.72 (bs, 1H), 3.16-3.24 (m, 1H), 3.27 (s, 3H), 3.78-3.87 (m, 1H), 3.90 (dd, *J* = 1.6, 9.8 Hz, 1H), 4.05-4.12 (m, 2H), 4.61 (d, *J* = 11.5 Hz, 1H), 4.90 (d, *J* = 11.5 Hz, 1H), 5.08 (bs, 1H), 5.18 (m, 1H), 5.63-5.80 (m, 2H), 7.27-7.41 (m, 11H), 7.65 (d, *J* = 6.5 Hz, 4H). **^{1}H NMR** ($CDCl_3$, 400 MHz) δ (ppm): 0.82-0.91 (m, 1H), 1.00 (s, 9H), 1.04 (d, *J* = 6.0 Hz, 3H), 1.06-1.10 (m, 1H), 1.13 (s, 9H), 1.17 (d, *J* = 9.3 Hz, 1H), 1.25 (s, 2H), 1.26-1.37 (m, 2H), 1.40-1.49 (m, 1H), 1.54 (s, 9H), 1.55-1.61 (m, 1H), 1.62-1.72 (m, 2H), 1.75-1.92 (m, 4H), 2.05 (dd, *J* = 5.6, 9.4 Hz, 1H), 2.28-2.37 (m, 1H), 2.42 (dt, *J* = 3.0, 13.6 Hz, 1H), 2.53 (m, 1H), 2.58 (dd, *J* = 4.7, 9.8 Hz, 1H), 3.19-3.24 (m, 1H), 3.28 (s, 3H), 3.87 (sext, *J* = 6.9 Hz, 1H), 3.94 (dd, *J* = , 9.7 Hz, 1H), 4.07-4.18 (m, 2H), 4.56 (d, *J* = 11.5 Hz, 1H), 4.69-4.79 (m, 1H), 4.93 (d, *J* = 11.5 Hz, 1H), 5.14-5.26 (m, 1H), 5.53-5.66 (m, 2H), 7.27-7.42 (m, 11H), 7.65 (d, J = 7.3 Hz, 4H), 7.71 (bs, 1H). **^{13}C NMR** ($CDCl_3$, 150 MHz) δ (ppm): 13.7, 14.1, 17.3, 17.3, 17.4, 19.1, 19.1, 20.4, 21.0, 21.2, 22.7, 27.0, 27.2, 27.7, 29.3, 29.7, 30.6, 31.9, 56.0, 60.4, 64.4, 71.8, 96.1, 97.6, 99.8, 127.5, 128.8, 130.9, 132.4, 135.9, 167.9, 170.9, 171.3. **HRMS**: $C_{49}H_{68}NO_5Si$, Calculated $[M+H]^+$: 778.4867, Found $[M+H]^+$: 778.4865. $[\alpha]_D^{20}$ = -5.4 (c = 0.3, $CHCl_3$).

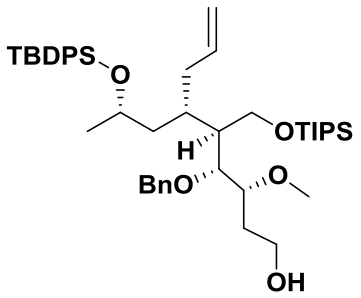

1.87

(3*R*,4*R*,5*S*,6*S*)-4-(benzyloxy)-6-((*S*)-2-((*tert*-butyldiphenylsilyl)oxy)propyl)-3-methoxy-5-(((triisopropylsilyl)oxy)methyl)non-8-en-1-ol (1.87). Pivalate ester **1.54** (240 mg, 0.284 mmol) was suspended in anhydrous dichloromethane (28.0 mL) and cooled to -78 °C. Diisobutylaluminum hydride (1.0 M in dichloromethane, 0.850 mL, 0.852 mmol) was added dropwise, and the resulting solution was stirred for 1 h until TLC indicated the reaction was complete. The reaction was quenched by addition of saturated aqueous sodium potassium tartrate, warmed to room temperature, and stirred until the organic layer became clear. The mixture was extracted with dichloromethane, dried over sodium sulfate, and condensed *in vacuo* to give a clear oil. This oil was purified by flash chromatography (0-35% ethyl acetate in hexanes) to provide the desired free primary alcohol **1.87** as a clear, colorless oil (200 mg, 93%).

^{1}H NMR ($CDCl_3$, 400 MHz) δ (ppm): 1.00 (s, 9H), 1.02 (d, *J* = 6.1 Hz, 3H), 1.05 (s, 21H), 1.43 (quin, *J* = 6.8 Hz, 1H), 1.57-1.63 (m, 1H), 1.65-1.74 (m, 2H), 1.75-1.81 (m, 1H), 1.98-2.07 (m, 1H), 2.10-2.16 (m, 2H), 2.87 (d, *J* = 6.3 Hz, 1H), 3.41 (s, 3H), 3.58 (dd, *J* = 10.5, 6.2 Hz, 1H), 3.66 (dd, *J* = 10.7, 3.6 Hz, 1H), 3.71-3.82 (m, 4H), 3.91 (sext, *J* = 6.1 Hz, 1H), 4.69 (dd, *J* = 156.8, 11.4 Hz, 2H), 4.81-4.85 (m, 2H), 5.42-5.52 (m, 1H) 7.23-7.41 (m, 11H), 7.65-7.68 (m, 4H). **^{13}C NMR** ($CDCl_3$, 100 MHz) δ (ppm): 12.1, 18.2, 19.3, 23.5, 27.1, 31.3, 33.0, 35.6, 42.9, 46.5, 57.0, 61.4, 62.1, 68.6, 74.2, 78.2, 85.0, 115.6, 127.5, 127.5, 127.6, 128.0, 128.3, 129.5, 129.6, 134.6, 135.1, 136.0, 138.6, 138.9. **HRMS**: $C_{46}H_{73}O_5Si_2$, Calculated $[M+H]^+$: 761.4997, Found $[M+]^+$: 761.4995. $[\alpha]_D^{20}$ = -8.2 (c = 1.0, $CHCl_3$).

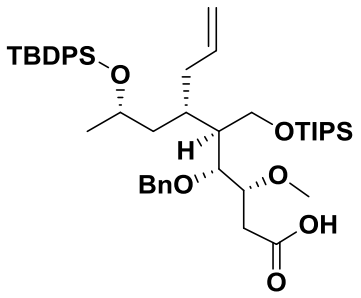

1.88

(3*R*,4*R*,5*S*,6*S*)-4-(benzyloxy)-6-((*S*)-2-((tert-butyldiphenylsilyl)oxy)propyl)-3-methoxy-5-(((triisopropylsilyl)oxy)methyl)non-8-enoic acid (1.88). Alcohol **1.87** (200 mg, 0.263 mmol) was suspended in dichloromethane/dimethylsulfoxide (4:1 v/v, 13.0 mL) and cooled to 0 °C. Triethylamine (0.370 mL, 2.63 mmol) was added followed by addition of sulfur trioxide pyridine complex (167 mg, 1.05 mmol). The resulting solution was stirred for 4 h at 0 °C, quenched by addition of water, extracted with dichloromethane, dried over sodium sulfate, and condensed *in vacuo* to give a pale yellow oil. This oil was purified by flash chromatography (0-20% ethyl acetate in hexanes) to provide the aldehyde as a clear, colorless oil (185 mg, 93%). To a stirring solution of this aldehyde (182 mg, 0.240 mmol) in *tert*-butanol (9.00 mL) was added 2-methyl-2-butene (0.260 mL, 2.40 mmol). In a separate vial, monobasic sodium phosphate (252 mg, 1.82 mmol) was dissolved in water (9.00 mL) and sodium chlorite (163 mg, 1.80 mmol) was added. The *tert*-butanol solution was cooled to 0 °C and the chlorite/phosphate solution in water was added dropwise. The resulting yellow solution was stirred at 0 °C for 30 min and was then quenched with saturated aqueous sodium thiosulfate and acidified to pH 3. The aqueous solution was then extracted with ethyl acetate, dried over sodium sulfate, and concentrated *in vacuo* to give a clear oil. This oil was purified by flash chromatography (0-50% ethyl acetate in hexanes) yielding carboxylic acid **1.88** as a clear, colorless oil (180 mg, 97%).

^{1}H NMR ($CDCl_3$, 400 MHz) δ (ppm): 1.00 (s, 9H), 1.02 (d, *J* = 6.3 Hz, 3H), 1.04-1.06 (m, 21H), 1.43 (quin, *J* = 6.7 Hz, 1H), 1.59-1.73 (m, 3H), 2.05-2.14 (m, 2H), 2.59 (dd, *J* = 16.5, 3.0 Hz, 1H), 2.73 (dd, *J* = 16.3, 8.7 Hz, 1H), 3.60 (s, 3H), 3.57 (dd, *J* = 10.4, 6.4 Hz, 1H), 3.67 (dd, *J* = 10.9, 3.9 Hz, 1H), 3.83 (dd, *J* = 9.0, 1.8 Hz, 1H), 3.90 (sext, *J* = 6.1 Hz, 1H), 4.05 (dt, *J* = 8.2, 2.2 Hz, 1H), 4.68 (dd, *J* = 141.9, 11.4 Hz, 2H), 4.81-4.85 (m, 2H), 5.41-5.51 (m, 1H) 7.23-7.41 (m, 11H), 7.64-7.67 (m, 4H). **^{13}C NMR** ($CDCl_3$, 100 MHz) δ (ppm): 12.02, 18.22, 19.27, 23.42, 27.11, 32.94, 35.08, 35.55, 42.86, 46.51, 57.47, 61.78, 68.56, 74.49, 77.35, 78.42, 80.90, 115.73, 127.50,

127.54, 127.63, 127.99, 128.34, 129.49, 129.61, 134.55, 135.08, 135.99, 136.01, 138.43, 138.67, 176.17.

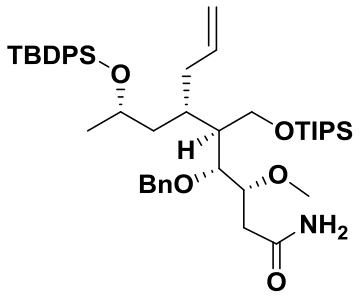

1.89

(3*R*,4*R*,5*S*,6*S*)-4-(benzyloxy)-6-((*S*)-2-((*tert*-butyldiphenylsilyl)oxy)propyl)-3-methoxy-5-(((triisopropylsilyl)oxy)methyl)non-8-enamide (1.89). Acid **1.88** (225 mg, 0.290 mmol) was suspended in dimethylformamide (1.50 mL). 1-Ethyl-3-(3-dimethylaminopropyl)carbodiimide hydrochloride (83.4 mg, 0.440 mmol) and 1-hydroxybenzotriazole (58.8 mg, 0.440 mmol) were added subsequently at room temperature, followed by addition of diisopropylethylamine (0.200 mL, 1.16 mmol) and ammonium chloride (31.0 mg, 0.580 mmol). The resulting solution was stirred for 6 h at room temperature until TLC indicated complete conversion. The reaction was quenched by addition of water, extracted with dichloromethane, dried over sodium sulfate, and condensed *in vacuo* to give a pale yellow residue. This residue was purified by flash chromatography (0-50% ethyl acetate in hexanes then 75% ethyl acetate in hexanes) to give amide **1.89** as a clear colorless oil (180 mg, 80%).

^{1}H NMR ($CDCl_3$, 400 MHz) δ (ppm): 1.00 (s, 9H), 1.02 (d, *J* = 6.1 Hz, 3H), 1.04-1.07 (m, 21H), 1.44 (quin, *J* = 6.8 Hz, 1H), 1.63-1.73 (m, 3H), 2.01-2.08 (m, 1H), 2.16-2.22 (m, 1H), 2.43 (dd, *J* = 15.8, 3.0 Hz, 1H), 2.53 (dd, *J* = 15.8, 8.4 Hz, 1H), 3.41 (s, 3H), 3.62-3.71 (m, 2H), 3.86-3.95 (m, 3H), 4.67 (dd, *J* = 124.8, 11.5 Hz, 2H), 4.79-4.84 (m, 2H), 5.16 (bs, 1H), 5.42-5.52 (m, 1H), 5.98 (bs, 1H), 7.23-7.41 (m, 11H), 7.64-7.66 (d, *J* = 7.6 Hz, 4H). **^{13}C NMR** ($CDCl_3$, 100 MHz) δ (ppm): 12.0, 18.9, 19.3, 23.5, 27.1, 33.1, 35.8, 36.4, 43.1, 46.1, 57.2, 61.7, 68.6, 74.3, 78.2, 81.0, 115.6, 127.5, 127.5, 127.6, 127.8, 128.4, 129.5, 129.6, 134.7, 135.0, 136.0, 138.6, 138.9, 174.1. **HRMS**: $C_{46}H_{72}NO_5Si_2$, Calculated $[M+H]^+$: 774.4949, Found $[M+H]^+$: 774.4951. $[\alpha]_D^{20}$ = -15.4 (c = 1.2, $CHCl_3$).

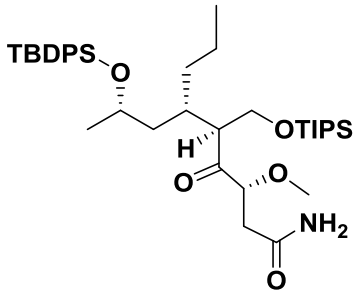

1.90

(3*R*,5*S*,6*S*,8*S*)-8-((*tert*-butyldiphenylsilyl)oxy)-3-methoxy-4-oxo-6-propyl-5-(((triisopropylsilyl)oxy)methyl)nonanamide (1.90). Amide **1.89** (180 mg, 0.232 mmol) was suspended in anhydrous ethyl acetate (23.0 mL). 10% palladium on activated carbon (62.0 mg, 0.058 mmol) was added and the flask was sealed and evacuated then back-filled with argon (3 x). The flask was then evacuated and refilled with hydrogen (3x) from a balloon. The reaction was stirred for 8 h at room temperature until the reaction was complete by TLC. The mixture was filtered through celite and washed liberally with ethyl acetate. The filtrate was condensed *in vacuo* to give the secondary alcohol as a clear, colorless oil that was carried on to the next step without further purification (158 mg, 99%). The resultant alcohol (152 mg, 0.222 mmol) was suspended in anhydrous dichloromethane (22.0 mL) with 4 Å molecular sieves (100 mg). The reaction was cooled to 0 °C and 4-methylmorpholine *N*-oxide (52.0 mg, 0.443 mmol) was added followed by tetrapropylammonium perruthenate (15.6 mg, 0.044 mmol). The reaction was warmed to room temperature and stirred for 2 h. Upon complete conversion as indicated by TLC, the mixture was filtered through celite and washed liberally with dichloromethane. The filtrate was condensed *in vacuo* to give a dark green residue that was purified by flash chromatography (0-75% ethyl acetate in hexanes) to give hydroxyketoamide **1.90** as a clear, colorless oil (129 mg, 85 %).

^{1}H NMR ($CDCl_3$, 400 MHz) δ (ppm): 0.67 (t, *J* = 6.8 Hz, 3H), 0.79-0.93 (m, 3H), 1.02 (s, 30H), 1.09 (d, *J* = 6.1 Hz, 3H), 1.25 (ddd, *J* = 13.7, 8.1, 4.1 Hz, 2H), 1.41 (ddd, *J* = 13.7, 8.9, 4.6 Hz, 1H), 1.65-1.73 (m, 1H), 2.37 (dd, *J* = 14.8, 8.1 Hz, 1H), 2.59 (dd, *J* = 15.3, 4.1 Hz, 1H), 3.00 (ddd, *J* = 8.7, 6.8, 4.8 Hz, 1H), 3.38 (s, 3H), 3.70 (dd, *J* = 9.5, 4.7 Hz, 1H), 3.78-3.83 (m, 2H), 4.17 (dd, *J* = 8.1, 4.0 Hz, 1H), 5.27 (bs, 1H), 5.86 (bs, 1H), 7.34-7.43 (m, 6H), 7.65-7.68 (m, 4H). **^{13}C NMR** ($CDCl_3$, 100 MHz) δ (ppm): 12.0, 14.5, 18.1, 18.8, 19.3, 22.8, 27.1, 32.3, 34.0, 37.0, 42.3, 53.1, 58.3, 63.6, 68.2, 83.9, 127.7, 127.7, 129.7, 134.7, 136.0, 136.0, 172.0, 212.4. **HRMS**:

$C_{39}H_{66}NO_5Si_2$, Calculated $[M+H]^+$: 684.4480, Found $[M+H]^+$: 684.4485. $[\alpha]_D^{20}$ = -17.4 (c = 0.5, $CHCl_3$).

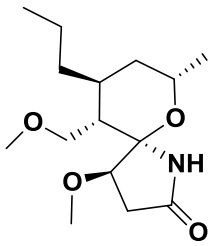

1.91

(4*R*,5*R*,7*S*,9*S*,10*S*)-4-methoxy-10-(methoxymethyl)-7-methyl-9-propyl-6-oxa-1-azaspiro[4.5]decan-2-one (1.91). Hydroxyketoamide **1.90** (68.0 mg, 0.099 mmol) was suspended in anhydrous methanol (30.0 mL). Concentrated hydrochloric acid (0.026 mL, 0.300 mmol) was added at room temperature and the reaction was allowed to stir for 10 h. After this time the reaction was quenched by dropwise addition of saturated aqueous sodium bicarbonate and extracted with ethyl acetate. The organic layers were combined, dried over sodium sulfate, and condensed *in vacuo* to give a clear, colorless residue. The crude residue was purified by flash chromatography (0-85% ethyl acetate in hexanes) to yield the desired marineosin A model stereoisomer **1.91** as a clear, colorless oil (22.0 mg, 82%).

^{1}H NMR ($CDCl_3$, 400 MHz) δ (ppm): 0.89-0.94 (m, 5H), 1.14-1.16 (m, 3H), 1.20 (d, *J* = 6.6 Hz, 3H), 1.93-1.96 (m, 1H), 2.34-2.37 (m, 1H) 2.52 (m, 2H) 3.22 (dd, *J* = 10.4, 4.4 Hz, 1H), 3.28-3.31 (m, 1H), 3.31 (s, 3H), 3.44 (s, 3H), 3.74-3.79 (m, 1H), 4.15 (dd, *J* = 9.6, 8.0 Hz, 1H), 6.23 (bs, 1H). **^{13}C NMR** ($CDCl_3$, 150 MHz) δ (ppm): 14.0, 22.2, 26.0, 30.6, 35.2, 40.6, 55.9, 58.2, 62.0, 65.4, 70.4, 72.7, 79.2, 90.3, 175.3.

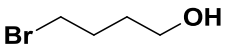

1.92

4-bromobutan-1-ol (1.92). To neat, refluxing tetrahydrofuran (67.5 mL, 832 mmol) was added 48% aqueous hydrobromic acid (31.0 mL, 274 mmol) dropwise. The reaction mixture was held at reflux for 2 hours. After cooling to room temperature, the reaction was neutralized with saturated aqueous sodium bicarbonate, extracted with diethyl ether, dried over sodium sulfate, and concentrated to provide 31.4 g (75%) of alcohol **1.92**. Spectral data matches that of commercial-

grade material.

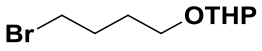

1.94

2-(4-bromobutoxy)tetrahydro-2*H*-pyran (1.94). To a stirred solution of alcohol **1.92** (1.95 g, 12.7 mmol) in diethyl ether (12.0 mL) at 0 °C was added *p*-TsOH (5.00 mg, 0.02 mmol) followed by dropwise addition of 3,4-dihydro-2*H*-pyran **1.93** (1.50 mL, 16.6 mmol). The reaction mixture was allowed to warm to room temperature. After 1 h, the reaction mixture was washed with saturated aqueous sodium bicarbonate and brine. The organic layer was dried over potassium carbonate, filtered, and concentrated to provide 2.70 g (90%) of pyran **1.94**. Spectral data matches that recorded by Grieco, *et al*.[32]

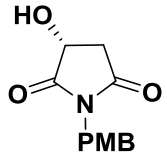

1.97

(*R*)-3-hydroxy-1-(4-methoxybenzyl)pyrrolidine-2,5-dione (1.97). To a solution of (*R*)-2-hydroxysuccinic acid **1.96** (3.20 g, 24.0 mmol) in 50% aqueous methanol (5 mL) was slowly added *para*-methoxybenzyl amine (3.14 mL, 24.0 mmol). Methanol was removed under reduced pressure and the reaction mixture was partitioned with *m*-xylene (64 mL) and heated to 190 °C. Water was azeotropically removed with a Dean-Stark trap. After 24 hours, the solvent was removed under reduced pressure and the residue was partitioned with ethanol (25 mL) and concentrated. Recrystallization from benzene provided 4.40 g (78%) of maleimide **1.97**.

^{1}H NMR ($CDCl_3$, 400 MHz) δ (ppm): 2.66 (dd, *J* = 4.8, 18.2 Hz, 1H), 2.93 (bs, 1H), 3.05 (dd, *J* = 8.5, 18.2 Hz, 1H), 3.78 (s, 3H), 4.56-4.65 (m, 3H), 6.83 (d, *J* = 8.7 Hz, 2H), 7.32 (d, *J* = 8.7 Hz, 2H). **^{13}C NMR** ($CDCl_3$, 100 MHz) δ (ppm): 37.1, 41.8, 55.2, 66.8, 113.9, 127.4, 130.3, 159.3, 174.0, 178.3. **HRMS**: $C_{12}H_{13}NO_4Na$, Calculated $[M+Na]^+$: 258.0742, Found $[M+Na]^+$: 258.0741. $[\alpha]_D^{20}$ = +43.1 (c = 1.0, CH_3OH).

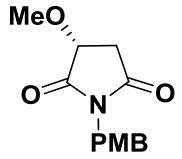

1.98

(*R*)-3-methoxy-1-(4-methoxybenzyl)pyrrolidine-2,5-dione (1.98). To a solution of maleimide **1.97** (4.15 g, 20.3 mmol) in acetonitrile (40 mL) at room temperature was added silver(I) oxide (4.69 g, 20.3 mmol) and iodomethane (3.60 mL, 57.9 mmol). The reaction mixture was refluxed for 1 h. After cooling to room temperature, the reaction mixture was filtered, concentrated, and purified by column chromatography (0-20% ethyl acetate in hexanes) to provide 3.92 g (78%) of ether **1.98**.

^{1}H NMR ($CDCl_3$, 400 MHz) δ (ppm): 2.60 (dd, *J* = 4.2, 18.2 Hz, 1H), 2.98 (dd, *J* = 8.2, 18.2 Hz, 1H), 3.60 (s, 3H), 3.78 (s, 3H), 4.18 (dd, *J* = 4.2, 8.2 Hz, 1H), 4.59 (d, *J* = 2.4 Hz, 2H), 6.83 (d, *J* = 8.7 Hz, 2H), 7.32 (d, *J* = 8.7 Hz, 2H). **^{13}C NMR** ($CDCl_3$, 100 MHz) δ (ppm): 35.5, 41.3, 54.9, 58.4, 74.5, 113.7, 127.5, 123.0, 159.0, 173.6, 175.1. **HRMS**: $C_{13}H_{15}NO_4Na$, Calculated $[M+Na]^+$: 272.0899, Found $[M+Na]^+$: 272.0900. $[\alpha]_D^{20}$ = +45.7 (c = 1.0, CH_3OH).

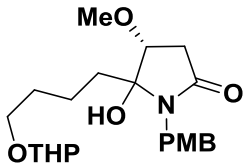

1.99

(4*R*)-5-hydroxy-4-methoxy-1-(4-methoxybenzyl)-5-(4-((tetrahydro-2*H*-pyran-2-yl)oxy)butyl)pyrrolidin-2-one (1.99). A flame-dried flask was charged with magnesium powder (447 mg, 18.4 mmol) and placed under an inert argon atmosphere. The magnesium was suspended in anhydrous tetrahydrofuran (21.0 mL) and pyran **1.94** (1.40 mL, 7.50 mmol) was added. After warming to 50 °C, additional pyran **1.94** (2.00 mL, 10.7 mmol) was added dropwise. The reaction mixture was heated periodically until it sustained reflux. A separate flame-dried flask was charged with ether **1.98** (1.50 g, 6.00 mmol) and THF (30.0 mL). After cooling to −20 °C, the solution of Grignard **1.95** was added dropwise via syringe. The reaction mixture was kept between −10 °C and −15 °C. After 2.5 h, water (5.00 mL) was added and the reaction was allowed to reach room temperature. The product was extracted with diethyl ether, washed with brine, dried over sodium

sulfate, and concentrated. The residue was purified on by column chromatography (0-30% ethyl acetate in hexanes) to provide 6.61 g (80%) of tertiary alcohol **1.99**.

^{1}H NMR ($CDCl_3$, 400 MHz) δ (ppm): 1.48-1.59 (m, 5H), 1.61-1.75 (m, 2H), 1.77-1.90 (m, 1H), 2.12-2.24 (m, 2H), 2.57 (d, *J* = 17.9 Hz, 1H), 2.71 (dddd, *J* = 1.9, 7.2, 17.8 Hz, 1H), 3.27 (s, 3H), 3.29-3.34 (m, 1H), 3.45-3.50 (m, 1H), 3.63-3.71 (m, 1H), 3.77 (s, 3H), 3.80-3.85 (m, 1H), 4.49-4.52 (m, 1H), 4.55- 4.66 (m, 3H), 4.85 (q, *J* = 6.8 Hz, 1H), 6.81 (d, *J* = 8.6 Hz, 2H), 7.13 (d, *J* = 8.6 Hz, 2H). **^{13}C NMR** ($CDCl_3$, 100 MHz) δ (ppm): 19.6, 19.8, 23.4, 23.5, 25.4 (2C), 30.1, 30.2, 30.7, 30.8, 36.0 (2C), 42.9 (2C), 55.1, 55.2, 62.3, 62.6, 66.5, 66.7, 72.0 (2C), 98.9, 99.0, 107.0, 107.1, 113.9 (2C), 127.9, 128.3, 128.4, 139.2, 139.3, 158.8 (2C), 173.0, 173.1. **HRMS**: $C_{22}H_{33}NO_6Na$, Calculated $[M+Na]^+$: 430.2206, Found $[M+Na]^+$: 430.2210. $[\alpha]_D^{20}$ = -15.0 (c = 0.6, $CHCl_3$).

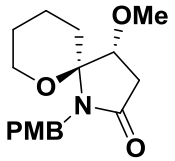

1.101

(4*R*,5*S*)-4-methoxy-1-(4-methoxybenzyl)-6-oxa-1-azaspiro[4.5]decan-2-one (1.101). To a stirred solution of tertiary alcohol **1.99** (390 mg, 1.00 mmol) in dichloromethane (6.00 mL) at 0 °C was added *p*-TsOH monohydrate (41.0 mg, 0.200 mmol). After 30 minutes, the solvent was removed and the residue was purified by flash chromatography (0-30% ethyl acetate in hexanes) to provide 244 mg (80%) of spiroaminal **1.101**.

^{1}H NMR ($CDCl_3$, 400 MHz) δ (ppm): 1.39-1.51 (m, 4H), 1.63-1.70 (m, 1H), 1.85-1.92 (m, 1H), 2.47 (d, *J* = 17.4 Hz, 1H), 2.65 (dd, *J* = 5.5, 17.4 Hz, 1H), 3.32 (s, 3H), 3.61 (m, 1H), 3.73 (s, 3H), 3.84 (dd, *J* = 2.4, 11.2 Hz, 1H), 3.95 (d, *J* = 5.5 Hz, 1H), 4.11 (d, *J* = 16.0 Hz, 1H), 4.70 (d, *J* = 16.0 Hz, 1H), 6.78 (d, *J* = 8.7 Hz, 2H), 7.14 (d, *J* = 8.7 Hz, 2H). **^{13}C NMR** ($CDCl_3$, 100 MHz) δ (ppm): 20.0, 24.6, 27.9, 34.3, 41.8, 55.0, 56.6, 64.7, 74.9, 94.9, 113.5, 127.9, 130.5, 158.2, 174.5. **HRMS**: $C_{17}H_{24}NO_4$, Calculated $[M+H]^+$: 306.1705, Found $[M+H]^+$: 306.1702. $[\alpha]_D^{20}$ = -50.6 (c = 1.0, $CHCl_3$).

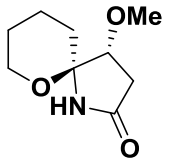

1.102

(4*R*,5S)-4-methoxy-6-oxa-1-azaspiro[4.5]decan-2-one (1.102). To a stirred solution of spiroaminal **1.101** (258 mg, 0.850 mmol) in acetonitrile (27.0 mL) and water (3.50 mL) was added ceric ammonium nitrate (1.40 g, 2.50 mmol). After 1.5 h, a second portion of CAN (467 mg, 0.800 mmol) was added. After 1 h, the acetonitrile was removed under reduced pressure and the product was extracted with dichloromethane. The combined organic layers were washed with brine, dried over sodium sulfate, and concentrated. The residue was purified by column chromatography (0-30% ethyl acetate in hexanes) to provide 105 mg (67%) of amide **1.102**.

^{1}H NMR ($CDCl_3$, 400 MHz) δ (ppm): 1.54-1.63 (m, 2H), 1.63-1.73 (m, 1H), 1.73-1.83 (m, 3H), 2.29 (dd, *J* = 1.7, 17.2 Hz, 1H), 2.70 (dd, *J* = 5.6, 17.2 Hz, 1H), 3.34 (s, 3H), 3.66-3.72 (m, 3H), 8.64 (bs, 1H). **^{13}C NMR** ($CDCl_3$, 100 MHz) δ (ppm): 19.4, 25.2, 29.3, 35.7, 57.3, 62.7, 82.4, 91.8, 177.3. **HRMS**: $C_9H_{16}NO_3$, Calculated $[M+H]^+$: 186.1130, Found $[M+H]^+$: 186.1131. $[\alpha]_D^{20}$ = -97.1 (c = 1.1, $CHCl_3$).

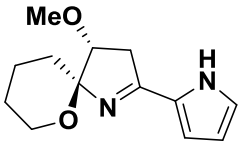

1.105

(4*R*,5*S*)-4-methoxy-2-(1*H*-pyrrol-2-yl)-6-oxa-1-azaspiro[4.5]dec-1-ene (1.105). A flame dried flask was charged with amide **1.102** (30.0 mg, 0.162 mmol) and placed under an inert argon atmosphere. After cooling to 0 °C, anhydrous dichloromethane (1.60 mL) and trifluoromethanesulfonic anhydride (27.0 μL, 0.162 mmol) were added. After 3 minutes, pyrrole (56.0 μL, 0.810 mmol) was added and at 10 minutes, the reaction was quenched with saturated aqueous sodium bicarbonate. The product was extracted with DCM, dried over sodium sulfate, and concentrated. The residue was purified by flash chromatography (0-70% ethyl acetate in hexanes) to provide 30.5 mg (80%) of pyrrole **1.105**.

^{1}H NMR ($CDCl_3$, 400 MHz) δ (ppm): 1.54-1.78 (m, 5H), 1.86-1.99 (m, 2H), 2.78 (dd, *J* = 5.3, 16.5 Hz, 1H), 3.21 (dd, *J* = 6.8, 16.5 Hz, 1H), 3.44 (s, 3H), 3.72 (d, *J* = 10.8 Hz, 1H), 3.84 (t, *J* =

6.2 Hz, 1H), 4.15 (dt, *J* = 2.8, 11.1 Hz, 1H), 6.21 (t, *J* = 3.2 Hz, 1H), 6.57 (d, *J* = 3.5 Hz, 1H), 6.90 (s, 1H). **^{13}C NMR** ($CDCl_3$, 100 MHz) δ (ppm): 19.6, 25.8, 29.2, 38.7, 58.2, 64.2, 85.3, 102.8, 110.7, 112.8, 121.1, 126.3, 164.6. **HRMS**: $C_{13}H_{19}N_2O_2$, Calculated $[M+H]^+$: 235.1447, Found $[M+H]^+$: 235.1447. $[\alpha]_D^{20}$ = -65.2 (c = 1.6, $CHCl_3$).

Chapter II

Synthesis and Optimization of a Selective Dopamine Receptor 4 Antagonist for Use as a PET Tracer and an *in vivo* Tool to Study Cocaine Addiction

2.1. Introduction

Dopamine receptors are involved in many important central nervous system (CNS) processes and are indicated in diseases such as schizophrenia, attention deficit hyperactivity disorder (ADHD), Parkinson's disease (PD), and substance addiction.[33] Since the discovery of five subtypes of the dopamine receptors, great effort has been made to synthesize highly selective ligands in order to study each receptor's involvement in disease. To this end, this chapter reports on the structure-activity relationship (SAR) of a novel, morpholine-based dopamine receptor 4 (D_4) antagonist. The goal of this project is to optimize this scaffold to be an *in vivo* probe as well as a positron emission tomography (PET) tracer to study the role of D_4 receptors in cocaine addiction.

2.1.1. Dopamine Receptors

Dopamine (DA, **Figure 2.1**) is an important catecholamine neurotransmitter in mammals and is the endogenous ligand of five distinct dopamine receptors.[33] The dopamine receptors are G-protein coupled receptors (GPCRs) that fall into two families based on their homology and function: the D_1-like family (D_1 and D_5) and the D_2-like family (D_2, D_3, and D_4) (**Figure 2.1**). D_1 and D_2 receptors are the most numerous DA receptors in the CNS and the earliest to be discovered. Conversely, it took almost twenty years to discover the D_3, D_4, and D_5 receptors, which have relatively low levels of expression.[34] The D_1-like family couples to $G\alpha_{s/olf}$ proteins, leading to activation of the enzyme adenylyl cyclase (AC) and an increase in cyclic adenosine monophosphate (cAMP) levels. The D_2-like family couples to $G\alpha_{i/o}$ proteins which induce the opposite effect from $G\alpha_{s/olf}$ proteins, inhibition of AC and a decrease of cAMP concentrations.[33] As a member of the D_2-like family, D_4 is 53% homologous to the D_2 receptor in its transmembrane domain, making the development of a selective ligand difficult.[33]

(a)

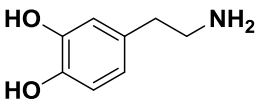

(b)

	Dopamine Receptors	Associated G-protein	Function
D_1-like family	D_1, D_5	$G\alpha_{s/olf}$	increase cAMP
D_2-like family	D_2, D_3, D_4	$G\alpha_{i/o}$	decrease cAMP

Figure 2.1. (a) Structure of dopamine. **(b)** The dopamine receptor families.

Dopamine regulation through the nigrostriatal, mesolimbic, and mesocortical pathways has been shown to be involved in reward, motivation, motor control, and cognition.[35] It has been shown that high levels of DA can lead to increased motor activity and "impulsive" behaviors while low levels can cause torpor and slowed reaction.[33] There are many CNS conditions associated with dopaminergic dysfunction, including Parkinson's disease, attention deficit hyperactivity disorder, Tourette's syndrome, and psychoses as seen in schizophrenia, Huntington's disease, and Alzheimer's disease.[34]

The D_1 and D_2 receptors have been explored in greater depth than the other DA receptors and have been shown to be critically involved in reward, reinforcement, and locomotor activity.[36] Most information reported about the D_4 receptor's function is highly debated. Knockout studies of the D_4 receptor gene (*DRD4*) show phenotypes suggesting a physiological role for D_4 in locomotion and drug sensitivity.[34] *DRD4* knockout mice demonstrated a reduction in overall locomotion and were more sensitive to the stimulation of locomotor activity elicited by cocaine.[35] Genetic association studies have also added relevant information about the role of D_4 in various disease states, showing a strong association for D_4 with ADHD, alcoholism, and nicotine dependence (**Figure 2.2**).[37] However, these results are preliminary data that must be studied in animal models using selective D_4 ligands to confirm the association.

Disorder	Genetic Association
ADHD Alcoholism Nicotine dependence	Strong
Autism Depression, Bipolar OCD Eating disorders	Mild/ Debatable
Sleep disorders Delirium, dementia, etc. Schizophrenia	Not confirmed/ Not known

Figure 2.2. D_4 involvement in disease as shown by genetic association studies.[37]

There are a number of polymorphisms in the D_4 receptor gene coding sequence. The most extensive is found in the third exon that encodes the third intracellular loop (IL3) of the receptor. This exon contains a variable number of tandem repeats (VNTR), in which a 48-base pair sequence (16 amino acids) exists as a 2- to 11-fold repeat ($D_{4.2}$ to $D_{4.11}$).[38] A similar polymorphism has been found in primates and dogs, but not in rodents.[38] In the global population of humans, $D_{4.4}$ is the most common at 64%, $D_{4.7}$ is found in 21% of people, and $D_{4.2}$ is 8% abundant.[34] Correspondingly, there are two isoforms of the D_2 receptor, D_{2L} and D_{2S}. The D_{2L} receptor (dopamine receptor 2 long form) contains a 29 amino acid insertion in the IL3 that is not observed in the D_{2S} receptor (dopamine receptor 2 short form).[35] The variations found in the third intracellular loop of the dopamine receptors could be important regarding their coupling to G-proteins. However, any differences in function have not been defined and ligand binding affinity for D_4 does not significantly change across polymorphisms.

D_4 receptors have been found to be expressed in the cerebral cortex, amygdala, hippocampus, and striatum through studies such as Northern blot, reverse transcription polymerase chain reaction, and *in situ* hybridization.[38] It is also been demonstrated that D_4 is highly expressed

in the retina. D_4 receptors are not exclusive to the brain; they are also present in the cardiac atrium, lymphocytes, and kidneys.[38] D_4 receptors are postsynaptic and their stimulation not only inhibits adenylyl cyclase, but also inositol phosphate hydrolysis and arachidonic acid release. Stimulation also causes the opening of G-protein coupled inward rectifying potassium channels (GIRK) and the closing of calcium channels (**Figure 2.3**).[34]

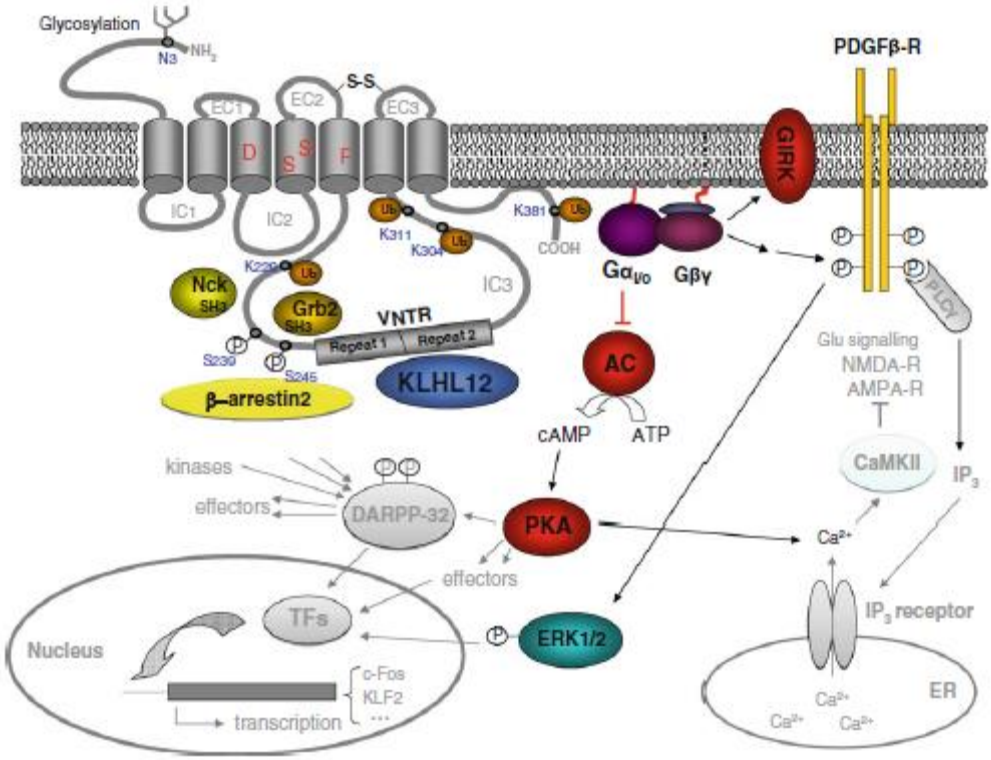

Figure 2.3. The $D_{4.2}$ receptor and its signaling cascade.[38]

2.1.2. PET Imaging

Positron emission tomography is a technique that has become commonplace in the drug discovery and medical communities. PET is a non-invasive procedure that uses positron emitting isotopes to measure the uptake, location, concentration, and elimination of a labeled molecule in the body.[39] The radioisotope undergoes beta decay, emitting positrons from its nucleus which travel through the local tissue until they interact with an electron, annihilating both.[40] This collision produces a pair of gamma photons that travel at the same speed but roughly 180 degrees from each other. When the photons reach the detectors surrounding the test subject, light is produced and converted to an electrical signal, allowing a computer to design an image revealing

where the photons originated.[40] The total analysis reveals the locations with the highest concentrations of the labeled PET tracer.

There are many isotopes that can be used in PET imaging including nitrogen-13, oxygen-15, bromine-76, and iodine-124.[41] However, the most commonly used isotopes are carbon-11 (for its convenient incorporation into organic molecules) and fluorine-18 (for its reasonable half-life of 110 minutes).[41]

2.2. Literature Review

2.2.1. Dopamine Receptor 4 Antagonists

There has long been interest in small molecule regulation of dopamine receptors. Dopamine receptor 4 antagonists quickly gained attention in the mid-1990s after it was found that clozapine (**Figure 2.4**) binds to D_4 with a higher affinity than D_2 (**Table 2.1**). Clozapine is an atypical antipsychotic used to treat schizophrenia and while it does bind D_4 receptors, it also inhibits the serotonin (5-HT), muscarinic (M), adrenaline (α), and histamine (H) receptors.[42,43] Scientists once thought that clozapine's efficacy in schizophrenia was due to its activity at D_4, beginning the race to synthesize selective D_4 antagonists. This hypothesis was later found to be incorrect. Shown in **Table 2.1** is a summary of antagonists that are at least 500-fold selective for D_4 over D_2. The structures of these antagonists all contain 1,4-disubstituted piperidine or piperazine cores (**Figure 2.4**, highlighted in red). While their selectivity for D_4 over D_2 is good, the basicity of the alkylated nitrogen causes many of these compounds to have activity at other biogenic amine receptors, limiting their use as tool compounds.

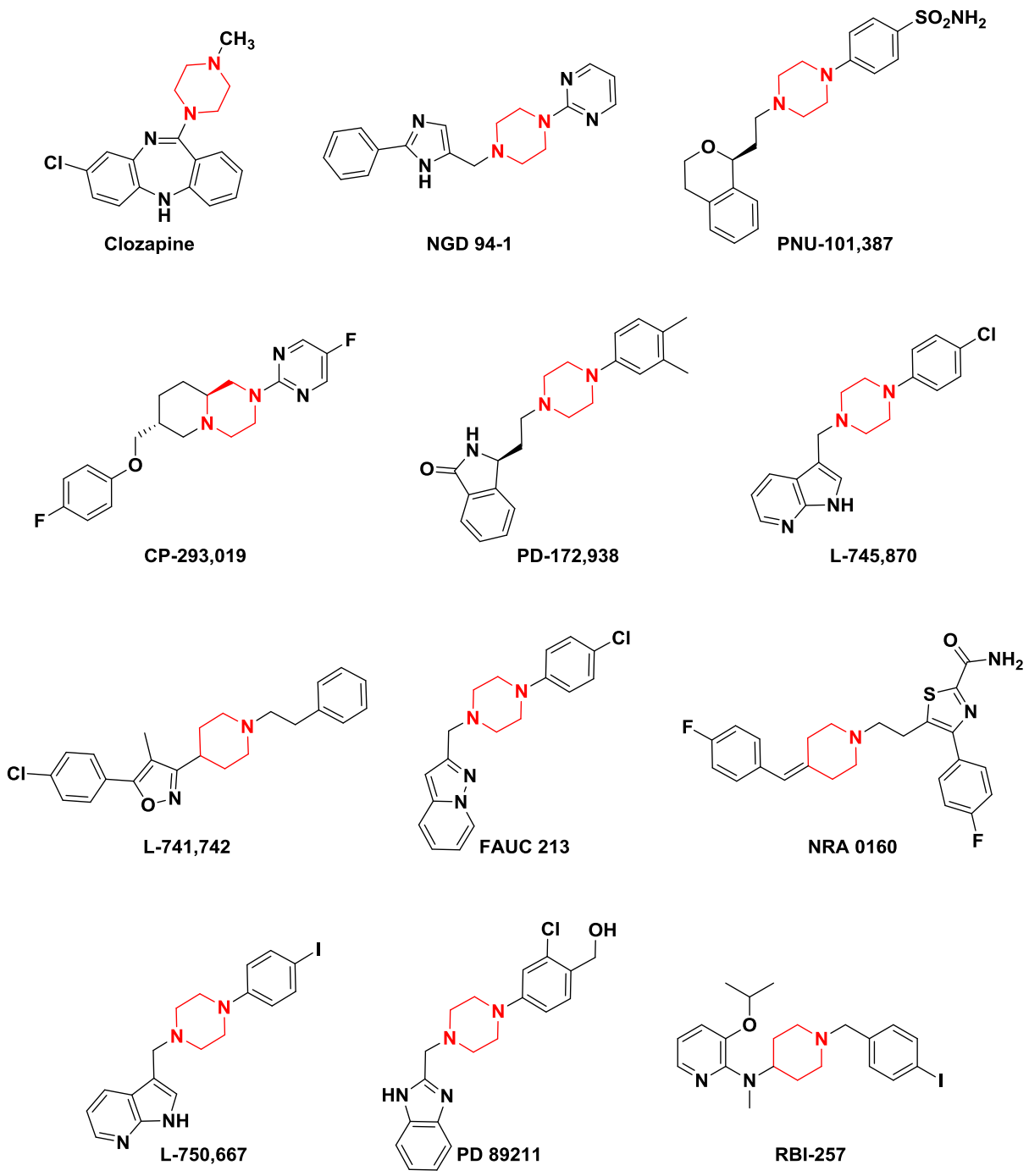

Figure 2.4. Structures of "selective" D_4 antagonists.

Table 2.1. Summary of D_4 antagonists with >500-fold selectivity over D_2.

	K_i (nM)		
	D_2	D_4	D_4:D_2
Clozapine	220	32	7
NGD 94-1	2230	3.6	620
PNU-101,387	4300	7.2	597
CP-293,019	3310	3.8	871
PD-172,938	5800	7.8	743
L-745,870	2000	0.4	5000
L-741,742	>1700	3.5	>485
FAUC 213	3400	2.2	1545
NRA 0160	>10,000	0.5	>20,000
L-750,667	>1700	0.5	>3400
PD 89211	>5000	3.6	>1300
RBI-257	568	0.33	1721

Of particular interest to the work presented in this chapter, there has been a report of 2,4-disubstituted morpholines as D_4 ligands. **Table 2.2** summarizes an SAR study of D_4 antagonists containing morpholine and oxazepane cores.[44] Shown are compounds that exhibited greater than 10 nM binding affinity for $D_{4.2}$. All compounds were also tested against D_2, with none having activity up to 10 μM; however, activity at other receptors was not reported. Using their modeling software, the group concluded that the two π system substituents and the basic nitrogen of the core are necessary to maintain high affinity and selectivity for D_4 receptors.[44]

Table 2.2. SAR of morpholines and oxazepanes as D_4 ligands.[44]

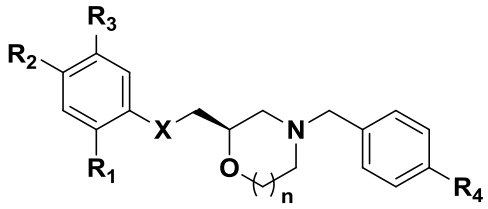

R_1	R_2	R_3	R_4	X	n	K_i (nM)
OMe	Cl	H	Cl	O	1	2.8
OEt	H	Cl	Cl	O	1	2.9
OMe	H	Cl	Cl	NH	1	4.5
OH	Cl	H	Cl	NH	1	5.4
OMe	Cl	H	Br	O	2	2.0
OEt	H	H	Cl	O	2	4.9
COMe	H	Cl	Cl	O	2	5.5
OEt	Cl	H	Cl	O	2	7.0
OEt	H	Cl	Cl	O	2	9.3

2.2.2. Cocaine Addiction

There have been many studies showing that long alleles of *DRD4* (greater than 7 repeats in the third intracellular loop) are implicated in personality traits such as excessive impulsivity, novelty-seeking, and risk-taking behavior.[45] These traits play a large factor in drug-taking behavior, leading to studies of the D_4 receptor's involvement in addiction. While many genetic association studies have been debated, there is evidence of a higher prevalence of *DRD4* long alleles in methamphetamine and nicotine users.[45] These results need to be confirmed by the development and use of animal models with selective ligands of the D_4 receptor.

Initial studies using *DRD4* knockout mice were inconclusive with respect to the gene's role in drug-taking behavior, so alternative animal models are more useful to study addiction.[45] There are several models that can be used to test stimulant-taking behavior, with drug self-administration as the gold standard to study drugs of abuse. The Lindsley lab is especially interested in the ability of D_4 antagonists to treat cocaine addiction and its symptoms. Cocaine addiction is a widespread

problem, with approximately 4.8 million Americans having abused the drug in 2009, and there are currently no approved medications for its treatment.[46]

In the clinic, both D_1 and D_2 antagonists failed to reduce the symptoms patients claimed to experience due to cocaine addiction. Buspirone (**Figure 2.5**), an FDA-approved drug for generalized anxiety disorder, acts as an antagonist at the D_3 and D_4 receptors (K_is of 98 and 29 nM, respectively) but is commonly characterized as a serotonin 5-HT_{1A} partial agonist (K_i = 29 nM).[43,46] Bergman and co-workers studied buspirone in intravenous cocaine self-administration models in nonhuman primates (NHP), and found that cocaine intake was completely extinguished with buspirone pretreatment in the range of currently prescribed oral doses (**Figure 2.5**).[46] These results were not seen in food-maintained behavior, suggesting no effect on motivation due to buspirone treatment. The authors propose that these results are not due to buspirone's 5-HT_{1A} activity, as a previously tested 5-HT_{1A} selective agonist, gepirone (**Figure 2.5**), did not produce changes in self-administration behavior.[46] There have been other studies using D_4 antagonists in various cocaine addiction models with results that are intriguing but incomplete.[47]

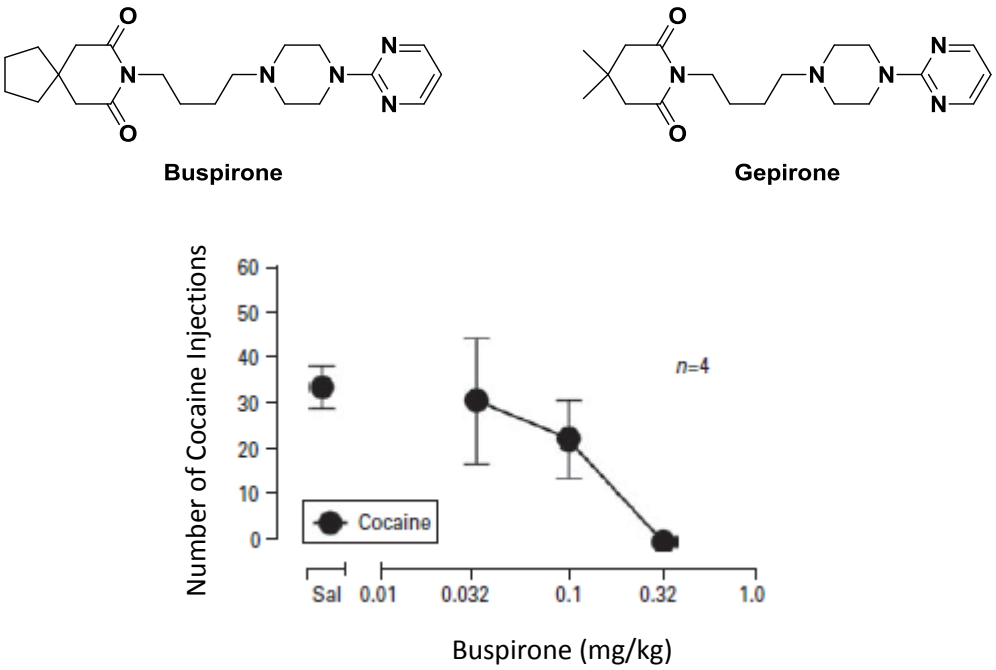

Figure 2.5. Efficacy of buspirone to attenuate cocaine self-administration in NHP.

While our lab is mainly interested in cocaine addiction, other stimulants like nicotine and amphetamines have been studied in relation to D_4. Yan *et al.* showed that L-745,870 (**Figure 2.4**)

blocked the reinstatement of nicotine-seeking brought on by either reexposure to nicotine or cues paired with the drug.[48] They also found that L-745,870 did not affect reinstatement of food-seeking. This suggests that D_4 receptors are involved in drug-seeking relapse and D_4 antagonists could prolong abstinence; however, other stimulants should be tested to confirm this hypothesis. Another study demonstrated that D_4 receptors play a role in behavioral sensitization to amphetamine in rats.[49] When PNU-101,387 (**Figure 2.4**) was dosed with amphetamine, the amphetamine-induced increase in dopamine release was blocked.[49] This finding reveals the possibility that D_4 is important in the establishment of addiction through the development of sensitization to drugs of abuse.

The D_4 receptor has been shown not to be involved in the rewarding effects of stimulants through drug discrimination and conditioned place preference models.[45] Instead, it seems D_4 may mediate relapse and other aspects of stimulant-seeking as seen in self-administration, reinstatement, and sensitization models.[45] This is a fascinating therapeutic area for D_4 antagonists as research continues to uncover information about the possible treatment of cocaine addiction.

2.2.3. PET Imaging of Dopamine 4 Receptors

Various techniques like autoradiography and receptor-specific antibodies have been used to determine the location of D_4 receptors in the brain.[50] These studies have led to general conclusions about where D_4 is expressed and have found that D_4 receptor densities are quite low in the brain. To detect small receptor populations using PET, a radioligand must have very high binding affinity (generally picomolar range), complete selectivity for its target, high blood-brain barrier (BBB) penetrance, and low nonspecific binding.[51] Important to these last two criteria is the tracer's lipophilicity, with optimum log P values for CNS drugs being 2.0 to 3.5.[51]

There are several reports in which compounds with high affinity for D_4 and reasonable selectivity have been analyzed as potential PET tracers. Many of these failed to attain PET tracer status due to factors like rapid metabolism and nonspecific binding. Only a few studies have attempted to use PET to image D_4 receptors. PB-12 (**Table 2.3**) is one such compound; it is highly selective over the other dopamine receptors (>17,000-fold) and, although it shows activity at serotonin and adrenergic receptors, PB-12 is still maintains >3,800-fold selectivity.[52]

Table 2.3. Reported potencies of PB-12.[52]

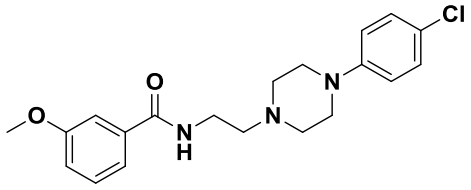

PB-12

IC_{50} (nM)								
$D_{4.4}$	D_{2L}	D_3	D_1	D_5	α_1	5-HT_{1A}	σ_1	σ_2
0.057	3800	>1000	>1000	>1000	270	220	>1000	>1000

PB-12 was labeled with carbon-11 at the methoxy carbon and used in PET imaging in a cynomolgus monkey.[50] After injection of [^{11}C]PB-12, rapid and high accumulation of radioactivity in the brain was seen, revealing no specific binding. Two separate experiments were performed using a pretreatment of L-745,870 or unlabeled PB-12 thirty minutes before injection of the radioligand. It would be expected that the D_4 receptors would be blocked by these antagonists resulting in an observable difference in the PET images. However, this effect was not seen, as no change in radioligand distribution was observed, again suggesting that the radioactivity detected was due to nonspecific binding.[50] Langer *et al.* postulated that this result may be caused by the lipophilicity of PB-12 (log P = 3.25) being high enough to bind to many other proteins and lipids in the brain.[50]

The scaffold of PB-12 continued to be used as a lead to find D_4 antagonists with lower lipophilicity. A report from 2010 revealed that the binding affinity of PB-12 is actually much lower than previously reported (K_i = 5.0 nM).[51] This may have led to the failure of the initial study summarized above. This new study identified **2.1** (**Table 2.4**) as a potentially improved PET tracer. Piperidine **2.1** showed no significant displacement of specific ligands for the receptors shown below at 1 μM and was also less lipophilic than PB-12 (log P = 2.55).

Table 2.4. Structure and binding data of **2.1**.[51]

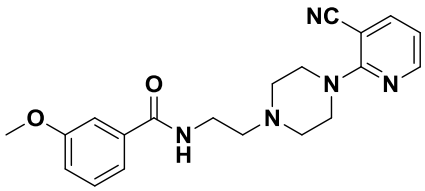

2.1

			% displacement at 1 μM						
cmp	log P	D_4 K_i (nM)	D_{2L}	σ_1	D_3	5-HT_{1A}	5-HT_{2A}	5-HT_{2C}	CB_1
PB-12	3.31	5.0	7.8	22					
2.1	2.55	1.5	4.4	8.3	5.1	9.3	24	3.2	6.5

Intravenous injection of [^{11}C]**2.1** into a rhesus monkey showed swift uptake in all brain regions followed by a rapid decline of radioactivity.[51] This suggests no specific or nonspecific binding occurred; however, radioactive accumulation in the retina was seen. Lacivita *et al.* concluded that imaging D_4 receptors using PET would require a ligand with a higher binding affinity than 1.5 nM due to low receptor density.[51]

The promise of a D_4 antagonist as a treatment for cocaine addiction as well as the lack of successful PET tracers for D_4 are the basis for our interest in developing a highly selective and potent D_4 antagonist.

2.3. Preliminary Data

The lead compound for this project was first reported in a Merck patent in 1995 followed by a subsequent publication.[53,54] Morpholine **2.5** was claimed to be a selective D_4 antagonist with one enantiomer being preferred, but the active stereoisomer was not reported. Morpholine **2.5** was prepared in three steps, including a chiral high-performance liquid chromatography (HPLC) purification to obtain the individual enantiomers in 10% overall yield (**Scheme 2.1a**).

The Lindsley lab chose to synthesize this pharmaceutically relevant morpholine based on our recently developed methodology (**Scheme 2.1b**).[55] Inspired by Jørgensen's work, 4-phenylbutanal (**2.6**) was asymmetrically α-chlorinated with pyrrolidine catalyst **2.7** and the resulting aldehyde was immediately reduced with sodium borohydride ($NaBH_4$) to preserve enantiopurity.[56] Alcohol **2.8** was converted into a leaving group with triflic anhydride (Tf_2O) and

displaced with *N*-benzylethanolamine. The primary alcohol was then free to perform S_N2 displacement of the chlorine, inverting the stereochemistry at that carbon. Hydrogenation of the benzyl protecting group and *N*-alkylation with benzimidazole **2.4** delivered **(*R*)-2.5**. This route greatly improved upon the previously reported synthesis with up to 95% enantiomeric excess (ee) and 35% overall yield.

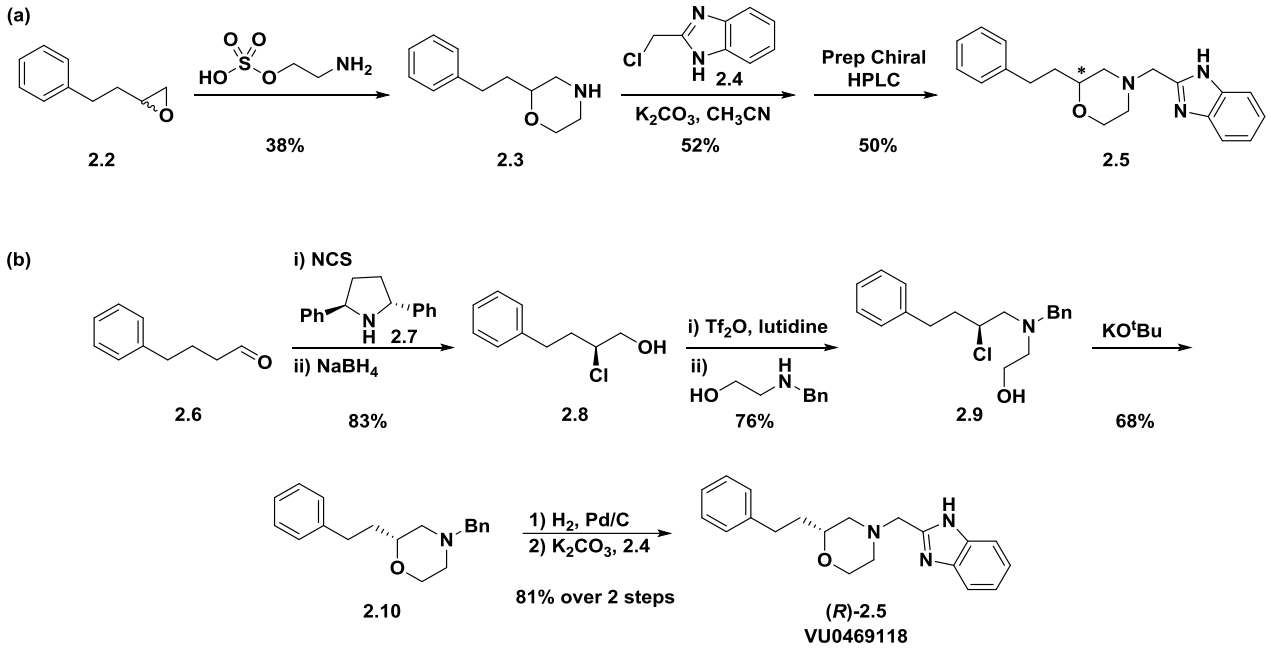

Scheme 2.1. Synthesis of morpholine **2.5** from **(a)** Merck, 1995[53] and **(b)** Lindsley, 2012[55].

Both enantiomers and the racemate of morpholine **2.5** were synthesized and evaluated against the full family of dopamine receptors in binding assays (**Table 2.5**). Morpholine **2.5** is completely inactive at D_1, D_2, and D_5, and >75-fold more selective for D_4 than D_3. Additionally, only the (*R*)-enantiomer is active at the D_4 receptor with K_i = 70 nM and IC_{50} = 180 nM.

Table 2.5. Binding and potency of the enantiomers of **2.5** against the dopamine receptors.[55]

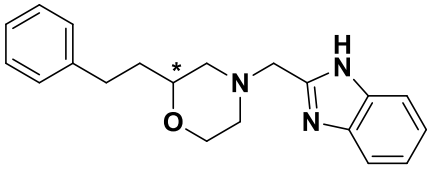

compound	D_1		D_2		D_3		D_4		D_5	
	K_i	IC_{50}	K_i	IC_{50}	K_i	IC_{50}	K_i	IC_{50}	K_i	IC_{50}
(±)-2.5	>100	>100	>100	>100	10.8	31.8	0.14	0.36	>100	>100
(*R*)-2.5	>100	>100	>100	>100	15.7	46.2	0.07	0.18	>100	>100
(*S*)-2.5	>100	>100	>100	>100	25.9	76.4	>100	>100	>100	>100

K_i and IC_{50} values are in μM, and represent at least three independent measurements.

VU0469118 (**(*R*)-2.5**) was subsequently submitted for drug metabolism and pharmacokinetics (DMPK) studies to determine its potential as an *in vivo* probe and PET tracer. **Table 2.6** describes the DMPK characteristics desired for such a ligand and compares them to the properties of VU0469118. VU0469118 meets almost all of the desired qualities for an *in vivo* tool. It has a high free fraction, ideal ClogP, high brain exposure, and no significant activity against any of the 68 GPCRs, ion channels, and transporters in the Lead Profiling Screen at Eurofins. The properties that still need to be improved upon for VU0469118 to become an *in vivo* tool are the binding affinity and the clearance, which is where our SAR study will focus. The SAR study for VU0469118 as a PET tracer will focus on incorporating a handle for radiolabeling and improving binding affinity.

Table 2.6. Desired and actual characteristics of VU0469118.

		Ideal *in vivo* probe characteristics	Ideal PET tracer characteristics	VU0469118
Activity (nM)	K_i IC_{50}	10 50	1	70 180
Selectivity		active only at D_4	binds only D_4	>10 μM ancill. pharm.
Brain to plasma ratio (B:P)		>1	>1	1.8
Clearance (rCL_{HEP}, mL/min/kg)		<20	<45	65.1
Lipophilicity (ClogP)			2.0-3.5	2.8

2.4. Structure-Activity Relationship Study of VU0469118

There are three obvious functionalities of VU0469118 to study SAR – the western phenyl, the benzimidazole, and the morpholine core (**Figure 2.6**). The benzimidazole substituent was chosen to study first as its addition was the final step of the known synthetic route to access VU0469118. A new route was devised to synthesize western phenyl derivatives so that the diversification step was closer to the end of the synthesis. Also, many core modifications were planned to study SAR.

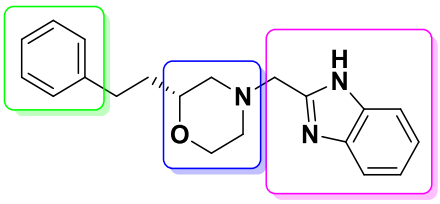

Figure 2.6. Functionalities of VU0469118 to derivatize: western phenyl (green), morpholine core (blue), benzimidazole (pink).

2.4.1. Benzimidazole Derivatives

In order to synthesize derivatives of the benzimidazole, the previously described synthesis of VU0469118 was employed using DL-proline as the catalyst for α-chlorination (**Scheme 2.2**).[57] It was important to synthesize this library as the racemate because changing the substituent on the

morpholine nitrogen could switch the enantiopreference of the receptor for the ligand. After common intermediate **2.3** was synthesized, the derivitization steps were optimized for rapid library synthesis and purification of the crude material via automated reverse-phase HPLC with minimal workup. Five different types of linkages off the morpholine nitrogen were studied in this initial library. All compounds were submitted to Eurofins Panlabs where they were tested at a single point of 10 μM in a competition study of D_4 receptors incubated with [^{3}H]spiperone (K_d = 0.46 nM). The results were considered significant if the percent inhibition was greater than 50%, meaning that 50% of the radioligand was displaced from the receptor by our compound.

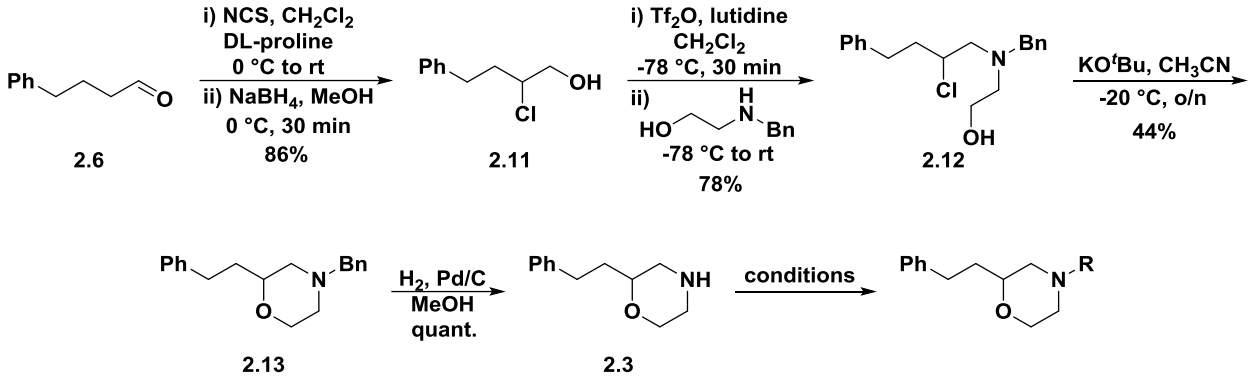

Scheme 2.2. Route to the library of benzimidazole derivatives.

The synthesis and inhibition data of benzyl linked derivatives is shown in **Figure 2.7**. Structure-activity relationship information was immediately evident from the data collected for these compounds. *Para*-substituted benzyl derivatives were preferred while substitutions at the *ortho* and *meta* positions were less active. Also, all isomers of the pyridyl substituent were inactive.[57]

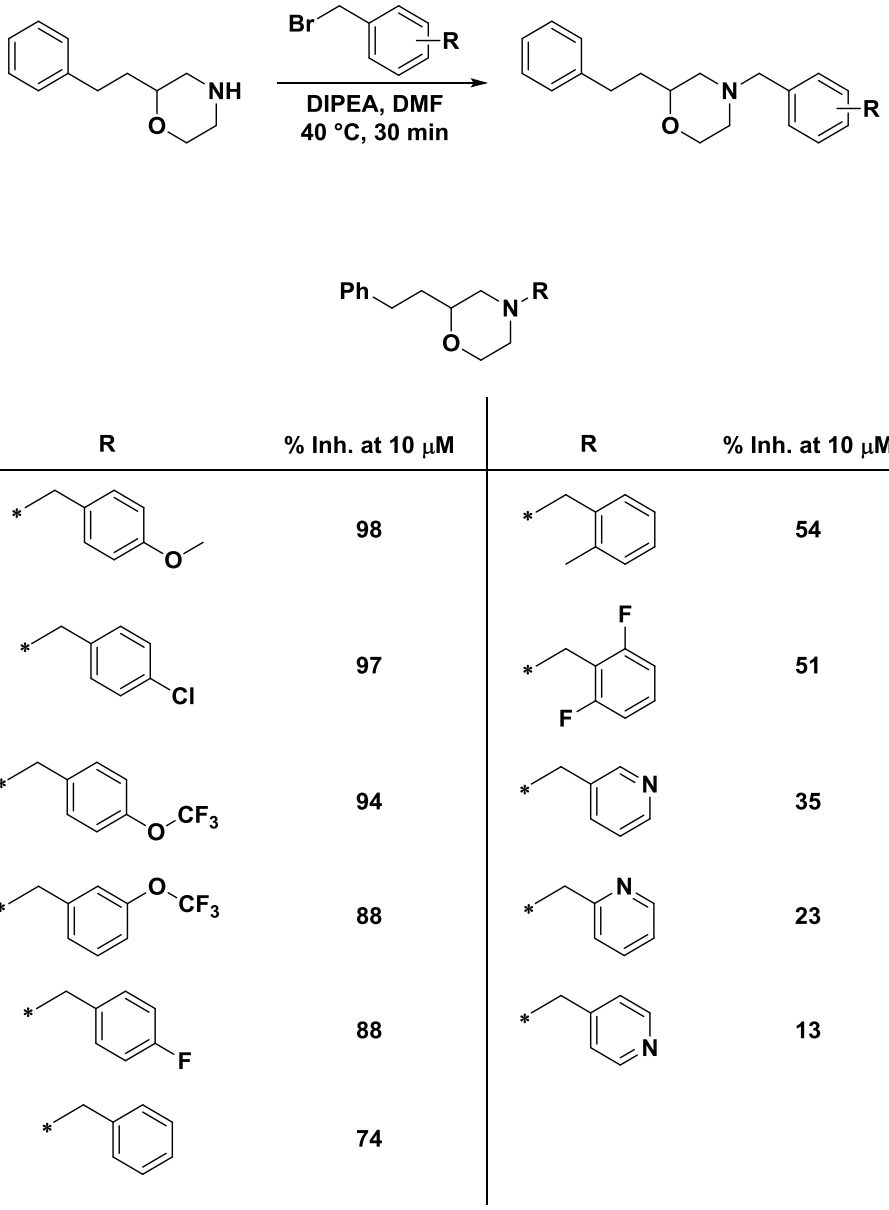

Figure 2.7. Synthesis and inhibition data of benzyl linked derivatives.

Other types of linkages were studied off the morpholine nitrogen as well. **Scheme 2.3** shows the synthesis of amides, ureas, sulfonamides, and *N*-aryl derivatives. As shown in **Table 2.7**, none of these compounds were considered active. Interestingly, when compared to the identical aryl groups that were benzyl linked, a significant loss in inhibition is seen.[57]

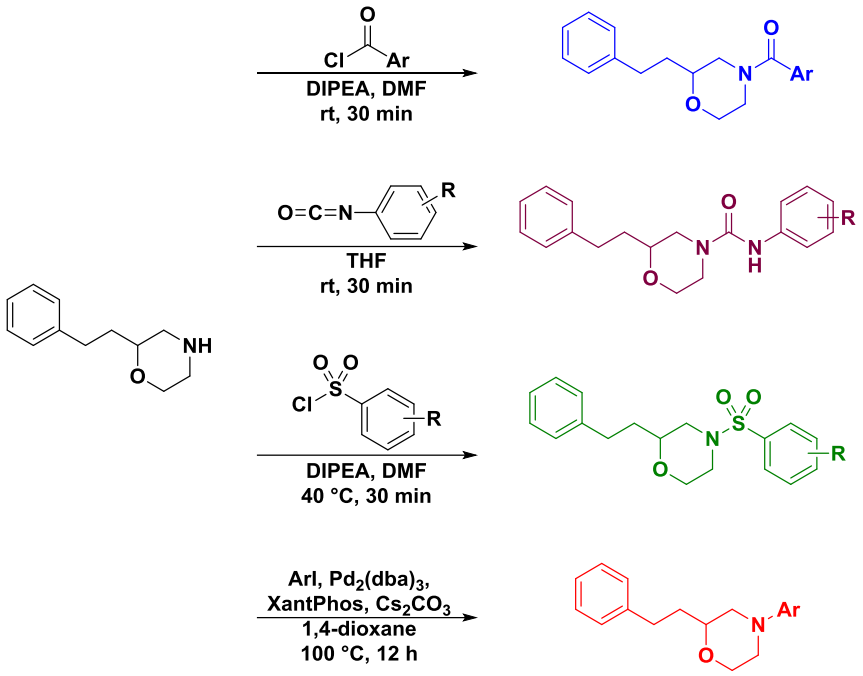

Scheme 2.3. Synthesis of amides, ureas, sulfonamides, and *N*-aryl derivatives.

Table 2.7. Inhibition comparison of benzyl linked derivatives to other linkages.

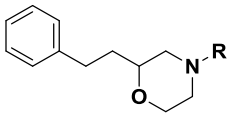

R	% Inh. at 10 μM	R	% Inh. at 10 μM	R	% Inh. at 10 μM
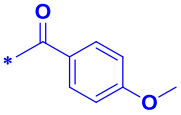	-5	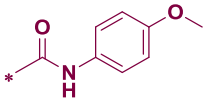	-2	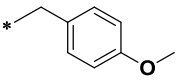	98
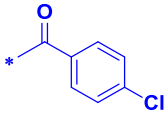	7	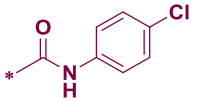	16	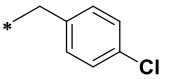	97
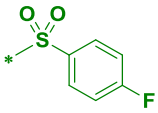	-8	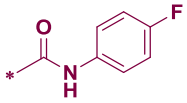	5	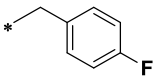	88
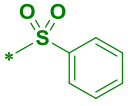	2	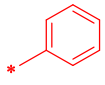	5	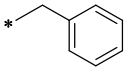	74
		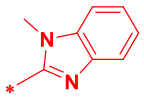	17	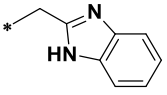	98

Figure 2.8 provides a summary of the inactive compounds from this first library. Any compound lacking a methylene between the nitrogen and aryl group proved to be inactive. Pyridyl derivatives also did not significantly inhibit spiperone's binding to the D_4 receptor. There are a few theories as to why this SAR appears: (1) the basicity of the nitrogen, which is key for binding, could be greatly reduced; (2) a specific length of linker may be necessary to fill a pocket of the binding site; (3) an oxygen coming off the linker could have unfavorable steric and/or electronic interactions in the pocket.

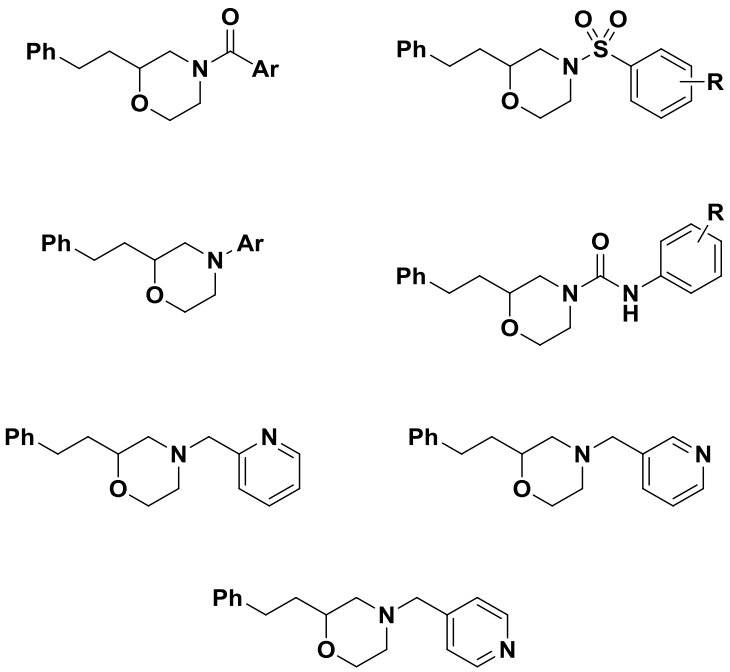

Figure 2.8. Summary of inactive compounds with <35% inhibition of D_4.

Additional binding data was obtained for the active compounds (**Table 2.8**). VU0517161 exhibited a 98% inhibition corresponding to 46 nM K_i and 170 nM IC_{50}. VU0517057 was slightly less active with a 97% inhibition, 81 nM K_i, and 290 nM IC_{50}. Importantly, this library was racemic, and it was expected that one stereoisomer would be more active than the other.

Table 2.8. Summary of active compounds and their binding affinity.

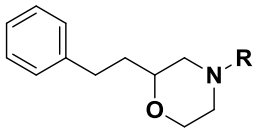

VU#	R	% Inh. at 10 μM	IC_{50} (μM)	K_i (μM)
VU0517161	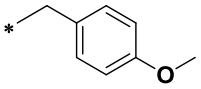	98	0.170	0.046
VU0517057	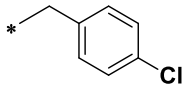	97	0.290	0.081
VU0517355	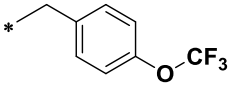	94	0.160	0.043
VU0517381	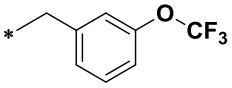	88	0.390	0.110
VU0517120	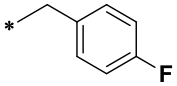	88	1.14	0.320
VU0517051	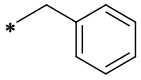	74	1.48	0.410
VU0517380	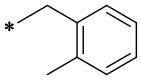	54	3.68	1.02
VU0517302	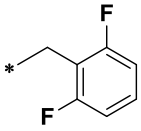	51	3.88	1.07

Next, the (*R*)- and (*S*)-enantiomers of the top two compounds were resolved and tested. The (*R*)-enantiomer was once again confirmed as the active isomer. Selectivity data was also attained for the dopamine receptors (**Table 2.9**). VU0603864, with the *para*-methoxy substituent, had the highest binding affinity of 28 nM. However, it did have slight activity at D_{2L} and D_3, but maintained 100-fold selectivity over these receptors. VU0603865 (R = Cl) exhibited a binding affinity of 36 nM and greater than 20 μM potency across the other dopamine receptors, showing excellent selectivity.[57]

Table 2.9. Dopamine receptor binding data.

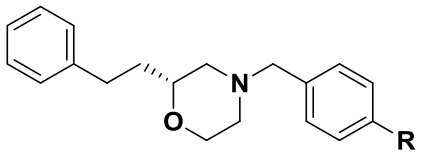

VU#	R	Subtype	IC_{50} (μM)	K_i (μM)
VU0603864	OCH_3	D_1	>20	
		D_{2S}	>20	
		D_{2L}	16.5	5.5
		D_3	8.2	2.8
		D_4	0.100	0.028
		D_5	>20	
VU0603865	Cl	D_1	>20	
		D_{2S}	>20	
		D_{2L}	>20	
		D_3	>20	
		D_4	0.130	0.036
		D_5	>20	

VU0603865 was chosen for further DMPK testing due to its complete selectivity and high affinity for the D_4 receptor (**Table 2.10**). Similar to VU0469118, VU0603865 was predicted to have high clearance in both rat and human. VU0603865 had good free fraction in both species and showed no significant activity against cytochrome P450 (CYP) enzymes, an improvement over the initial hit. In an *in vivo* tissue distribution study, VU0603865 was found to readily cross the blood-brain barrier with total brain concentrations of ~1 μM at 15 minutes. This compound was also tested in Eurofins Lead Profiling screen of 68 GPCRs, ion channels, and transporters at 10 μM. It was found to only significantly bind (>50%) to five receptors: adrenergic, α_{1A} (77%); histamine, H_1 (93%); sigma, σ_1 (99%); dopamine transporter, DAT (72%); and norepinephrine transporter, NET (68%).[57]

Table 2.10. DMPK comparison of VU0469118 and VU0603865.

	VU0469118	VU0603865
K_i (nM)	70	36
In vitro PK properties		
Microsome predicted hepatic clearance (mL/min/kg)		
Rat CL_{HEP}	65.1	67.5
Human CL_{HEP}	17.9	15.7
Percent free compound in plasma		
Rat f_u	13.3	3.9
Human f_u	1.2	6.1
CYP450 inhibition (μM)		
CYP1A2	13.1	>30
CYP2C9	4.8	>30
CYP2D6	12.0	18.0
CYP3A4	15.6	>30
In vivo PK properties		
Rat IP (10 mg/kg, 0.25 h)		
B:P	1.8	2.0
$[Brain]_{free}$ (nM)	78.3	38.4

Due to its pharmacological profile and selectivity, VU0603865 was declared an MLPCN (Molecular Libraries Probe Production Centers Network) probe, ML398.[57] As ML398 is a potent, selective, and brain penetrant D_4 antagonist, we wanted to test its ability to reverse hyperlocomotion induced by cocaine. **Figure 2.9** shows the results of this test using both VU0469118 and ML398. Locomotion was measured by the number of laser beam breaks per minute using the SmartFrame open field activity chamber. Cocaine alone significantly increased activity in rats over vehicle. Both compounds were dosed with cocaine at 3 mg/kg and 10 mg/kg. VU0469118 did not show a statistically significant reduction in hyperlocomotion up to 10 mg/kg. However, ML398 did significantly reverse cocaine-induced hyperlocomotion at 10 mg/kg.[57]

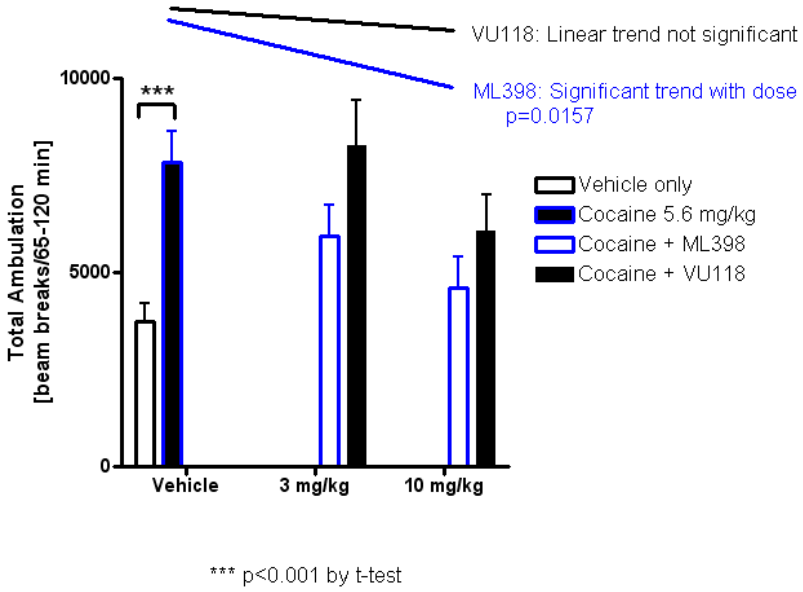

Figure 2.9. Effects of VU0469118 and ML398 on reversing cocaine-induced hyperlocomotion in rats.

While this is exciting data for the development of an *in vivo* tool, there are still properties about this compound that could be improved. Also, the development of a PET tracer would require a compound exhibiting much higher binding affinity. To this end, further enantiopure methylene-linked libraries were synthesized around the benzimidazole using the previously described enantioselective route (**Scheme 2.1b**). **Table 2.11** shows the results of these libraries.

This study provided very interesting SAR data. The naphthyl substitution lead to a compound with 1.3 nM binding affinity, the most potent to date for this project. It was found that very small changes in the benzimidazole ring system caused complete loss of activity. For example, methylation of one of the nitrogens (VU0651665) or replacement of one nitrogen with sulfur or oxygen (VU0651731, VU0651677) resulted in nearly inactive compounds.

Table 2.11. Potency and binding affinity of benzimidazole library.

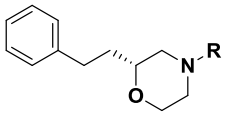

VU#	R	IC_{50} (nM)	K_i (nM)	VU#	R	IC_{50} (nM)	K_i (nM)
VU0651632	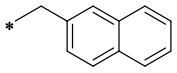	4.8	1.3	VU6000122	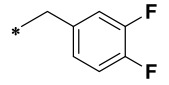	970	270
VU0652020	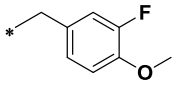	59	16	VU0651675	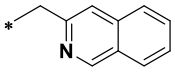	1240	340
VU0651729	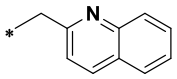	100	28	VU6000124	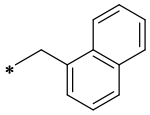	1800	500
VU0651633	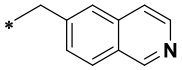	100	29	VU0651733	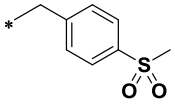	2190	610
VU6000121	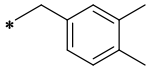	120	33	VU0651731	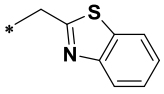	3660	1010
VU0651676	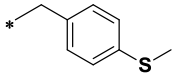	130	35	VU0651677	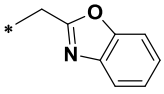	7180	1990
VU0651730	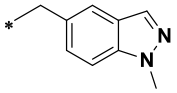	150	41	VU0651634	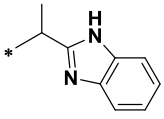	8540	2370
VU0651732	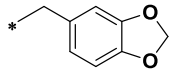	190	54	VU0652016	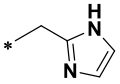	>10,000	>10,000
VU6000123	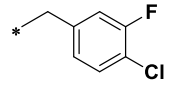	210	57	VU0651665	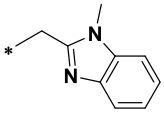	>10,000	>10,000
VU0652019	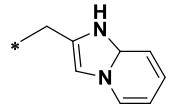	430	120				

Selectivity data was obtained for the best three compounds from this library (**Table 2.12**). None of these three were completely selective over the other dopamine receptors as they all exhibited weak D_3 activity. However, they were still >100-fold selective over D_3, with VU0651632 being 2,000-fold selective.

Table 2.12. Selectivity data for VU0651632, VU0652020, and VU0651729.

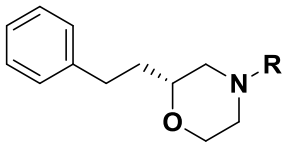

VU#	R	Subtype	IC_{50}	K_i
VU0651632	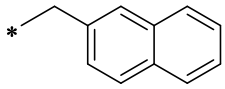	D_4	4.8 nM	1.3 nM
		D_3	7.7 μM	2.6 μM
		D_1, D_{2L}, D_{2S}, D_5	>20 μM	
VU0652020	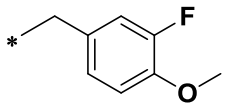	D_4	59 nM	16 nM
		D_3	8.8 μM	3.0 μM
		D_{2L}	19.5 μM	6.5 μM
		D_1, D_{2S}, D_5	>20 μM	
VU0651729	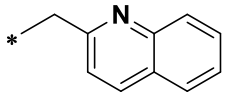	D_4	100 nM	28 nM
		D_3	8.7 μM	2.9 μM
		D_1, D_{2L}, D_{2S}, D_5	>20 μM	

The pharmacokinetic properties of the four most potent compounds in the second benzimidazole library were determined (**Table 2.13**). The hepatic clearance remained very high, almost hepatic blood flow. Also, the fraction unbound and CYP450 enzyme inhibition were much worse than ML398. These properties could be due to the higher lipophilicity of these compounds. Unfortunately, the DMPK properties of these compounds excludes them from further *in vivo* testing.

Table 2.13. In vitro PK properties of the most potent benzimidazole substituents.

	VU0651632	VU0652020	VU0651729	VU0651633
Microsome predicted hepatic clearance (mL/min/kg)				
Rat CL_{HEP}	67.8	68.5	68.8	67.2
Human CL_{HEP}	16.7	17.7	19.3	19.7
Percent free compound in plasma				
Rat f_u	0.5	2.1	2.6	2.9
Human f_u	0.2	1.8	0.9	2.2
CYP450 inhibition (μM)				
CYP1A2	14.1	14.0	11.6	1.34
CYP2C9	>30	24.9	15.0	1.34
CYP2D6	14.8	9.2	7.0	0.51
CYP3A4	>30	>30	14.6	<0.1

Even with its poor DMPK properties, our most potent compound, VU0651632, is in the desired range of binding affinity for PET imaging. The next goal for this project was to synthesize a compound with a functionality that could be labeled with fluorine-18 while lowering lipophilicity and maintaining binding affinity.

2.4.2. Phenyl Derivatives

In order to study the SAR of the western phenyl portion of the hit (see **Figure 2.6**), a new route had to be devised for ease of derivitization. **Scheme 2.4** shows this new synthesis. Ethanolamine was alkylated under microwave conditions with naphthyl bromide. Aminoalcohol **2.14** was then utilized in an epoxide opening to provide the desired morpholine core as well as an oxazepane byproduct. Incorporating the chiral epoxide sets the desired stereochemistry for this scaffold. Primary alcohol **2.15** was oxidized using Dess–Martin Periodinane followed by a Seyferth–Gilbert homologation with the Ohira–Bestmann modification to provide terminal alkyne **2.18**. Sonogashira coupling under microwave conditions provided the diversification point for the library. Finally, hydrogenation yielded the desired phenyl derivatives.

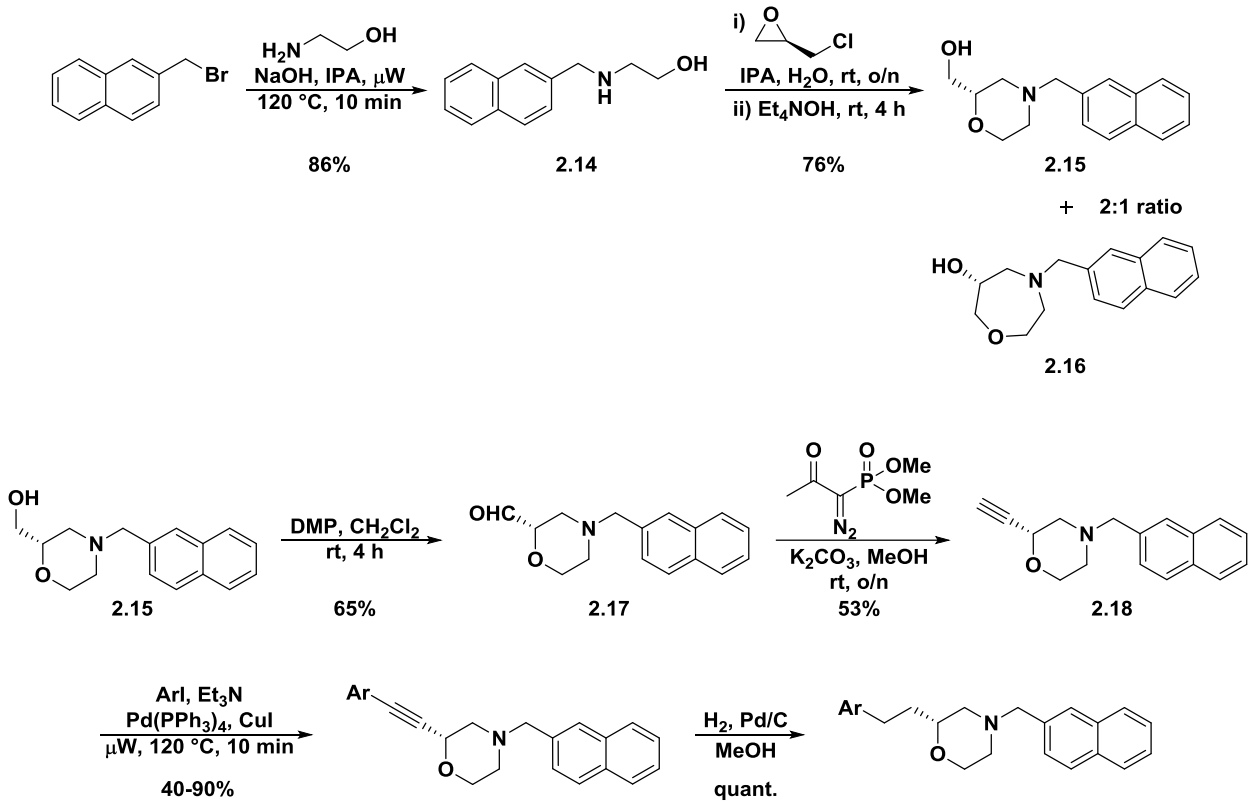

Scheme 2.4. Synthetic route toward western phenyl derivatives.

Due to the high lipophilicity of the naphthyl derivative, we were most interested in installing polar groups to help decrease log P. **Table 2.14** shows the library and binding data for these derivatives. Various 2-fluoropyridines were synthesized in the hopes of becoming radioligands. The Vanderbilt Institute of Imaging Science prefers to install fluorine-18 through an aromatic nucleophilic substitution reaction with a 2-chloropyridine. These fluoro-pyridines unfortunately resulted in significant loss of binding affinity. This SAR study revealed that *ortho*-substituted polar groups are well tolerated and generally give binding affinities in the 16-40 nM range.

Table 2.14. Binding affinities and potencies of western phenyl derivatives.

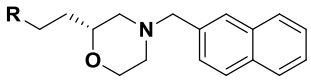

VU#	R	IC_{50} (nM)	K_i (nM)	VU#	R	IC_{50} (nM)	K_i (nM)
VU6000128	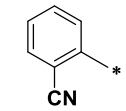	56	16	VU0657026	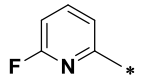	290	80
VU0650725	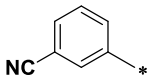	73	20	VU0657080	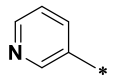	570	160
VU6000119	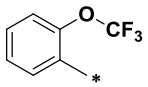	97	27	VU6000126	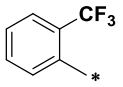	1040	290
VU6000125	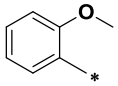	140	40	VU6000127	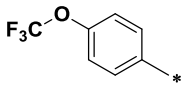	2830	780
VU0657071	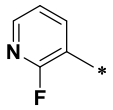	260	73	VU6000120	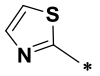	3800	1100
VU0657082	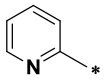	280	77				

It was later found through the synthesis of ML398 using the route in **Scheme 2.4** that the enantiopurity of this library was not known due to ee loss somewhere along the route. While this library still contains useful data concerning SAR, the synthetic scheme must be evaluated for the loss of enantiopurity and the problem reactions must be fixed in order to continue the investigation of phenyl derivatives.

2.5. Future Directions

There is ongoing effort in the lab to study the structure-activity relationship of this novel D_4 antagonist. More derivatives of the western phenyl ring are planned, including a matrix library with the best moieties found so far replacing the phenyl and benzimidazole. When a suitable 2-fluoropyridine analog is found, PET studies will commence to study the location of D_4 receptors in the brain.

There are also plans for variations of the core region of the morpholine antagonist (**Figure 2.10**). The oxazepane byproduct (**2.16**) formed in the route to the phenyl derivatives will be an interesting core change. Also, replacing the oxygen in the morpholine ring with a gem di-fluoro group could provide potent analogs with novel intellectual property.

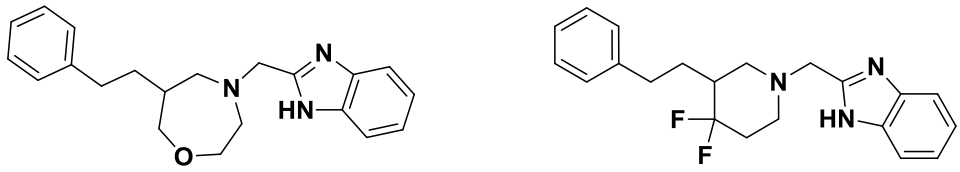

Figure 2.10. Ideas for core changes.

The synthesis of the oxazepane core will begin with the same epoxide opening previously shown (**Scheme 2.5**). Displacement of the alcohol will be facilitated by the triflate with deprotonated phenylacetylene. Simultaneous hydrogenation and hydrogenolysis will reduce the alkyne and remove the benzyl group. Finally, the nitrogen can be alkylated with any benzyl substituent. These analogs will be racemic; if there are a few worth pursuing, the enantiomers will be resolved by supercritical fluid chromatography (SFC). This scaffold is slightly different than the compounds reported by Audouze *et al.*; while their compounds were 2,4-disubstitued oxazepanes, these will be 3,5-disubstitued.[44]

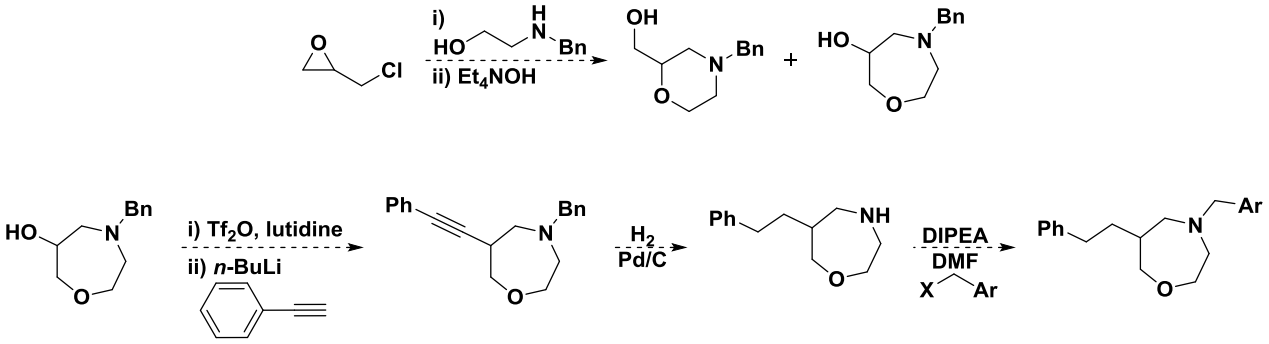

Scheme 2.5. Planned synthesis of oxazepane core.

The synthesis of the di-fluoro piperidine begins with piperidinone **2.19** (**Scheme 2.6**). Alkylation of the nitrogen will be followed by addition of phenethyliodide. The ester will be

removed under acidic conditions and DAST will be used to convert the ketone to a gem-di-fluoro group.

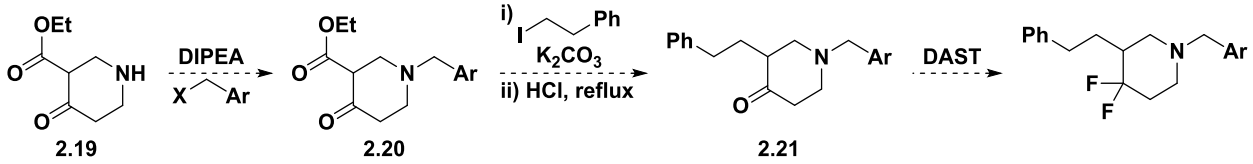

Scheme 2.6. Planned synthesis of the di-fluoro piperidine core.

2.6. Conclusions

There is still much to be explored about the role of D_4 receptors in various disease states. We hope to add to the limited knowledge by synthesizing a highly selective antagonist with low nanomolar binding affinity. Our initial compound, VU0469118, already exhibited many of the properties needed for an *in vivo* probe and a PET tracer. An initial SAR study identified ML398 which has shown efficacy in the cocaine mechanism. By further increasing the binding affinity while maintaining other important pharmacokinetic characteristics, we hope to find a candidate that can be used as an *in vivo* tool and a PET tracer to study cocaine addiction and its symptoms.

2.7. Experimental Methods

All reagents and solvents were commercial grade and purified prior to use when necessary. Analytical thin layer chromatography (TLC) was performed on Sorbent Technologies HL 0.25 mm silica gel plates with UV indicator. Visualization was accomplished by irradiation under a 254 nm UV lamp and/or the use of an iodine chamber. Chromatography on silica gel was performed using Silica Gel 60 (230-400 mesh) from Sorbent Technologies. ^{1}H and ^{13}C NMR spectra were recorded on a Bruker DRX-400 (400 and 100 MHz, respectively) NMR instrument. Chemical shifts are reported in ppm from the solvent resonance as an internal standard. Data are reported as follows: chemical shift, multiplicity (s = singlet, d = doublet, t = triplet, m = multiplet, bs = broad singlet), coupling constant (Hz), and number of protons. Low resolution mass spectra were obtained on an Agilent 6130 Quadrupole LC/MS with electrospray ionization (R_T = retention time). Optical rotations were measured on a JASCO P-2000 digital polarimeter at room temperature. Concentration (c) in g/100 mL and solvent are given in parentheses. Preparative purification was performed on a Gilson chromatograph using a Luna 5u C_{18}(2) 100A AXIA column (30x50 mm) using a water/acetonitrile gradient. Chiral separations were performed on a Thar Investigator II supercritical fluid chromatograph (SFC) using Lux Cellulose 4 (10x250 mm), Chiralpak IA (10x250 mm), and Chiralpak ID (10x250 mm) columns. A Micromass Q-Tof API-US mass spectrometer was used to acquire high resolution mass spectrometry (HRMS) data. The value Δ is the error in the measurement (in ppm) given by the equation $\Delta = [(ME - MT)/ MT] \times 106$, where *M*E is the experimental mass and *M*T is the theoretical mass. The HRMS results were obtained with ES as the ion source and leucine enkephalin as the reference.

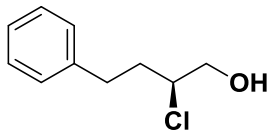

2.8

(*S*)-2-chloro-4-phenylbutan-1-ol (2.8). Suspended 4-phenylbutanal (147 mg, 0.992 mmol) in anhydrous dichloromethane (4.0 mL) and cooled to 0 °C. (2*R*,5*R*)-Diphenylpyrrolidine (22.0 mg, 0.099 mmol) added followed by *N*-chlorosuccinimide (172 mg, 1.29 mmol). The progress of this reaction was monitored by proton NMR (the starting material aldehyde peak being converted to the mono-chlorinated aldehyde). Once complete, methanol (4.0 mL) was added at 0 °C followed

by the slow addition of sodium borohydride (187 mg, 4.96 mmol). Continued stirring for 30 minutes before water was added and the solution was extracted with dichloromethane. After drying over sodium sulfate, filtering, and concentrating, the crude material was purified by column chromatography (0-45% ethyl acetate in hexanes). Pure chloro-alcohol was collected (158 mg, 86%) in 93% ee.

^{1}H NMR ($CDCl_3$, 400 MHz) δ (ppm): 1.99-2.09 (m, 3H), 2.73-2.80 (m, 1H), 2.87-2.94 (m, 1H), 3.67-3.82 (m, 2H), 3.96-4.02 (m, 1H), 7.20-7.33 (m, 5H). **^{13}C NMR** ($CDCl_3$, 100 MHz) δ (ppm): 32.3, 35.8, 64.0, 66.9, 126.2, 128.4, 128.5, 140.6. $[\alpha]_D^{20}$ = -48.4 (c = 1.0, CH_3OH). Spectral data matches that recorded by M. O'Reilly and C. Lindsley, Organic Letters, *14*, 2910.

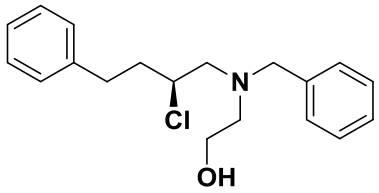

2.9

(*S*)-2-(benzyl(2-chloro-4-phenylbutyl)amino)ethanol (2.9). (*S*)-2-chloro-4-phenylbutan-1-ol (0.530 g, 2.87 mmol) was suspended in anhydrous dichloromethane (28.0 mL) and to this 2,6-lutidine (3.3 mL, 28.7 mmol) was added. This solution was cooled to -78 °C before triflic anhydride (0.63 mL, 3.73 mmol) was added dropwise. This was stirred 30 minutes and the triflate was confirmed to be formed by proton NMR. *N*-benzylethanolamine (2.1 mL, 14.3 mmol) in anhydrous dichloromethane (2.0 mL) was added to the solution dropwise. The reaction was allowed to warm to room temperature slowly overnight and the consumption of the triflate was established by NMR. Diethyl ether (100 mL) and water (100 mL) was added and the organic layer was separated from the aqueous, dried over sodium sulfate, filtered, and concentrated *in vacuo*. The crude product was purified by column chromatography (0-20% ethyl acetate in hexanes) to yield the chloro-aminoalcohol (0.715 g, 78%).

^{1}H NMR ($CDCl_3$, 400 MHz) δ (ppm): 1.88-1.99 (m, 1H), 2.07-2.18 (m, 1H), 2.63-2.96 (m, 7H), 3.53-3.76 (m, 4H), 3.90-3.99 (m, 1H), 7.20-7.40 (m, 10H). **^{13}C NMR** ($CDCl_3$, 100 MHz) δ (ppm): 32.3, 37.6, 56.3, 58.8, 59.3, 60.3, 61.1, 126.1, 127.4, 128.4, 128.5, 128.5, 129.0, 138.2, 140.8. **LCMS:** R_T 0.892 min, *m/z* = 319.9 $[M+H]^+$, >99% @ 215 nm. $[\alpha]_D^{20}$ = -15.1 (c = 1.0, CH_3OH). Spectral data matches that recorded by M. O'Reilly and C. Lindsley, Organic Letters, *14*, 2910.

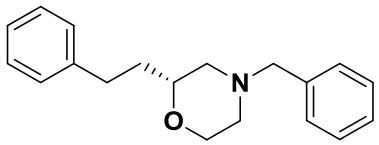

2.10

(*R*)-4-benzyl-2-phenethylmorpholine (2.10). Suspended (*S*)-2-(benzyl(2-chloro-4-phenylbutyl) amino)ethanol (0.660 g, 2.08 mmol) in anhydrous acetonitrile (100 mL) and cooled to -20 °C. Potassium *tert*-butoxide (1.17 g, 10.4 mmol) was added and the progress of the reaction was followed by TLC. Upon consumption of starting material, water and diethyl ether were added to the reaction and it was extracted with ether, dried over sodium sulfate, filtered, and concentrated. The crude material was purified by column chromatography (0-40% ethyl acetate in hexanes) to give the morpholine (0.316 g, 54%).

^{1}H NMR ($CDCl_3$, 400 MHz) δ (ppm): 1.63-1.74 (m, 1H), 1.78-1.89 (m, 1H), 1.92 (t, *J* = 10.7 Hz, 1H), 2.21 (td, *J* = 3.2, 11.1 Hz, 1H), 2.63-2.86 (m, 4H), 3.50-3.58 (m, 3H), 3.70 (td, *J* = 2.4, 11.1 Hz, 1H), 3.92 (d, *J* = 11.1 Hz, 1H), 7.18-7.24 (m, 3H), 7.25-7.39 (m, 7H). **^{13}C NMR** ($CDCl_3$, 100 MHz) δ (ppm): 31.5, 35.3, 53.2, 58.6, 63.3, 66.7, 74.8, 125.7, 127.1, 128.2, 128.3, 128.4, 129.1, 137.7, 142.0. **LCMS:** R_T 0.924 min, *m/z* = 282.0 $[M+H]^+$, >99% @ 215 nm. $[\alpha]_D^{20}$ = +30.3 (c = 1.0, CH_3OH). Spectral data matches that recorded by M. O'Reilly and C. Lindsley, Organic Letters, *14*, 2910.

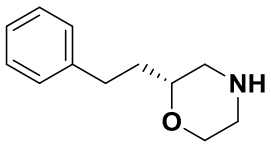

(*R*)-2.3

(*R*)-2-phenethylmorpholine ((*R*)-2.3). Suspended (*R*)-4-benzyl-2-phenethylmorpholine (88.0 mg, 0.313 mmol) in anhydrous methanol (6.3 mL). The flask was purged three times alternating vacuum and argon. To this was added 10% Pd/C (6.6 mg, 0.063 mmol) and the flask was purged three times alternating vacuum and hydrogen gas. The reaction was followed by TLC and LCMS until it was complete. The solution was then filtered through celite with methanol, concentrated, and carried on crude.

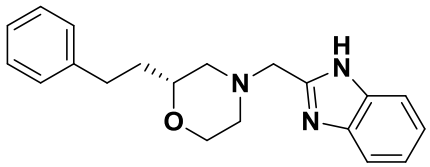

(*R*)-2.5, VU0469118

(*R*)-4-((1*H*-benzo[*d*]imidazol-2-yl)methyl)-2-phenethylmorpholine (VU0469118).

^{1}H NMR ($CDCl_3$, 400 MHz) δ (ppm): 1.53-1.63 (m, 1H), 1.73-1.84 (m, 1H), 2.04 (*J* = 10.28, 1H), 2.34 (td, *J* = 3.4, 11.6 Hz, 1H), 2.56-2.78 (m, 4H), 3.42-3.44 (m, 1H), 3.67 (td, *J* = 2.1, 11.6 Hz, 1H), 3.77-3.90 (m, 3H), 7.12-7.21 (m, 3H), 7.23-7.31 (m, 4H), 7.62 (bs, 2H). **^{13}C NMR** ($CDCl_3$, 100 MHz) δ (ppm): 31.4, 35.0, 53.4, 56.6, 58.7, 66.5, 74.7, 114.9, 122.4, 125.8, 128.4 (2C), 138.7, 141.7, 151.8. $[\alpha]_D^{20}$ = +38.3 (c = 1.0, CH_3OH). Spectral data matches that recorded by M. O'Reilly and C. Lindsley.

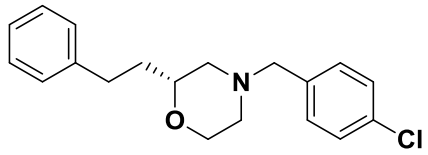

ML398

(*R*)-4-(4-chlorobenzyl)-2-phenethylmorpholine (VU0603865, ML398). In a microwave vial, suspended (*R*)-2-phenethylmorpholine (0.100 g, 0.523 mmol) in anhydrous acetonitrile (2.6 mL). Potassium carbonate (0.361 g, 2.61 mmol) and 4-chlorobenzyl bromide (0.107 g, 0.523 mmol) were added. This was heated under microwave conditions to 120 °C for ten minutes. Water was added and the product was extracted with ethyl acetate. The organic layer was dried over sodium sulfate, filtered, and concentrated *in vacuo*. The crude material was purified by column chromatography (0-30% ethyl acetate in hexanes) to provide pure product (0.103 mg, 61%).

^{1}H NMR ($CDCl_3$, 400 MHz) δ (ppm): 1.73 (dm, *J* = 64 Hz, 2H), 1.88 (t, *J* = 10.4 Hz, 1H), 2.20 (dt, *J* = 3.1, 11.5 Hz, 1H), 2.59-2.71 (m, 3H), 2.73-2.84 (m, 1H), 3.45 (s, 2H), 3.45-3.53 (m, 1H), 3.65 (t, *J* = 11.3 Hz, 1H), 3.89 (d, *J* = 11.5 Hz, 1H), 7.15-7.22 (m, 3H), 7.23-7.32 (m, 6H). **^{13}C NMR** ($CDCl_3$, 100 MHz) δ (ppm): 31.5, 35.2, 53.1, 58.5, 62.4, 66.6, 74.8, 125.7, 128.3 (2C), 128.4, 130.3, 132.8, 136.3, 141.9. **LCMS:** R_T 0.850 min, *m/z* = 316.9 $[M+H]^+$, >99% @ 215 and 254 nm. **HRMS**: $C_{19}H_{23}NOCl$, Calculated $[M+H]^+$: 316.1468, Found $[M+H]^+$: 316.1470. $[\alpha]_D^{20}$ = +29.3 (c = 1.0, CH_3OH, 92% ee).

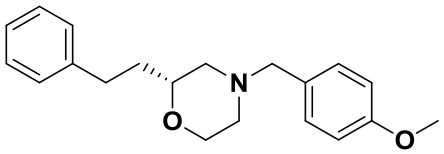

(*R*)-4-(4-methoxybenzyl)-2-phenethylmorpholine (VU0603864).

^{1}H NMR ($CDCl_3$, 400 MHz) δ (ppm): 1.58-1.71 (m, 1H), 1.75-1.91 (m, 2H), 2.15 (dt, *J* = 3.3, 11.4 Hz, 1H), 2.60-2.82 (m, 4H), 3.43 (s, 2H), 3.45-3.54 (m, 1H), 3.65 (dt, *J* = 2.4, 11.3 Hz, 1H), 3.81 (s, 3H), 3.88 (dm, *J* = 11.3 Hz, 1H), 6.86 (d, *J* = 8.6 Hz, 2H), 7.15-7.30 (m, 7H). **^{13}C NMR** ($CDCl_3$, 100 MHz) δ (ppm): 31.5, 35.3, 53.1, 55.2, 58.5, 62.6, 66.7, 74.8, 113.5, 125.7, 128.3, 128.4, 129.7, 130.3, 142.0, 158.7. **LCMS:** R_T 0.852 min, *m/z* = 312.0 $[M+H]^+$, >99% @ 215 and 254 nm. **HRMS**: $C_{20}H_{26}NO_2$, Calculated $[M+H]^+$: 312.1964, Found $[M+H]^+$: 312.1964. $[\alpha]_D^{20}$ = +44.4 (c = 0.33, CH_3OH, 92% ee).

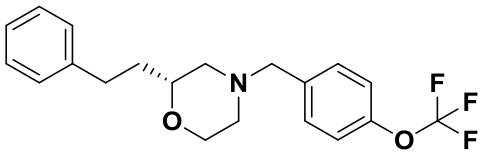

(*R*)-2-phenethyl-4-(4-(trifluoromethoxy)benzyl)morpholine (VU0603764).

^{1}H NMR ($CDCl_3$, 400 MHz) δ (ppm): 1.61-1.87 (m, 2H), 1.91 (t, *J* = 11.0 Hz, 1H), 2.19 (dt, *J* = 3.3, 11.3 Hz, 1H), 2.60-2.73 (m, 3H), 2.74-2.84 (m, 1H), 3.46 (s, 2H), 3.46-3.55 (m, 1H), 3.67 (dt, *J* = 2.4, 11.4 Hz, 1H), 3.87-3.93 (m, 1H), 7.14-7.23 (m, 5H), 7.25-7.31 (m, 2H), 7.32-7.38 (m, 2H). **^{13}C NMR** ($CDCl_3$, 100 MHz) δ (ppm): 31.5, 35.2, 53.1, 58.6, 62.3, 66.7, 74.8, 120.7, 125.7, 128.3, 128.4, 130.2, 136.6, 141.9, 148.2. **LCMS:** R_T 0.997 min, *m/z* = 365.9 $[M+H]^+$, >99% @ 215 and 254 nm. **HRMS**: $C_{20}H_{23}NO_2F_3$, Calculated $[M+H]^+$: 366.1681, Found $[M+H]^+$: 366.1679. $[\alpha]_D^{20}$ = +22.6 (c = 1.0, CH_3OH, 92% ee).

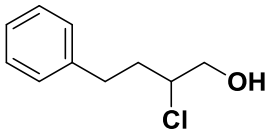

2.11

2-chloro-4-phenylbutan-1-ol (2.11). Suspended 4-phenylbutanal (1.16 g, 7.83 mmol) in anhydrous dichloromethane (31.0 mL) and cooled to 0 °C. DL-proline (180 mg, 1.56 mmol) was added followed by *N*-chlorosuccinimide (1.36 g, 10.2 mmol). The progress of this reaction was

monitored by proton NMR (the starting material aldehyde peak being converted to the mono-chlorinated aldehyde). Once complete, methanol (31.0 mL) was added at 0 °C followed by slow addition of sodium borohydride (1.48 g, 39.1 mmol). Continued stirring for 30 minutes before water was added and the solution was extracted with dichloromethane. After drying over sodium sulfate, filtering, and concentrating, the crude material was purified by column chromatography (0-45% ethyl acetate in hexanes). Pure racemic chloro-alcohol was collected (1.10 g, 76%).
^{1}H NMR ($CDCl_3$, 400 MHz) δ (ppm): 1.99-2.09 (m, 3H), 2.73-2.80 (m, 1H), 2.87-2.94 (m, 1H), 3.67-3.82 (m, 2H), 3.96-4.02 (m, 1H), 7.20-7.33 (m, 5H). **^{13}C NMR** ($CDCl_3$, 100 MHz) δ (ppm): 32.3, 35.8, 64.0, 66.9, 126.2, 128.4, 128.5, 140.6.

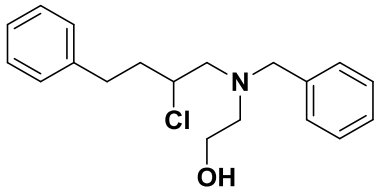

2.12

2-(benzyl(2-chloro-4-phenylbutyl)amino)ethanol (2.12). 2-chloro-4-phenylbutan-1-ol (0.537 g, 2.91 mmol) was suspended in anhydrous dichloromethane (29.0 mL) and to this 2,6-lutidine (3.37 mL, 29.1 mmol) was added. This solution was cooled to -78 °C before triflic anhydride (0.63 mL, 3.78 mmol) was added dropwise. This was stirred 30 minutes and the triflate was confirmed to be formed by proton NMR. *N*-benzylethanolamine (2.1 mL, 14.5 mmol) in anhydrous dichloromethane (2.0 mL) was added to the solution dropwise. The reaction was allowed to warm to room temperature slowly overnight and the consumption of the triflate was established by NMR. Diethyl ether (100 mL) and water (100 mL) was added and the organic layer was separated from the aqueous, dried over sodium sulfate, filtered, and concentrated *in vacuo*. The crude product was purified by column chromatography (0-20% ethyl acetate in hexanes) to yield the racemic chloro-aminoalcohol (0.718 g, 78%).
^{1}H NMR ($CDCl_3$, 400 MHz) δ (ppm): 1.88-1.99 (m, 1H), 2.07-2.18 (m, 1H), 2.63-2.96 (m, 7H), 3.53-3.76 (m, 4H), 3.90-3.99 (m, 1H), 7.20-7.40 (m, 10H). **^{13}C NMR** ($CDCl_3$, 100 MHz) δ (ppm): 32.3, 37.6, 56.3, 58.8, 59.3, 60.3, 61.1, 126.1, 127.4, 128.4, 128.5, 128.5, 129.0, 138.2, 140.8.
LCMS: R_T 0.892 min, *m/z* = 319.9 $[M+H]^+$, >99% @ 215 nm.

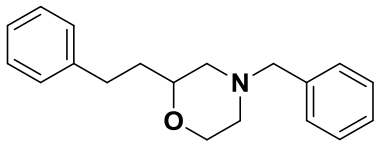

2.13

4-benzyl-2-phenethylmorpholine (2.13, VU0517051). Suspended 2-(benzyl(2-chloro-4-phenylbutyl) amino)ethanol (0.650 g, 2.05 mmol) in anhydrous acetonitrile (100 mL) and cooled to -20 °C. Potassium *tert*-butoxide (1.15 g, 10.2 mmol) was added and the progress of the reaction was followed by TLC. Upon consumption of starting material, water and diethyl ether were added to the reaction and it was extracted with ether, dried over sodium sulfate, filtered, and concentrated. The crude material was purified by column chromatography (0-40% ethyl acetate in hexanes) to give the racemic morpholine (0.316 g, 55%).

^{1}H NMR ($CDCl_3$, 400 MHz) δ (ppm): 1.63-1.74 (m, 1H), 1.78-1.89 (m, 1H), 1.92 (t, *J* = 10.7 Hz, 1H), 2.21 (td, *J* = 3.2, 11.1 Hz, 1H), 2.63-2.86 (m, 4H), 3.50-3.58 (m, 3H), 3.70 (td, *J* = 2.4, 11.1 Hz, 1H), 3.92 (d, *J* = 11.1 Hz, 1H), 7.18-7.24 (m, 3H), 7.25-7.39 (m, 7H). **^{13}C NMR** ($CDCl_3$, 100 MHz) δ (ppm): 31.5, 35.3, 53.2, 58.6, 63.3, 66.7, 74.8, 125.7, 127.1, 128.2, 128.3, 128.4, 129.1, 137.7, 142.0. **LCMS:** R_T 0.924 min, *m/z* = 282.0 $[M+H]^+$, >99% @ 215 nm.

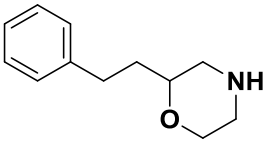

2.3

2-phenethylmorpholine (2.3). Suspended 4-benzyl-2-phenethylmorpholine (200 mg, 0.711 mmol) in anhydrous methanol (10.0 mL). The flask was purged three times alternating vacuum and argon. Added to this was 10% Pd/C (15.1 mg, 0.142 mmol) and the flask was purged three times alternating vacuum and hydrogen gas. The reaction was followed by TLC and LCMS until it was complete. The solution was then filtered through celite with methanol, concentrated, and carried on crude.

General procedure for *N*-alkylation:

2-phenethylmorpholine (7.5 mg, 0.04 mmol) was suspended in *N*,*N*-dimethylformamide (0.50 mL). To this was added Hunig's base (34 μL, 0.19 mmol) and the desired benzyl halide (0.05 mmol). The reaction was stirred at 40 °C for 30 minutes before being purified by automated reverse phase column chromatography.

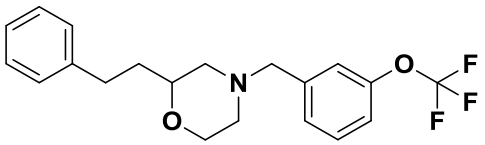

2-phenethyl-4-(3-(trifluoromethoxy)benzyl)morpholine (VU0517381).

^{1}H NMR ($CDCl_3$, 400 MHz) δ (ppm): 1.60-1.86 (m, 2H), 1.86-2.00 (m, 1H), 2.13-2.28 (m, 1H), 2.58-2.84 (m, 4H), 3.50 (bs, 2H), 3.60-3.76 (m, 1H), 3.84-3.94 (m, 1H), 7.09-7.14 (m, 1H), 7.14-7.23 (m, 4H), 7.23-7.29 (m, 3H), 7.30-7.37 (m, 1H). **^{13}C NMR** ($CDCl_3$, 100 MHz) δ (ppm): 31.5, 35.2, 52.9, 58.3, 62.4, 66.4, 74.7, 119.1, 119.6, 121.4, 125.7, 127.3, 128.3 (2C), 129.6, 141.8, 149.3. **LCMS:** R_T 0.987 min, *m/z* = 365.9 $[M+H]^+$, >99% @ 215 and 254 nm.

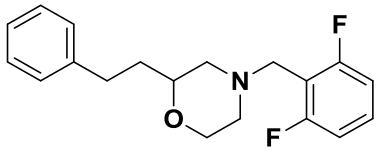

4-(2,6-difluorobenzyl)-2-phenethylmorpholine (VU0517302).

^{1}H NMR ($CDCl_3$, 400 MHz) δ (ppm): 1.60-1.86 (m, 2H), 1.93-2.06 (m, 1H), 2.22-2.35 (m, 1H), 2.59-2.84 (m, 4H), 3.50 (bs, 1H), 3.59-3.78 (m, 3H), 3.84-3.94 (m, 1H), 6.86-6.94 (m, 2H), 7.14-7.20 (m, 3H), 7.22-7.30 (m, 3H). **^{13}C NMR** ($CDCl_3$, 100 MHz) δ (ppm): 31.5, 35.3, 48.7, 52.0, 57.5, 66.5, 74.7, 111.0, 111.2, 125.7, 128.3, 128.4, 129.5, 141.9, 160.7, 160.8, 163.2 (2C). **LCMS:** R_T 0.880 min, *m/z* = 317.9 $[M+H]^+$, >99% @ 215 and 254 nm.

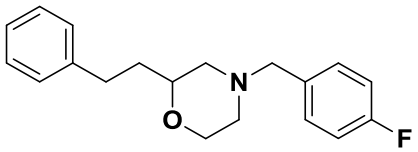

4-(4-fluorobenzyl)-2-phenethylmorpholine (VU0517120).

^{1}H NMR ($CDCl_3$, 400 MHz) δ (ppm): 1.60-1.85 (m, 2H), 1.85-1.94 (m, 1H), 2.13-2.24 (m, 1H), 2.60-2.73 (m, 3H), 2.73-2.83 (m, 1H), 3.46 (s, 2H), 3.48-3.56 (m, 1H), 3.61-3.73 (m, 1H), 3.86-3.93 (m, 1H), 7.01 (t, *J* = 8.6 Hz, 1H), 7.15-7.21 (m, 3H), 7.24-7.32 (m, 4H). **^{13}C NMR** ($CDCl_3$, 100 MHz) δ (ppm): 31.5, 35.3, 53.0, 58.4, 62.4, 66.6, 74.8, 114.9, 115.1, 125.7, 128.3, 128.4, 130.5, 130.6, 141.9. **LCMS:** R_T 0.842 min, *m/z* = 300.0 $[M+H]^+$, >99% @ 215 and 254 nm.

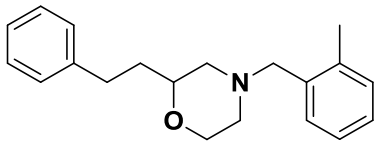

4-(2-methylbenzyl)-2-phenethylmorpholine (VU0517380).

^{1}H NMR ($CDCl_3$, 400 MHz) δ (ppm): 1.60-1.86 (m, 2H), 1.90-2.00 (m, 1H), 2.10-2.30 (m, 1H), 2.36 (s, 3H), 2.57-2.73 (m, 3H), 2.72-2.83 (m, 1H), 3.44 (bs, 2H), 3.56-3.70 (m, 1H), 3.84-3.90 (m, 1H), 7.11-7.20 (m, 6H), 7.22-7.29 (m, 3H). **^{13}C NMR** ($CDCl_3$, 100 MHz) δ (ppm): 19.2, 31.6, 35.3, 53.2, 58.6, 61.1, 66.8, 74.9, 125.4, 125.7, 127.1, 128.3, 128.4, 129.8, 130.2, 137.5, 142.0. **LCMS:** R_T 0.946 min, *m/z* = 296.0 $[M+H]^+$, >99% @ 215 and 254 nm.

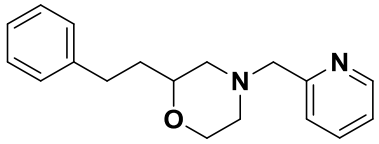

2-phenethyl-4-(pyridin-2-ylmethyl)morpholine (VU0517003).

LCMS: R_T 0.744 min, *m/z* = 283.1 $[M+H]^+$, >99% @ 215 and 254 nm.

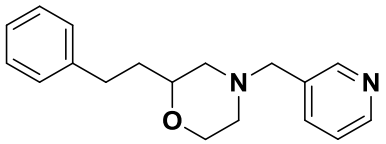

2-phenethyl-4-(pyridin-3-ylmethyl)morpholine (VU0517029).

LCMS: R_T 0.610 min, *m/z* = 283.0 $[M+H]^+$, >99% @ 215 and 254 nm.

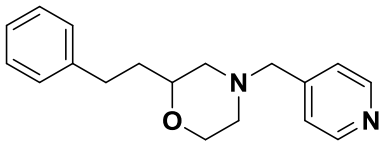

2-phenethyl-4-(pyridin-4-ylmethyl)morpholine (VU0517301).

LCMS: R_T 0.675 min, *m/z* = 283.0 $[M+H]^+$, >99% @ 215 and 254 nm.

General procedure for amide synthesis:

2-phenethylmorpholine (7.5 mg, 0.04 mmol) was suspended in *N*,*N*-dimethylformamide (0.50 mL). To this was added Hunig's base (34 μL, 0.19 mmol) and the desired acid chloride (0.05 mmol). The reaction was stirred at room temperature for one hour before being purified by automated reverse phase column chromatography.

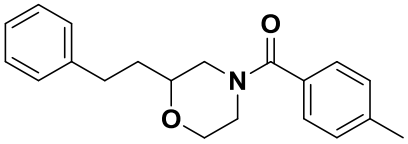

(2-phenethylmorpholino)(*p*-tolyl)methanone (VU0517002).

LCMS: R_T 1.128 min, *m/z* = 310.0 $[M+H]^+$, >99% @ 215 and 254 nm.

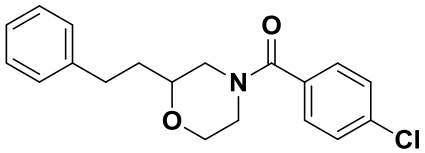

(4-chlorophenyl)(2-phenethylmorpholino)methanone (VU0517030).

LCMS: R_T 1.142 min, *m/z* = 330.9 $[M+H]^+$, >99% @ 215 and 254 nm.

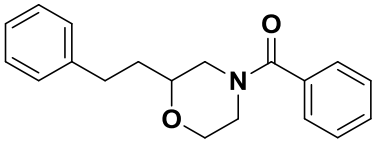

(2-phenethylmorpholino)(phenyl)methanone (VU0517052).

LCMS: R_T 1.072 min, *m/z* = 296.0 $[M+H]^+$, >99% @ 215 and 254 nm.

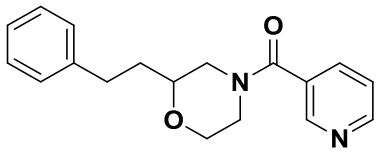

(2-phenethylmorpholino)(pyridin-3-yl)methanone (VU0517053).

LCMS: R_T 0.813 min, *m/z* = 296.9 $[M+H]^+$, >99% @ 215 and 254 nm.

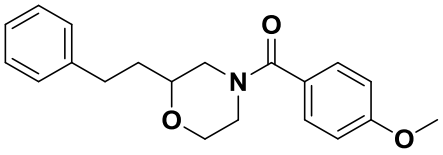

(4-methoxyphenyl)(2-phenethylmorpholino)methanone (VU0517134).

LCMS: R_T 1.074 min, *m/z* = 326.0 $[M+H]^+$, >99% @ 215 and 254 nm.

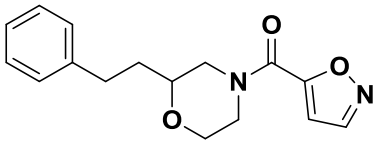

Isoxazol-5-yl(2-phenethylmorpholino)methanone (VU0517298).

LCMS: R_T 0.992 min, *m/z* = 286.9 $[M+H]^+$, >92% @ 215 nm.

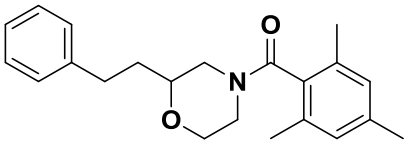

Mesityl(2-phenethylmorpholino)methanone (VU0517299).

LCMS: R_T 1.207 min, *m/z* = 338.0 $[M+H]^+$, >99% @ 215 and 254 nm.

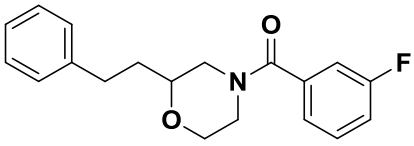

(3-fluorophenyl)(2-phenethylmorpholino)methanone (VU0517300).

LCMS: R_T 1.104 min, *m/z* = 313.9 $[M+H]^+$, >94% @ 215 nm.

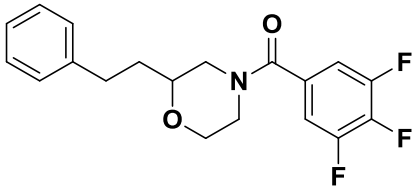

(2-phenethylmorpholino)(3,4,5-trifluorophenyl)methanone (VU0517354).

LCMS: R_T 1.163 min, *m/z* = 349.9 $[M+H]^+$, >97% @ 215 nm.

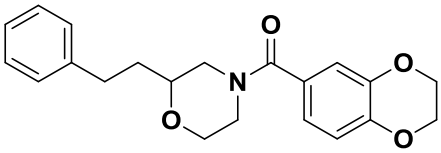

(2,3-dihydrobenzo[*b*][1,4]dioxin-6-yl)(2-phenethylmorpholino)methanone (VU0517379).

LCMS: R_T 1.074 min, *m/z* = 353.9 $[M+H]^+$, >96% @ 215 nm.

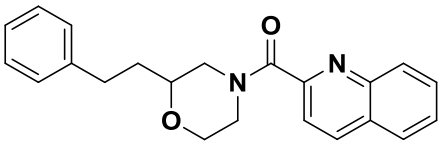

(2-phenethylmorpholino)(quinolin-2-yl)methanone (VU0517523).

LCMS: R_T 1.118 min, *m/z* = 346.9 $[M+H]^+$, >95% @ 215 nm.

General procedure for Buchwald–Hartwig coupling:

2-phenethylmorpholine (7.5 mg, 0.04 mmol) was suspended in 1,4-dioxane (0.50 mL). To this was added tris(dibenzylideneacetone)dipalladium(0) (1.8 mg, 0.002 mmol), 4,5-bis(diphenylphosphino)-9,9-dimethylxanthene (2.3 mg, 0.004 mmol), cesium carbonate (32 mg, 0.10 mmol), and the desired aryl bromide (0.033 mmol). The reaction was stirred under argon at 100 °C for 18 hours. When complete, the reaction was quenched with water and extracted with ethyl acetate before being purified by automated reverse phase column chromatography.

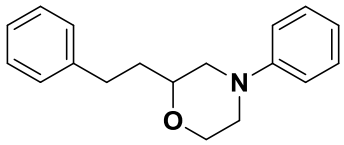

2-phenethyl-4-phenylmorpholine (VU0517240).

LCMS: R_T 1.177 min, *m/z* = 268.0 $[M+H]^+$, >95% @ 215 nm.

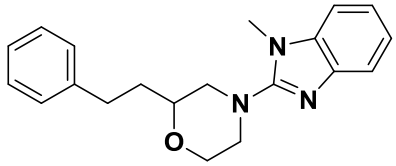

4-(1-methyl-1*H*-benzo[*d*]imidazol-2-yl)-2-phenethylmorpholine (VU0517535).

LCMS: R_T 0.931 min, *m/z* = 322.0 $[M+H]^+$, >99% @ 215 and 254 nm.

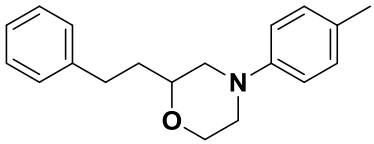

2-phenethyl-4-(*p*-tolyl)morpholine (VU0517595).

LCMS: R_T 1.117 min, *m/z* = 282.0 $[M+H]^+$, >99% @ 215 and 254 nm.

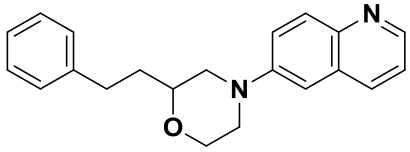

2-phenethyl-4-(quinolin-6-yl)morpholine (VU0517596).

LCMS: R_T 0.961 min, *m/z* = 319.0 $[M+H]^+$, >99% @ 215 and 254 nm.

General procedure for urea synthesis:

2-phenethylmorpholine (7.5 mg, 0.04 mmol) was suspended in tetrahydrofuran (0.50 mL). To this was added the desired aryl isocyanate (0.05 mmol). The reaction was stirred at room temperature for one hour before being purified by automated reverse phase column chromatography.

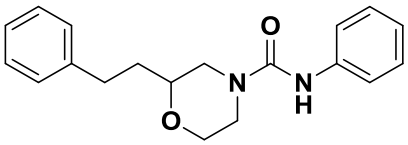

2-phenethyl-*N*-phenylmorpholine-4-carboxamide (VU0517262).

LCMS: R_T 1.127 min, *m/z* = 311.0 $[M+H]^+$, >99% @ 215 and 254 nm.

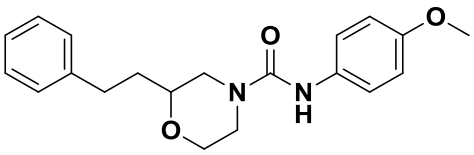

***N*-(4-methoxyphenyl)-2-phenethylmorpholine-4-carboxamide (VU0517319).**

LCMS: R_T 1.098 min, *m/z* = 340.9 $[M+H]^+$, >99% @ 215 and 254 nm.

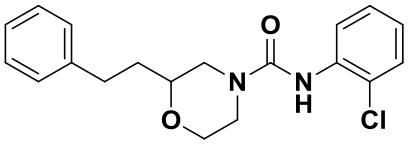

***N*-(2-chlorophenyl)-2-phenethylmorpholine-4-carboxamide (VU0517320).**

LCMS: R_T 1.185 min, *m/z* = 345.9 $[M+H]^+$, >99% @ 215 and 254 nm.

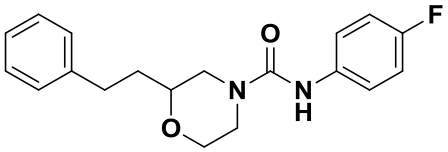

***N*-(4-fluorophenyl)-2-phenethylmorpholine-4-carboxamide (VU0517328).**

LCMS: R_T 1.127 min, *m/z* = 328.9 $[M+H]^+$, >99% @ 215 and 254 nm.

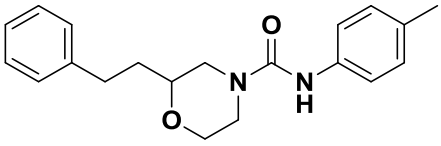

2-phenethyl-*N*-(*p*-tolyl)morpholine-4-carboxamide (VU0517347).

LCMS: R_T 1.150 min, *m/z* = 325.0 $[M+H]^+$, >99% @ 215 and 254 nm.

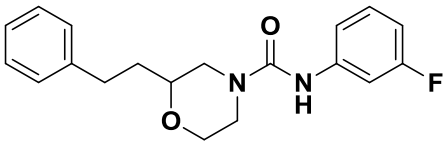

***N*-(3-fluorophenyl)-2-phenethylmorpholine-4-carboxamide (VU0517348).**

LCMS: R_T 1.151 min, *m/z* = 328.9 $[M+H]^+$, >95% @ 215 nm.

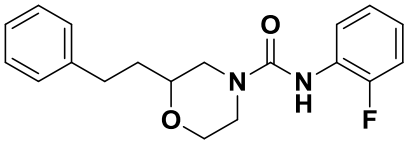

***N*-(2-fluorophenyl)-2-phenethylmorpholine-4-carboxamide (VU0517572).**

LCMS: R_T 1.107 min, *m/z* = 328.9 $[M+H]^+$, >94% @ 215 nm.

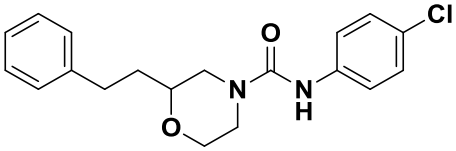

***N*-(4-chlorophenyl)-2-phenethylmorpholine-4-carboxamide (VU0517647).**

LCMS: R_T 1.181 min, *m/z* = 345.9 $[M+H]^+$, >99% @ 215 and 254 nm.

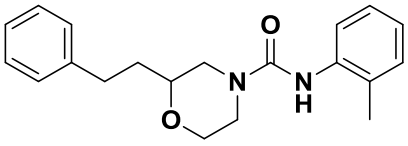

2-phenethyl-*N*-(*o*-tolyl)morpholine-4-carboxamide (VU0517574).

LCMS: R_T 1.107 min, *m/z* = 325.0 $[M+H]^+$, >99% @ 215 and 254 nm.

General procedure for sulfonamide synthesis:

2-phenethylmorpholine (7.5 mg, 0.04 mmol) was suspended in *N*,*N*-dimethylformamide (0.50 mL). To this was added Hunig's base (34 µL, 0.19 mmol) and the desired sulfonyl chloride (0.05 mmol). The reaction was stirred at 40 °C for one hour before being purified by automated reverse phase column chromatography.

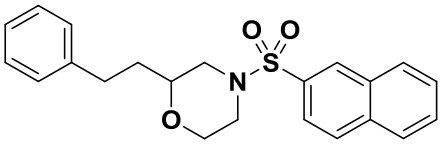

4-(naphthalen-2-ylsulfonyl)-2-phenethylmorpholine (VU0517473).

LCMS: R_T 1.236 min, *m/z* = 382.1 $[M+H]^+$, >99% @ 215 and 254 nm.

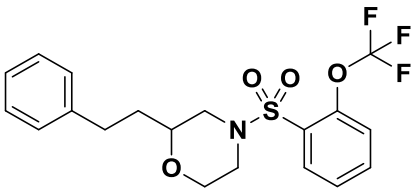

2-phenethyl-4-((2-(trifluoromethoxy)phenyl)sulfonyl)morpholine (VU0517474).

LCMS: R_T 1.292 min, *m/z* = 415.8 $[M+H]^+$, >95% @ 215 nm.

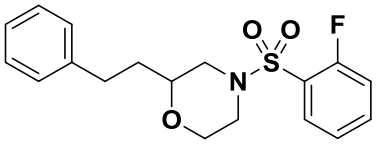

4-((2-fluorophenyl)sulfonyl)-2-phenethylmorpholine (VU0517475).

LCMS: R_T 1.206 min, *m/z* = 349.9 $[M+H]^+$, >95% @ 215 nm.

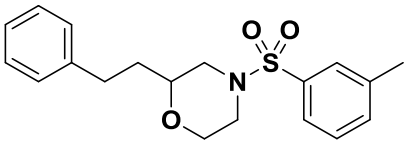

2-phenethyl-4-(*m*-tolylsulfonyl)morpholine (VU0517476).

LCMS: R_T 1.247 min, *m/z* = 345.9 $[M+H]^+$, >99% @ 215 and 254 nm.

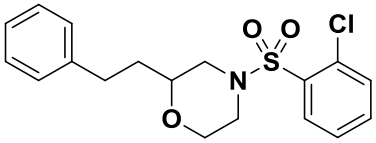

4-((2-chlorophenyl)sulfonyl)-2-phenethylmorpholine (VU0517550).

LCMS: R_T 1.233 min, *m/z* = 366.8 $[M+H]^+$, >99% @ 215 and 254 nm.

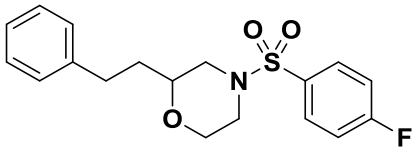

4-((4-fluorophenyl)sulfonyl)-2-phenethylmorpholine (VU0517570).

LCMS: R_T 1.216 min, *m/z* = 349.9 $[M+H]^+$, >99% @ 215 and 254 nm.

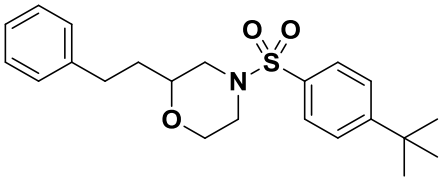

4-((4-(*tert*-butyl)phenyl)sulfonyl)-2-phenethylmorpholine (VU0517594).

LCMS: R_T 1.372 min, *m/z* = 387.9 $[M+H]^+$, >95% @ 215 nm.

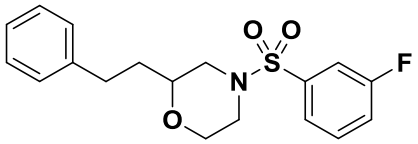

4-((3-fluorophenyl)sulfonyl)-2-phenethylmorpholine (VU0517651).

LCMS: R_T 1.221 min, *m/z* = 349.9 $[M+H]^+$, >95% @ 215 nm.

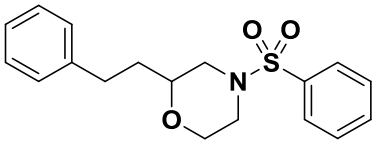

2-phenethyl-4-(phenylsulfonyl)morpholine (VU0517653).

LCMS: R_T 1.131 min, *m/z* = 332.1 $[M+H]^+$, >99% @ 215 and 254 nm.

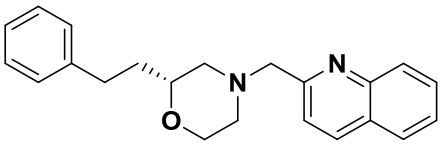

(*R*)-2-phenethyl-4-(quinolin-2-ylmethyl)morpholine (VU0651729).

^{1}H NMR ($CDCl_3$, 400 MHz) δ (ppm): 1.60-1.88 (m, 2H), 2.04-2.16 (m, 1H), 2.34-2.46 (m, 1H), 2.60-2.70 (m, 1H), 2.71-2.83 (m, 3H), 3.58 (bs, 1H), 3.69-3.80 (m, 1H), 3.85 (s, 2H), 3.88-3.95

(m, 1H), 7.14-7.19 (m, 3H), 7.23-7.29 (m, 2H), 7.50-7.56 (m, 1H), 7.64 (d, *J* = 8.4 Hz, 1H), 7.68-7.74 (m, 1H), 7.81 (d, *J* = 8.1 Hz, 1H), 8.09 (d, *J* = 8.5 Hz, 1H), 8.14 (d, *J* = 8.5 Hz, 1H). **^{13}C NMR** ($CDCl_3$, 100 MHz) δ (ppm): 31.5, 35.2, 53.3, 58.7, 65.3, 66.6, 74.8, 121.1, 125.7, 126.2, 127.4, 127.5, 128.3, 128.4, 129.0, 129.4, 136.4, 141.9, 147.6. **LCMS:** R_T 0.929 min, *m/z* = 333.0 $[M+H]^+$, >91% @ 215 nm. **HRMS**: $C_{22}H_{25}N_2O$, Calculated $[M+H]^+$: 333.1967, Found $[M+H]^+$: 333.1966. $[\alpha]_D^{20}$ = +19.9 (c = 1.0, CH_3OH, 92% ee).

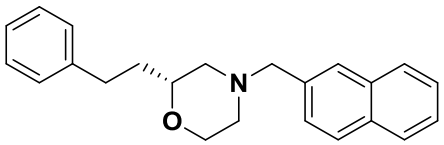

(*R*)-4-(naphthalen-2-ylmethyl)-2-phenethylmorpholine (VU0651632).

^{1}H NMR ($CDCl_3$, 400 MHz) δ (ppm): 1.51-1.79 (m, 2H), 1.82-1.96 (m, 1H), 2.10-2.25 (m, 1H), 2.50-2.61 (m, 1H), 2.61-2.77 (m, 3H), 3.46 (bs, 1H), 3.52-3.72 (m, 3H), 3.78-3.87 (m, 1H), 7.06-7.11 (m, 3H), 7.14-7.20 (m, 2H), 7.35-7.46 (m, 3H), 7.66 (s, 1H), 7.70-7.78 (m, 3H). **^{13}C NMR** ($CDCl_3$, 100 MHz) δ (ppm): 31.5, 35.2, 53.1, 58.3, 63.2, 66.4, 74.6, 125.7, 125.8, 126.0, 127.4, 127.6, 127.7, 128.0, 128.3, 128.4, 132.8, 133.2, 141.8. **LCMS:** R_T 0.933 min, *m/z* = 331.9 $[M+H]^+$, >99% @ 215 and 254 nm. **HRMS**: $C_{23}H_{26}NO$, Calculated $[M+H]^+$: 332.2014, Found $[M+H]^+$: 332.2017. $[\alpha]_D^{20}$ = +24.8 (c = 1.0, CH_3OH, 92% ee).

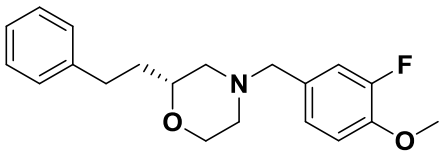

(*R*)-4-(3-fluoro-4-methoxybenzyl)-2-phenethylmorpholine (VU0652020).

^{1}H NMR ($CDCl_3$, 400 MHz) δ (ppm): 1.52-1.78 (m, 2H), 1.79 (t, *J* = 10.5 Hz, 1H), 2.08 (dt, *J* = 3.0, 11.4 Hz, 1H), 2.51-2.64 (m, 3H), 2.65-2.74 (m, 1H), 3.33 (s, 2H), 3.38-3.47 (m, 1H), 3.54-3.63 (m, 1H), 3.77-3.84 (m, 4H), 6.81 (t, *J* = 8.4 Hz, 1H), 6.88-6.94 (m, 1H), 7.00 (dd, *J* = 1.9, 12.2 Hz, 1H), 7.07-7.13 (m, 3H), 7.16-7.22 (m, 2H). **^{13}C NMR** ($CDCl_3$, 100 MHz) δ (ppm): 31.5, 35.3, 53.0, 56.2, 58.4, 62.2, 66.6, 74.8, 113.0, 116.6, 116.7, 124.6, 125.7, 128.3, 128.4, 141.9, 151.0, 153.5. **LCMS:** R_T 0.825 min, *m/z* = 330.0 $[M+H]^+$, >99% @ 215 and 254 nm. **HRMS**: $C_{20}H_{25}NO_2F$, Calculated $[M+H]^+$: 330.1869, Found $[M+H]^+$: 330.1870. $[\alpha]_D^{20}$ = +26.8 (c = 1.0, CH_3OH, 92% ee).

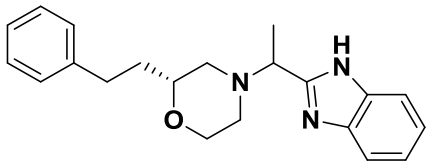

(2*R*)-4-(1-(1*H*-benzo[*d*]imidazole-2-yl)ethyl)-2-phenethylmorpholine (VU0651634).

Mixture of diastereomers: **^{1}H NMR** ($CDCl_3$, 400 MHz) δ (ppm): 1.54 (s, 3H), 1.56 (s, 3H), 1.60-1.73 (m, 2H), 1.76-1.89 (m, 2H), 2.14 (t, *J* = 10.6 Hz, 1H), 2.30 (t, *J* = 10.6 Hz, 1H), 2.43 (dt, *J* = 3.0, 11.5 Hz, 1H), 2.58-2.71 (m, 6H), 2.71-2.81 (m, 2H), 3.46-3.58 (m, 2H), 3.64-3.77 (m, 2H), 3.90-4.04 (m, 3H), 7.13-7.21 (m, 5H), 7.23-7.29 (m, 4H). **^{13}C NMR** ($CDCl_3$, 100 MHz) δ (ppm): 13.4, 14.0, 31.3, 31.4, 34.9, 35.1, 47.9, 51.6, 52.9, 57.1, 59.2, 59.4, 66.6, 74.8 (2C), 125.8, 128.3, 128.4, 141.6. **LCMS:** R_T 0.868 min, *m/z* = 336.0 $[M+H]^+$, >99% @ 215 and 254 nm. **HRMS**: $C_{21}H_{25}N_3O$, Calculated $[M+H]^+$: 335.1998, Found $[M+H]^+$: 335.2001.

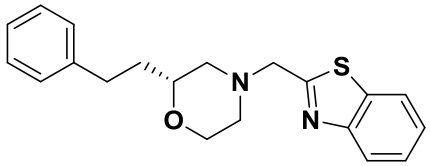

(*R*)-4-(benzo[*d*]thiazol-2-ylmethyl)-2-phenethylmorpholine (VU0651731).

^{1}H NMR ($CDCl_3$, 400 MHz) δ (ppm): 1.63-1.90 (m, 2H), 2.11-2.25 (m, 1H), 2.40-2.55 (m, 1H), 2.61-2.82 (m, 2H), 2.82-2.94 (m, 2H), 3.60 (bs, 1H), 3.70-3.83 (m, 1H), 3.90-4.05 (m, 3H), 7.15-7.21 (m, 3H), 7.24-7.30 (m, 1H), 7.36 (t, *J* = 7.4 Hz, 1H), 7.47 (t, *J* = 7.6 Hz, 1H), 7.88 (d, *J* = 7.9 Hz, 1H), 7.99 (d, *J* = 8.0 Hz, 1H). **^{13}C NMR** ($CDCl_3$, 100 MHz) δ (ppm): 31.5, 35.1, 53.2, 58.5, 60.3, 66.5, 74.8, 121.7, 122.8, 124.9, 125.8, 125.9, 128.3, 128.4, 135.4, 141.8, 153.2. **LCMS:** R_T 0.933 min, *m/z* = 339.0 $[M+H]^+$, >99% @ 215 and 254 nm. **HRMS**: $C_{20}H_{22}N_2OS$, Calculated $[M+H]^+$: 338.1453, Found $[M+H]^+$: 338.1457. $[\alpha]_D^{20}$ = +40.05 (c = 0.5, CH_3OH).

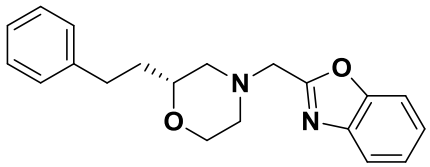

(*R*)-2-((2-phenthylmorpholino)methyl)benzo[*d*]oxazole (VU0651677).

^{1}H NMR ($CDCl_3$, 400 MHz) δ (ppm): 1.62-1.88 (m, 2H), 2.11-2.26 (m, 1H), 2.40-2.56 (m, 1H), 2.60-2.83 (m, 2H), 2.87 (d, *J* = 10.2 Hz, 2H), 3.62 (bs, 1H), 3.71-3.84 (m, 1H), 3.85-3.98 (m, 3H),

7.13-7.20 (m, 3H), 7.22-7.29 (m, 1H), 7.32-7.39 (m, 2H), 7.52-7.58 (m, 1H), 7.70-7.76 (m, 1H). **^{13}C NMR** ($CDCl_3$, 100 MHz) δ (ppm): 31.4, 35.1, 52.8, 55.3, 58.2, 66.3, 74.5, 110.7, 120.71, 124.4, 125.2, 125.8, 128.3, 128.4, 140.8, 141.7, 150.9. **LCMS:** R_T 0.904 min, *m/z* = 323.0 $[M+H]^+$, >99% @ 215 and 254 nm. **HRMS**: $C_{20}H_{22}N_2O_2$, Calculated $[M+H]^+$: 322.1681, Found $[M+H]^+$: 322.1687. $[\alpha]_D^{20}$ = +19.8 (c = 0.5, CH_3OH).

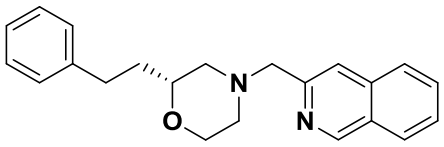

(*R*)-4-(isoquinolin-3-ylmethyl)-2-phenethylmorpholine (VU0651675).

^{1}H NMR ($CDCl_3$, 400 MHz) δ (ppm): 1.60-1.88 (m, 2H), 2.07-2.20 (m, 1H), 2.36-2.49 (m, 1H), 2.56-2.70 (m, 1H), 2.72-2.85 (m, 3H), 3.65 (bs, 1H), 3.71-3.82 (m, 1H), 3.83-3.95 (m, 3H), 7.14-7.19 (m, 3H), 7.23-7.28 (m, 2H), 7.54 (t, *J* = 7.4 Hz, 1H), 7.62-7.68 (m, 1H), 7.69-7.74 (m, 1H), 7.82 (d, *J* = 8.0 Hz, 1H), 8.08 (d, *J* = 8.6 Hz, 1H), 8.14 (d, *J* = 8.4 Hz, 1H). **^{13}C NMR** ($CDCl_3$, 100 MHz) δ (ppm): 31.4, 35.2, 53.3, 58.6, 65.2, 66.5, 74.7, 121.2, 125.7, 126.3, 127.4, 127.5, 128.3, 128.4, 129.0, 129.4, 136.5, 141.8, 147.6. **LCMS:** R_T 0.880 min, *m/z* = 333.0 $[M+H]^+$, >99% @ 215 and 254 nm. **HRMS**: $C_{22}H_{24}N_2O$, Calculated $[M+H]^+$: 332.1889, Found $[M+H]^+$: 332.1894. $[\alpha]_D^{20}$ = +21.1 (c = 0.1, CH_3OH, 92% ee).

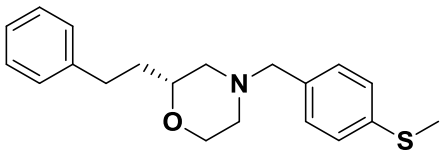

(*R*)-4-(4-(methylthio)benzyl)-2-phenethylmorpholine (VU0651676).

^{1}H NMR ($CDCl_3$, 400 MHz) δ (ppm): 1.60-1.86 (m, 2H), 1.86-1.97 (m, 1H), 2.13-2.26 (m, 1H), 2.49 (s, 3H), 2.59-2.83 (m, 4H), 3.41-3.60 (m, 3H), 3.62-3.75 (m, 1H), 3.89 (d, *J* = 11.4 Hz, 1H), 7.14-7.30 (m, 9H). **^{13}C NMR** ($CDCl_3$, 100 MHz) δ (ppm): 15.9, 31.5, 35.3, 53.0, 58.4, 62.6, 66.5, 74.7, 123.5, 125.7, 126.5, 128.3, 128.4, 129.7, 141.9. **LCMS:** R_T 0.907 min, *m/z* = 327.9 $[M+H]^+$, >99% @ 215 and 254 nm. **HRMS**: $C_{20}H_{25}NOS$, Calculated $[M+H]^+$: 327.1657, Found $[M+H]^+$: 327.1663. $[\alpha]_D^{20}$ = +29.1 (c = 0.5, CH_3OH, 92% ee).

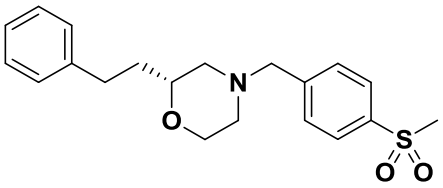

(*R*)-4-(4-(methylsulfonyl)benzyl)-2-phenethylmorpholine (VU0651733).

^{1}H NMR ($CDCl_3$, 400 MHz) δ (ppm): 1.60-1.87 (m, 2H), 1.90-2.01 (m, 1H), 2.19-2.31 (m, 1H), 2.60-2.73 (m, 3H), 2.73-2.84 (m, 1H), 3.06 (s, 3H), 3.47-3.64 (m, 3H), 3.64-3.76 (m, 1H), 3.91 (d, *J* = 11.3 Hz, 1H), 7.14-7.22 (m, 3H), 7.24-7.31 (m, 2H), 7.55 (d, *J* = 7.2 Hz, 2H), 7.90 (d, *J* = 8.2 Hz, 2H). **^{13}C NMR** ($CDCl_3$, 100 MHz) δ (ppm): 31.4, 35.2, 44.4, 53.1, 58.5, 62.4, 66.5, 74.7, 125.8, 127.4, 128.3, 128.4, 129.7, 141.8. **LCMS:** R_T 0.785 min, *m/z* = 359.9 $[M+H]^+$, >99% @ 215 and 254 nm. **HRMS**: $C_{20}H_{25}NO_3S$, Calculated $[M+H]^+$: 359.1555, Found $[M+H]^+$: 359.1557. $[\alpha]_D^{20}$ = +25.1 (c = 0.5, CH_3OH).

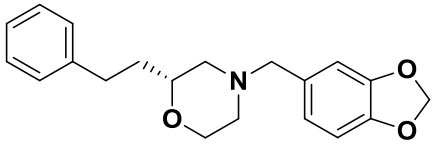

(*R*)-4-(benzo[*d*]dioxol-5-ylmethyl)-2-phenethylmorpholine (VU0651732).

^{1}H NMR ($CDCl_3$, 400 MHz) δ (ppm): 1.60-1.71 (m, 1H), 1.75-1.92 (m, 2H), 2.16 (t, *J* = 11.0 Hz, 1H), 2.59-2.83 (m, 4H), 3.41 (s, 2H), 3.51 (bs, 1H), 3.67 (t, J = 11.6 Hz, 1H), 3.85-3.92 (m, 1H), 5.95 (s, 2H), 6.75 (s, 2H), 6.85 (s, 1H), 7.15-7.21 (m, 3H), 7.24-7.30 (m, 2H). **^{13}C NMR** ($CDCl_3$, 100 MHz) δ (ppm): 31.5, 35.3, 53.0, 58.4, 62.9, 66.6, 74.8, 100.8, 107.8, 109.4, 122.2, 125.7, 128.3, 128.4, 141.9, 147.6. **LCMS:** R_T 0.857 min, *m/z* = 325.9 $[M+H]^+$, >99% @ 215 and 254 nm. **HRMS**: $C_{20}H_{23}NO_3$, Calculated $[M+H]^+$: 325.1678, Found $[M+H]^+$: 325.1683. $[\alpha]_D^{20}$ = +31.3 (c = 0.5, CH_3OH).

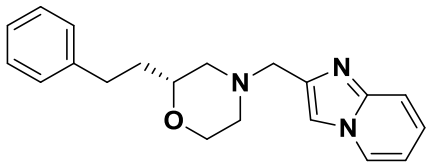

(*R*)-4-(imidazo[1,2-*a*]pyridin-2-ylmethyl)-2-phenethylmorpholine (VU0652019).

^{1}H NMR ($CDCl_3$, 400 MHz) δ (ppm): 1.60-1.87 (m, 2H), 2.02 (t, *J* = 10.6 Hz, 1H), 2.32 (dt, *J* = 3.5, 11.5 Hz, 1H), 2.59-2.82 (m, 2H), 2.82-2.90 (m, 2H), 3.53-3.62 (m, 1H), 3.68-3.78 (m, 3H),

3.87-3.93 (m, 1H), 6.76 (dt, *J* = 1.0, 6.8 Hz, 1H), 7.11-7.19 (m, 4H), 7.22-7.28 (m, 2H), 7.52 (s, 1H), 7.56 (d, *J* = 9.1 Hz, 1H), 8.10 (d, *J* = 6.8 Hz, 1H). **^{13}C NMR** ($CDCl_3$, 100 MHz) δ (ppm): 31.5, 35.3, 53.3, 56.7, 58.6, 66.5, 74.7, 111.1, 112.1, 117.4, 124.3, 125.4, 125.7, 128.2, 128.4, 141.9, 145.1. **LCMS:** R_T 0.676 min, *m/z* = 322.1 $[M+H]^+$, >99% @ 215 and 254 nm. **HRMS**: $C_{20}H_{23}N_3O$, Calculated $[M+H]^+$: 321.1841, Found $[M+H]^+$: 321.1844. $[\alpha]_D^{20}$ = +27.3 (c = 0.5, CH_3OH).

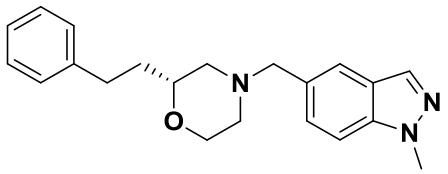

(*R*)-4-((1-methyl-1*H*-indazol-5-ylmethyl)-2-phenethylmorpholine (VU0651730).

^{1}H NMR ($CDCl_3$, 400 MHz) δ (ppm): 1.53-1.85 (m, 2H), 1.86-1.99 (m, 1H), 2.14-2.28 (m, 1H), 2.57-2.81 (m, 4H), 3.45-3.75 (m, 4H), 3.84-3.93 (m, 1H), 4.07 (s, 3H), 7.12-7.19 (m, 3H), 7.22-7.28 (m, 1H), 7.33-7.44 (m, 2H), 7.61 (s, 1H), 7.93 (s, 1H). **^{13}C NMR** ($CDCl_3$, 100 MHz) δ (ppm): 31.5, 35.3, 35.5, 53.1, 58.4, 63.2, 66.5, 74.7, 108.8, 121.2, 123.9, 125.7, 128.0, 128.2, 128.4, 132.5, 139.4, 141.9. **LCMS:** R_T 0.848 min, *m/z* = 335.9 $[M+H]^+$, >99% @ 215 and 254 nm. **HRMS**: $C_{21}H_{25}N_3O$, Calculated $[M+H]^+$: 335.1998, Found $[M+H]^+$: 335.2002. $[\alpha]_D^{20}$ = +23.8 (c = 0.333, CH_3OH, 92% ee).

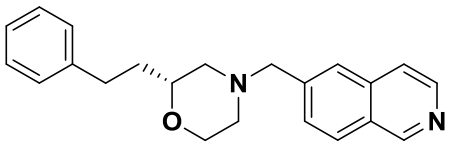

(*R*)-4-(isoquinolin-6-ylmethyl)-2-phenethylmorpholine (VU0651633).

^{1}H NMR ($CDCl_3$, 400 MHz) δ (ppm): 1.60-1.87 (m, 2H), 1.99 (t, *J* = 10.6 Hz, 1H), 2.24-2.35 (m, 1H), 2.58-2.82 (m, 4H), 3.53-3.62 (m, 1H), 3.66-3.79 (m, 3H), 3.87-3.94 (m, 1H), 7.12-7.20 (m, 3H), 7.22-7.29 (m, 2H), 7.61-7.68 (m, 2H), 7.75 (s, 1H), 7.94 (d, *J* = 8.4 Hz, 1H), 8.52 (d, *J* = 5.7 Hz, 1H), 9.23 (s, 1H). **^{13}C NMR** ($CDCl_3$, 100 MHz) δ (ppm): 31.4, 35.2, 53.1, 58.4, 63.0, 66.3, 74.6, 120.3, 125.7, 127.8, 128.1, 128.3 (2C), 128.7, 135.7, 141.8, 143.1, 152.1. **LCMS:** R_T 0.668 min, *m/z* = 333.2 $[M+H]^+$, >91% @ 215 nm. **HRMS**: $C_{22}H_{24}N_2O$, Calculated $[M+H]^+$: 332.1889, Found $[M+H]^+$: 332.1893. $[\alpha]_D^{20}$ = +30.5 (c = 0.333, CH_3OH, 92% ee).

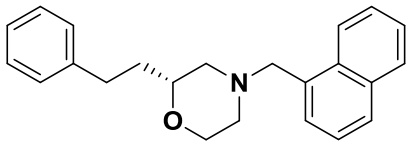

(*R*)-4-(naphthalen-1-ylmethyl)-2-phenethylmorpholine (VU6000124).

^{1}H NMR ($CDCl_3$, 400 MHz) δ (ppm): 1.59-1.87 (m, 2H), 1.92-2.05 (m, 1H), 2.20-2.34 (m, 1H), 2.56-2.66 (m, 1H), 2.66-2.83 (m, 3H), 3.43-3.55 (m, 1H), 3.57-3.72 (m, 1H), 3.82-3.98 (m, 3H), 7.12-7.19 (m, 3H), 7.22-7.28 (m, 2H), 7.37-7.45 (m, 2H), 7.46-7.56 (m, 2H), 7.75-7.83 (m, 1H), 7.83-7.94 (m, 1H), 8.28 (d, *J* = 7.2 Hz, 1H). **^{13}C NMR** ($CDCl_3$, 100 MHz) δ (ppm): 31.6, 35.3, 53.3, 58.8, 61.5, 66.7, 74.9, 124.7, 125.0, 125.6, 125.7, 128.2, 128.4, 132.5, 133.8. **LCMS:** R_T 0.862 min, *m/z* = 332.2 $[M+H]^+$, >96% @ 215 and 254 nm. **HRMS**: $C_{23}H_{25}NO$, Calculated $[M+H]^+$: 331.1936, Found $[M+H]^+$: 331.1940. $[\alpha]_D^{20}$ = +48.3 (c = 0.5, CH_3OH, 92% ee).

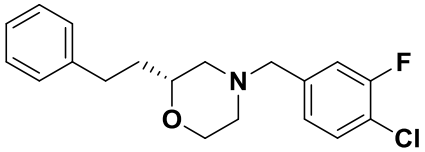

(*R*)-4-(4-chloro-3-fluorobenzyl)-2-phenethylmorpholine (VU6000123).

^{1}H NMR ($CDCl_3$, 400 MHz) δ (ppm): 1.60-1.86 (m, 2H), 1.86-1.98 (m, 1H), 2.11-2.30 (m, 1H), 2.57-2.72 (m, 3H), 2.72-2.84 (m, 1H), 3.36-3.59 (m, 3H), 3.59-3.76 (m, 1H), 3.84-3.94 (m, 1H), 7.00-7.09 (m, 1H), 7.13-7.21 (m, 4H), 7.23-7.29 (m, 2H), 7.32 (t, *J* = 7.8 Hz, 1H). **^{13}C NMR** ($CDCl_3$, 100 MHz) δ (ppm): 31.5, 35.2, 53.0, 58.4, 62.0, 66.5, 74.7, 125.2, 125.8, 128.3, 128.4, 130.3, 141.8, 156.8, 159.2. **LCMS:** R_T 0.806 min, *m/z* = 334.2 $[M+H]^+$, >99% @ 215 and 254 nm. **HRMS**: $C_{19}H_{21}ClFNO$, Calculated $[M+H]^+$: 333.1296, Found $[M+H]^+$: 333.1300. $[\alpha]_D^{20}$ = +30.2 (c = 0.5, CH_3OH, 92% ee).

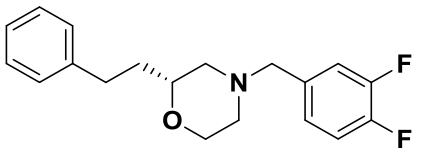

(*R*)-4-(3,4-difluorobenzyl)-2-phenethylmorpholine (VU6000122).

^{1}H NMR ($CDCl_3$, 400 MHz) δ (ppm): 1.59-1.86 (m, 2H), 1.86-2.01 (m, 1H), 2.13-2.31 (m, 1H), 2.57-2.85 (m, 4H), 3.35-3.61 (m, 3H), 3.61-3.82 (m, 1H), 3.85-3.95 (m, 1H), 6.99-7.14 (m, 2H), 7.14-7.23 (m, 4H), 7.23-7.32 (m, 2H). **^{13}C NMR** ($CDCl_3$, 100 MHz) δ (ppm): 31.5, 35.2, 52.9,

58.3, 61.9, 66.3, 74.6, 116.8, 117.0, 117.7, 125.8, 128.3 (2C), 141.8, 148.9, 151.6, 188.6. **LCMS:** R_T 0.749 min, *m/z* = 318.2 $[M+H]^+$, >96% @ 215 and 254 nm. **HRMS**: $C_{19}H_{21}F_2NO$, Calculated $[M+H]^+$: 317.1591, Found $[M+H]^+$: 317.1594. $[\alpha]_D^{20}$ = +23.4 (c = 0.5, CH_3OH, 92% ee).

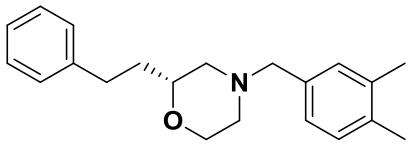

(*R*)-4-(3,4-dimethylbenzyl)-2-phenethylmorpholine (VU6000121).

^{1}H NMR ($CDCl_3$, 400 MHz) δ (ppm): 1.59-1.84 (m, 2H), 1.84-1.94 (m, 1H), 2.11-2.22 (m, 1H), 2.24 (s, 3H), 2.25 (s, 3H), 2.58-2.84 (m, 4H), 3.43 (s, 2H), 3.47-3.59 (m, 1H), 3.61-3.76 (m, 1H), 3.82-3.92 (m, 1H), 7.01-7.05 (m, 1H), 7.06-7.10 (m, 2H), 7.14-7.20 (m, 3H), 7.23-7.29 (m, 2H). **^{13}C NMR** ($CDCl_3$, 100 MHz) δ (ppm): 19.3, 19.7, 31.5, 35.3, 53.1, 58.6, 63.0, 66.7, 74.7, 125.7, 126.7, 128.2, 128.4, 129.4, 130.5, 136.4, 142.0. **LCMS:** R_T 0.825 min, *m/z* = 310.2 $[M+H]^+$, >99% @ 215 and 254 nm. **HRMS**: $C_{21}H_{27}NO$, Calculated $[M+H]^+$: 309.2093, Found $[M+H]^+$: 309.2094. $[\alpha]_D^{20}$ = +29.6 (c = 0.5, CH_3OH, 92% ee).

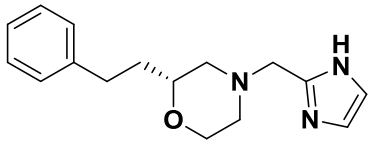

(*R*)-4-((1*H*-imidazol-2-yl)methyl)-2-phenethylmorpholine (VU0652016).

LCMS: R_T 0.701 min, *m/z* = 272.0 $[M+H]^+$, >99% @ 215 and 254 nm.

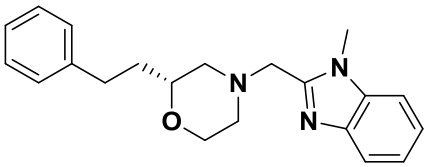

(*R*)-4-((1-methyl-1*H*-benzo[*d*]imidazol-2-yl)methyl)-2-phenethylmorpholine (VU0651665).

LCMS: R_T 0.889 min, *m/z* = 336.0 $[M+H]^+$, >99% @ 215 and 254 nm.

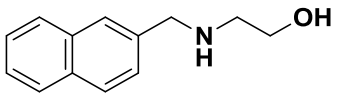

2.14

2-((naphthalen-2-ylmethyl)amino)ethan-1-ol (2.14). 2-(bromomethyl)naphthalene (1.00 g, 4.52 mmol) was suspended in isopropanol (15.0 mL) in a microwave vial. To this was added sodium hydroxide (181 mg, 4.52 mmol) and 2-aminoethan-1-ol (1.36 mL, 22.6 mmol). The vial was sealed and reacted in the microwave at 120 °C for 10 minutes. The solution was concentrated and purified by column chromatography (5-15% methanol in dichloromethane). Pure **2.14** was recovered as a white solid (766 mg, 84%).

^{1}H NMR ($CDCl_3$, 400 MHz) δ (ppm): 3.76 (t, *J* = 5.1 Hz, 2H), 3.65 (t, *J* = 5.1 Hz, 2H), 3.90 (s, 2H), 7.39-7.51 (m, 3H), 7.71 (s, 1H), 7.76-7.87 (m, 3H). **^{13}C NMR** ($CDCl_3$, 100 MHz) δ (ppm): 50.6, 53.4, 60.5, 125.5, 125.9, 126.3, 126.4, 127.5 (2C), 128.0, 132.5, 133.2, 137.0.

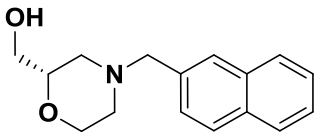

2.15

(*S*)-(4-(naphthalen-2-ylmethyl)morpholin-2-yl)methanol (2.15). Aminoalcohol **2.14** (656 mg, 3.26 mmol) was suspended in water and isopropanol (0.2 M, 1:1 v/v, 16 mL). (*R*)-(-)-Epichlorohydrin (0.27 mL, 3.42 mmol) was added and this was stirred overnight at room temperature. Tetraethylammonium hydroxide (35 wt% in water, 1.6 mL) was added the following morning and the reaction was allowed to stir for four hours. The solution was acidified to pH = 9 using 2N HCl then extracted with ethyl acetate, dried over sodium sulfate, and concentrated. Purification by column chromatography (60-100% ethyl acetate in hexanes) yielded desired morpholine **2.15** (426 mg) as well as oxazepane **2.16** (210 mg).

^{1}H NMR ($CDCl_3$, 400 MHz) δ (ppm): 2.06 (t, *J* = 10.7 Hz, 1H), 2.24 (dt, *J* = 3.3, 8.1 Hz, 1H), 2.68-2.79 (m, 2H), 3.51-3.78 (m, 6H), 3.87-3.94 (m, 1H), 7.43-7.53 (m, 3H), 7.74 (s, 1H), 7.78-7.87 (m, 3H). **^{13}C NMR** ($CDCl_3$, 100 MHz) δ (ppm): 53.0, 54.5, 63.3, 63.9, 66.4, 76.0, 125.6, 125.9, 127.2, 127.5, 127.6, 127.7, 127.8, 132.7, 133.1, 134.9. **HRMS**: $C_{16}H_{19}NO_2$, Calculated $[M+H]^+$: 257.1416, Found $[M+H]^+$: 257.1420. $[\alpha]_D^{20}$ = +13.3 (c = 1.0, CH_3OH).

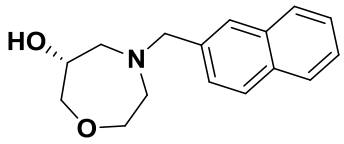

2.16

(*R*)-4-(naphthalen-2-ylmethyl)-1,4-oxazepan-6-ol (2.16).

^{1}H NMR ($CDCl_3$, 400 MHz) δ (ppm): 2.52-2.62 (m, 1H), 2.83-2.93 (m, 2H), 2.98-3.08 (m, 1H), 3.67-3.77 (m, 2H), 3.81 (s, 2H), 3.83-3.94 (m, 3H), 7.43-7.54 (m, 3H), 7.72 (s, 1H), 7.77-7.86 (m, 3H). **^{13}C NMR** ($CDCl_3$, 100 MHz) δ (ppm): 57.1, 57.8, 63.4, 68.9, 69.9, 76.1, 125.9, 126.2, 126.9, 127.7, 127.8, 128.4, 132.9, 133.3. **HRMS**: $C_{16}H_{19}NO_2$, Calculated $[M+H]^+$: 257.1416, Found $[M+H]^+$: 257.1418. $[\alpha]_D^{20}$ = +11.4 (c = 0.5, CH_3OH).

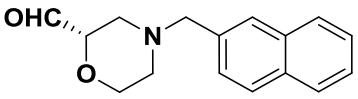

2.17

(*S*)-4-(naphthalen-2-ylmethyl)morpholine-2-carbaldehyde (2.17). In a flame-dried flask under argon, suspended alcohol 2.X (600 mg, 2.33 mmol) in anhydrous dichloromethane (23.0 mL). Added Dess-Martin Periodinane (1.48 g, 3.50 mmol) and stirred at room temperature overnight. This reaction was quenched with saturated, aqueous sodium bicarbonate and extracted with dichloromethane. After being dried over sodium sulfate and concentrated, the product was purified by column chromatography (30-80% ethyl acetate in hexanes). This gave pure aldehyde **2.17** (320 mg, 61%).

^{1}H NMR ($CDCl_3$, 400 MHz) δ (ppm): 2.25-2.32 (m, 1H), 2.32-2.40 (m, 1H), 2.65-2.72 (m, 1H), 2.90-2.98 (m, 1H), 3.70 (s, 2H), 3.74-3.83 (m, 1H), 3.98 (dt, *J* = 3.3, 11.5 Hz, 1H), 4.06-4.12 (m, 1H), 7.42-7.51 (m, 3H), 7.71 (s, 1H), 7.77-7.85 (m, 3H), 9.62 (s, 1H).

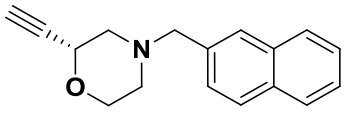

2.18

(*R*)-2-ethynyl-4-(naphthalen-2-ylmethyl)morpholine (2.18). In a flame-dried flask under argon, added aldehyde **2.17** (250 mg, 0.979 mmol) in anhydrous methanol (16.0 mL). Added to this was potassium carbonate (271 mg, 1.96 mmol) and dimethyl (1-diazo-2-

oxopropyl)phosphonate (226 mg, 1.18 mmol). This reaction was stirred at room temperature overnight. In the morning, the mixture was diluted with water, extracted with ethyl acetate, dried over sodium sulfate, and concentrated *in vacuo*. After purification by column chromatography (0-50% ethyl acetate in hexanes), pure alkyne **2.18** was recovered (115 mg, 47%).

^{1}H NMR ($CDCl_3$, 400 MHz) δ (ppm): 2.35-2.45 (m, 2H), 2.45-2.49 (m, 1H), 2.59-2.66 (m, 1H), 2.80-2.87 (m, 1H), 3.64-3.74 (m, 3H), 3.96 (dt, *J* = 3.3, 11.4 Hz, 1H), 4.35-4.42 (m, 1H), 7.44-7.54 (m, 3H), 7.76 (s, 1H), 7.80-7.88 (m, 3H).

General procedure for Sonogashira couplings and hydrogenations:

Alkyne **2.18** (15.0 mg, 0.060 mmol) was suspended in triethylamine (0.5 mL) in a microwave vial. The desired aryl iodide or aryl bromide (0.072 mmol) was added along with copper (I) iodide (0.006 mmol) and tetrakis(triphenylphosphine)palladium(0) (0.003 mmol). The microwave vial was sealed, purged with argon, and reacted in the microwave at 120 °C for 10 minutes. Product formation was confirmed by LCMS and the reaction mixture was diluted in dichloromethane and extracted from water. Purification was done by automated reverse phase column chromatography. These products were suspended in methanol and stirred under hydrogen with 10% palladium on carbon until the alkyne was reduced. Purification of these final compounds was done by automated reverse phase column chromatography.

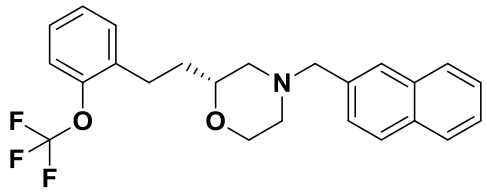

(*R*)-4-(naphthalen-2-ylmethyl)-2-(2-(trifluoromethoxy)phenethyl)morpholine (VU6000119).

^{1}H NMR ($CDCl_3$, 400 MHz) δ (ppm): 1.59-1.84 (m, 2H), 1.90-2.02 (m, 1H), 2.17-2.33 (m, 1H), 2.64-2.89 (m, 4H), 3.52 (bs, 1H), 3.59-3.76 (m, 3H), 3.83-3.94 (m, 1H), 7.14-7.21 (m, 3H), 7.21-7.25 (m, 1H), 7.42-7.53 (m, 3H), 7.73 (s, 1H), 7.77-7.86 (m, 3H). **^{13}C NMR** ($CDCl_3$, 100 MHz) δ (ppm): 25.7, 33.6, 53.1, 58.6, 63.4, 66.6, 74.7, 120.3, 125.6, 125.9, 126.6, 127.2, 127.3, 127.6 (2C), 127.7, 127.9, 130.8, 132.8, 133.2, 134.3, 147.6. **LCMS:** R_T 1.025 min, *m/z* = 415.9 $[M+H]^+$, >99% @ 215 and 254 nm.

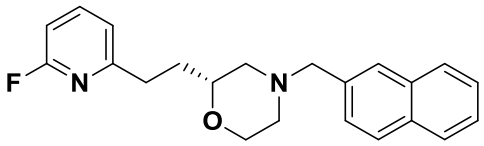

(*R*)-2-(2-(6-fluoropyridin-2-yl)ethyl)-4-(naphthalen-2-ylmethyl)morpholine (VU0657026).

^{1}H NMR ($CDCl_3$, 400 MHz) δ (ppm): 1.80-1.89 (m, 2H), 1.90-2.03 (m, 1H), 2.16-2.30 (m, 1H), 2.65-2.93 (m, 4H), 3.53 (bs, 1H), 3.59-3.77 (m, 3H), 3.83-3.91 (m, 1H), 6.69 (dd, *J* = 2.8, 8.2 H, 1H), 6.99 (dd, *J* = 2.4, 7.2 Hz, 1H), 7.42-7.52 (m, 3H), 7.62 (q, *J* = 8.2 Hz, 1H), 7.72 (s, 1H), 7.78-7.85 (m, 3H). **^{13}C NMR** ($CDCl_3$, 100 MHz) δ (ppm): 32.8, 33.1, 53.1, 58.5, 63.3, 66.5, 74.7, 106.2, 106.6, 119.9, 120.0, 125.7, 126.0, 127.3, 127.6, 127.7, 127.9, 132.8, 133.2, 141.0, 141.1, 160.8, 160.9, 161.9, 164.3. **LCMS:** R_T 0.882 min, *m/z* = 351.0 $[M+H]^+$, >99% @ 215 and 254 nm.

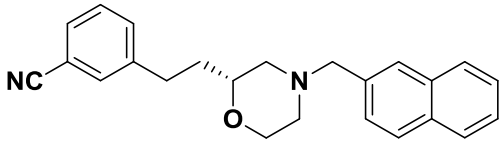

(*R*)-3-(2-(4-(naphthalen-2-ylmethyl)morpholin-2-yl)ethyl)benzonitrile (VU0657025).

^{1}H NMR ($CDCl_3$, 400 MHz) δ (ppm): 1.56-1.85 (m, 2H), 1.94 (t, *J* = 10.3 Hz, 1H), 2.18-2.32 (m, 1H), 2.61-2.85 (m, 4H), 3.45 (bs, 1H), 3.56-3.77 (m, 3H), 3.84-3.93 (m, 1H), 7.30-7.40 (m, 2H), 7.42-7.53 (m, 5H), 7.73 (s, 1H), 7.78-7.87 (m, 3H). **^{13}C NMR** ($CDCl_3$, 100 MHz) δ (ppm): 31.1, 34.7, 53.2, 58.4, 63.3, 66.6, 74.3, 112.3, 118.9, 125.7, 126.0, 127.3, 127.6 (2C), 128.0, 129.0, 129.6, 131.9, 132.8, 133.0, 133.2, 143.3. **LCMS:** R_T 0.948 min, *m/z* = 356.9 $[M+H]^+$, >99% @ 215 and 254 nm. **HRMS**: $C_{24}H_{24}N_2O$, Calculated $[M+H]^+$: 356.1889, Found $[M+H]^+$: 356.1893.

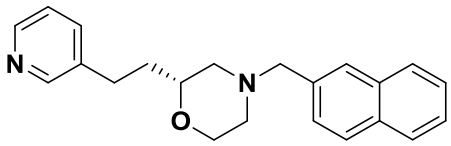

(*R*)-4-(naphthalen-2-ylmethyl)-2-(2-(pyridin-3-yl)ethyl)morpholine (VU0657080).

^{1}H NMR ($CDCl_3$, 400 MHz) δ (ppm): 1.58-1.85 (m, 2H), 1.93-2.04 (m, 1H), 2.22-2.36 (m, 1H), 2.59-2.70 (m, 1H), 2.71-2.87 (m, 3H), 3.57 (bs, 1H), 3.63-3.83 (m, 3H), 3.86-3.95 (m, 1H), 7.17 (dd, *J* = 4.8, 7.7 H, 1H), 7.43-7.54 (m, 4H), 7.75 (s, 1H), 7.78-7.87 (m, 3H), 8.38-8.48 (m, 2H). **^{13}C NMR** ($CDCl_3$, 100 MHz) δ (ppm): 28.6, 34.8, 53.0, 58.3, 63.2, 66.4, 74.2, 123.2, 125.8, 126.1,

127.3, 127.6, 127.7, 128.1, 132.8, 133.2, 135.8, 147.3, 149.9. **LCMS:** R_T 0.672 min, *m/z* = 332.9 $[M+H]^+$, >99% @ 215 and 254 nm. **HRMS**: $C_{22}H_{24}N_2O$, Calculated $[M+H]^+$: 332.1889, Found $[M+H]^+$: 332.1894.

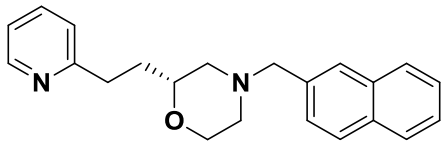

(*R*)-4-(naphthalen-2-ylmethyl)-2-(2-(pyridin-2-yl)ethyl)morpholine (VU0657082).

LCMS: R_T 0.664 min, *m/z* = 333.0 $[M+H]^+$, >99% @ 215 and 254 nm.

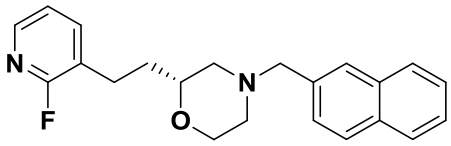

(*R*)-2-(2-(2-fluoropyridin-3-yl)ethyl)-4-(naphthalen-2-ylmethyl)morpholine (VU0657071).

LCMS: R_T 0.895 min, *m/z* = 350.9 $[M+H]^+$, >99% @ 215 and 254 nm.

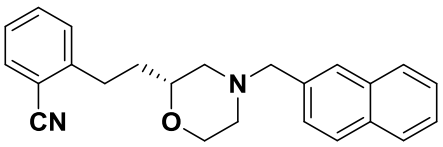

(*R*)-2-(2-(4-(naphthalen-2-ylmethyl)morpholin-2-yl)ethyl)benzonitrile (VU6000128).

LCMS: R_T 0.932 min, *m/z* = 356.9 $[M+H]^+$, >99% @ 215 and 254 nm.

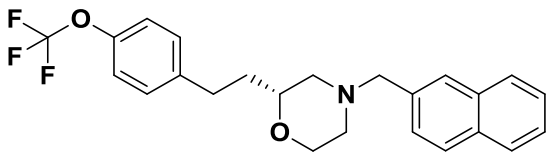

(*R*)-4-(naphthalen-2-ylmethyl)-2-(4-(trifluoromethoxy)phenethyl)morpholine (VU6000127).

LCMS: R_T 1.046 min, *m/z* = 415.9 $[M+H]^+$, >99% @ 215 and 254 nm.

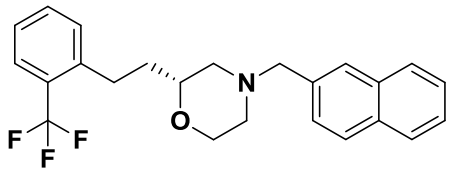

(*R*)-4-(naphthalen-2-ylmethyl)-2-(2-(trifluoromethyl)phenethyl)morpholine (VU6000126).

LCMS: R_T 1.075 min, *m/z* = 399.9 $[M+H]^+$, >99% @ 215 and 254 nm.

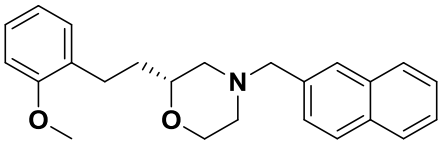

(*R*)-2-(2-methoxyphenethyl)-4-(naphthalen-2-ylmethyl)morpholine (VU6000125).

LCMS: R_T 1.001 min, *m/z* = 361.9 $[M+H]^+$, >99% @ 215 and 254 nm.

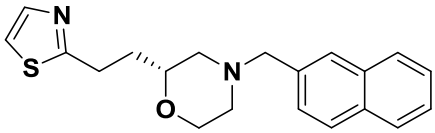

(*R*)-4-(naphthalen-2-ylmethyl)-2-(2-(thizol-2-yl)ethyl)morpholine (VU6000120).

LCMS: R_T 0.880 min, *m/z* = 338.9 $[M+H]^+$, >99% @ 215 and 254 nm.

REFERENCES

1. Newman, D. J. & Cragg, G. M. Natural Products as Sources of New Drugs over the Last 25 Years. *J. Nat. Prod.* **70,** 461–77 (2007).

2. Boonlarppradab, C., Kauffman, C. A., Jensen, P. R. & Fenical, W. Marineosins A and B, Cytotoxic Spiroaminals from a Marine-derived Actinomycete. *Org. Lett.* **10,** 5505–5508 (2008).

3. Fürstner, A. Chemistry and Biology of Roseophilin and the Prodigiosin Alkaloids: a Survey of the Last 2500 Years. *Angew. Chem. Int. Ed. Engl.* **42,** 3582–3603 (2003).

4. Aldrich, L. N., Dawson, E. S. & Lindsley, C. W. Evaluation of the Biosynthetic Proposal for the Synthesis of Marineosins A and B. *Org. Lett.* **12,** 1048–1051 (2010).

5. Cai, X. C., Wu, X. & Snider, B. B. Synthesis of the Spiroiminal Moiety of Marineosins A and B. *Org. Lett.* **12,** 1600–1603 (2010).

6. Salem, S. M. Biosynthesis of Marineosin, a Spiroaminal Undecylprodiginine Natural Product. (2012).

7. Cai, X. C. & Snider, B. B. Synthesis of the Spiroiminal Moiety and Approaches to the Synthesis of Marineosins A and B. *J. Org. Chem.* **78,** 12161–12175 (2013).

8. Lenz, R. & Ley, S. V. Tetra-n-propylammonium Perruthenate (TPAP)-catalysed Oxidations of Alcohols Using Molecular Oxygen as a Co-oxidant. *J. Chem. Soc. Perkin Trans.* **1,** 3291–3292 (1997).

9. Panarese, J. D. *et al.* Spiroaminal Model Systems of the Marineosins with Final Step Pyrrole Incorporation. *Tetrahedron Lett.* **54,** 2231–2234 (2013).

10. Aldrich, L. N. *et al.* Towards the Total Synthesis of Marineosin A: Construction of the Macrocyclic Pyrrole and an Advanced, Functionalized Spiroaminal Model. *European J. Org. Chem.* **20,** 4215–4218 (2013).

11. Williams, D. R., Kissel, W. S. & Li, J. J. Diastereoselection in the Conjugate Additions of Organoeopper Reagents to N-Enoyloxazolidinones. *Tetrahedron Lett.* **39,** 8593–8596 (1998).

12. Crimmins, M. T. & She, J. An Improved Procedure for Asymmetric Aldol Additions with N -Acyl Oxazolidinones, Oxazolidinethiones and Thiazolidinethiones. *Synlett* 1371–1374 (2004). doi:10.1055/s-2004-825626

13. Hoveyda, A. H., Evans, D. A. & Fu, G. C. Substrate-Directable Chemical Reactions. *Chem. Rev.* **93,** 1307–1370 (1993).

14. Finan, J. M. & Kishi, Y. Reductive Ring Openings of Allyl-Alcohol Epoxides. *Tetrahedron Lett.* **23,** 2719–2722 (1982).

15. Parikh, J. R. & Doering, W. E. Sulfur Trioxide in the Oxidation of Alcohols by Dimethyl Sulfoxide. *J. Am. Chem. Soc.* **89,** 5505–5507 (1967).

16. Dess, D. B. & Martin, J. C. Readily Accessible 12-I-5 Oxidant for the Conversion of Primary and Secondary Alcohols to Aldehydes and Ketones. *J. Org. Chem.* **48,** 4155–4156 (1983).

17. Stetter, H. Catalyzed Addition of Aldehydes to Activated Double Bonds - A New Synthetic Approach. *Angew. Chem. Int. Ed. Engl.* **15,** 639–712 (1976).

18. Knorr, L. . *Berichte der deutchen Chem. Gesellschaft* **17,** 2863 (1884).

19. Paal, C. . *Berichte der deutchen Chem. Gesellschaft* **17,** 2756 (1884).

20. Wilhelm, T. E., Belderrain, R., Brown, S. N. & Grubbs, R. H. Reactivity of Ru(H)(H2)Cl(PCy3)2 with Propargyl and Vinyl Chlorides : New Methodology To Give Metathesis-Active Ruthenium Carbenes. *Organometallics* **16,** 3867–3869 (1997).

21. Conrad, J. C., Parnas, H. H., Snelgrove, J. L. & Fogg, D. E. Highly Efficient Ru-Pseudohalide Catalysts for Olefin Metathesis. *J. Am. Chem. Soc.* **127,** 11882–11883 (2005).

22. Lindgren, B. O. & Nilsson, T. Preparation of Carboxylic Acids from Aldehydes (Including Hydroxylated Benzaldehydes) by Oxidation with Chlorite. *Acta Chem. Scand.* **27,** 888–890 (1973).

23. Wang, W. & Memurray, J. S. A Selective Method for the Preparation of Primary Amides: Synthesis of Fmoc-L-4- Carboxamidophenylalanine and other Compounds. *Tetrahedron Lett.* **40,** 2501–2504 (1999).

24. Zheng, J. F., Chen, W., Huang, S. Y., Ye, J. L. & Huang, P. Q. A Divergent Asymmetric Approach to Aza-spiropyran Derivative and (1S,8aR)-1-hydroxyindolizidine. *Beilstein J. Org. Chem.* **3,** 1–6 (2007).

25. Huang, P. Q. *et al.* A New Approach to (S)-4-hydroxy-2-pyrrolidinone and its 3-Substituted Analogues. *Tetrahedron: Asymmetry* **10,** 3309–3317 (1999).

26. Rapoport, H. & Castagnoli, N. 2,2'-Bipyrrole. *J. Am. Chem. Soc.* **84,** 2178–2181 (1962).

27. Baraznenok, I. L., Nenajdenko, V. G. & Balenkova, E. S. Chemical Transformations Induced by Triflic Anhydride. *Tetrahedron* **56,** 3077–3119 (2000).

28. Li, G., Zhang, X., Li, Q., Feng, P. & Shi, Y. A Concise Approach to the Spiroiminal Fragment of Marineosins. *Org. Biomol. Chem.* **11,** 2936–2938 (2013).

29. Barluenga, S., Moulin, E., Lopez, P. & Winssinger, N. Solution and Solid-phase Synthesis of Radicicol (Monorden) and Pochonin C. *Chem. Eur. J.* **11,** 4935–4952 (2005).

30. Evans, D. A. & Weber, A. E. Synthesis of the Cyclic Hexapeptide Echinocandin D. New Approaches to the Asymmetric Synthesis of B-Hydroxy a-Amino Acids. *J. Am. Chem. Soc.* **109,** 7151–7157 (1987).

31. Könning, D., Hiller, W. & Christmann, M. One-Pot Oxidation/Isomerization of Z-Allylic Alcohols with Oxygen as Stoichiometric Oxidant. *Org. Lett.* **14,** 5258–5261 (2012).

32. Grieco, P. A. & Larsen, S. D. An Intramolecular Immonium Ion Variation of the Diels-Alder Reaction: Synthesis of Dihydrocannivonine. *J. Org. Chem.* **51,** 3553–3555 (1986).

33. Missale, C., Nash, S. R., Robinson, S. W., Jaber, M. & Caron, M. G. Dopamine Receptors: From Structure to Function. *Physiol. Rev.* **78,** 189–225 (1998).

34. Oak, J. N., Oldenhof, J. & Van Tol, H. H. The Dopamine D4 Receptor: One Decade of Research. *Eur. J. Pharmacol.* **405,** 303–327 (2000).

35. Vallone, D., Picetti, R. & Borrelli, E. Structure and Function of Dopamine Receptors. *Neurosci. Biobehav. Rev.* **24,** 125–132 (2000).

36. Beaulieu, J. & Gainetdinov, R. R. The Physiology, Signaling, and Pharmacology of Dopamine Receptors. *Pharmacol. Rev.* **63,** 182–217 (2011).

37. Ptácek, R., Kuzelová, H. & Stefano, G. B. Dopamine D4 Receptor Gene DRD4 and its Association with Psychiatric Disorders. *Med. Sci. Monit.* **17,** RA215–220 (2011).

38. Rondou, P., Haegeman, G. & Van Craenenbroeck, K. The Dopamine D4 Receptor: Biochemical and Signalling Properties. *Cell. Mol. Life Sci.* **67,** 1971–1986 (2010).

39. Burns, H. D. *et al.* Positron Emission Tomography Neuroreceptor Imaging as a Tool in Drug Discovery , Research, and Development. *Curr. Opin. Chem. Biol.* **3,** 388–394 (1999).

40. Berger, A. Positron Emission Tomography. *Br. Med. J.* **326,** 1449 (2003).

41. Fernandes, E., Barbosa, Z., Clemente, G., Alves, F. & Abrunhosa, A. J. Positron Emitting Tracers in Pre-Clinical Drug Development. *Curr. Radiopharm.* **5,** 90–98 (2012).

42. Durif, F. *et al.* Clozapine Improves Dyskinesias in Parkinson Disease: A Double-blind, Placebo-controlled Study. *Neurology* **62,** 381–388 (2004).

43. Roth, B. & Driscoll, J. NIMH Psychoactive Drug Screening Program. *PDSP* (2014). at <http://pdsp.med.unc.edu/>

44. Audouze, K., Nielsen, E. Ø. & Peters, D. New Series of Morpholine and 1,4-Oxazepane Derivatives as Dopamine D4 Receptor Ligands: Synthesis and 3D-QSAR Model. *J. Med. Chem.* **47,** 3089–3104 (2004).

45. Di Ciano, P., Grandy, D. K. & Le Foll, B. Dopamine D4 Receptors in Psychostimulant Addiction. *Adv. Pharmacol.* **69,** 301–321 (2014).

46. Bergman, J. *et al.* Modification of Cocaine Self-administration by Buspirone (Buspar®): Potential Involvement of D3 and D4 Dopamine Receptors. *Int. J. Neuropsychopharmacol.* **16,** 445–458 (2013).

47. Acri, J. B. *Evidence for the Contribution of D4 Receptors to Cocaine Self-administration in Monkeys*. (2013).

48. Yan, Y. *et al.* Blockade of Dopamine D4 Receptors Attenuates Reinstatement of Extinguished Nicotine-Seeking Behavior in Rats. *Neuropsychopharmacology* **37,** 685–696 (2012).

49. Feldpausch, D. L. *et al.* The Role of Dopamine D4 Receptor in the Induction of Behavioral Sensitization to Amphetamine and Accompanying Biochemical and Molecular Adaptations. *J. Pharmacol. Exp. Ther.* **286,** 497–508 (1998).

50. Langer, O. *et al.* Carbon-11 PB-12: An Attempt to Visualize the Dopamine D4 Receptor in the Primate Brain with Positron Emission Tomography. *Nucl. Med. Biol.* **27,** 707–714 (2000).

51. Lacivita, E. *et al.* Design, Synthesis, Radiolabeling, and in Vivo Evaluation of Carbon-11 Labeled N-[2-[4-(3-cyanopyridin-2-yl)piperazin-1-yl]ethyl]-3-methoxybenzamide, a Potential Positron Emission Tomography Tracer for the Dopamine D4 Receptors. *J. Med. Chem.* **53,** 7344–7355 (2010).

52. Colabufo, N. a *et al.* Determination of Dopamine D4 Receptor Density in Rat Striatum Using PB12 as a Probe. *Eur. J. Pharmacol.* **427,** 1–5 (2001).

53. Leeson, P. D. & Showell, G. A. Morpholine Derivatives as Dopamine Receptor Subtype Ligands. (1995).

54. Showell, G. *et al.* Binding of 2,4-disubstituted Morpholines at Human D4 Dopamine Receptors. *Bioorg. Med. Chem.* **6,** 1–8 (1998).

55. O'Reilly, M. C. & Lindsley, C. W. A General, Enantioselective Synthesis of Protected Morpholines and Piperazines. *Org. Lett.* **14,** 2910–2913 (2012).

56. Halland, N., Braunton, A., Bachmann, S., Marigo, M. & Jørgensen, K. A. Direct organocatalytic asymmetric alpha-chlorination of aldehydes. *J. Am. Chem. Soc.* **126,** 4790–1 (2004).

57. Berry, C. B. *et al.* Discovery and Characterization of ML398, a Potent and Selective Antagonist of the D4 Receptor with in Vivo Activity. *ACS Med. Chem. Lett.* **5,** 1060–1064 (2014).